SELINUS UNIVERSITY
OF SCIENCES AND LITERATURE

ARTIFICIAL NEURAL NETWORK-BASED SAND PRODUCTION PREDICTION TECHNIQUE

By
Ir. TERRANCE DOUGLAS JAYASURIYA

A DISSERTATION

Presented to the Department of
Artificial Intelligence & Engineering Technology
at Selinus University

Faculty of Engineering & Technology
in fulfillment of the requirements

for the degree of

Doctor of Philosophy
in
Artificial Intelligence & Engineering Technology

2023

ACKNOWLEDGEMENTS

I would like to make a special thanks to my main general supervisor, Professor Salvatore Fava, for providing continual support, advice and untiring efforts. I would like to thank him for his patience and the constant assistance rendered towards me.

I would also like to acknowledge the Dean, Staff and Administration of the Department of Engineering and Information Technology of Selinus University who have given due assistance towards me. I would also like to take the opportunity to thank the Dean, Staff and Administration of the Post-Graduate Officer who have also always been of constant assistance.

I am most indebted to my dear wife and children for their constant love, encouragement, support and unceasing prayer for me. I would also like to acknowledge the encouragement and prayers from the rest of my family members, relatives, loved ones and dear friends that have helped me in one way or another, though simple yet remembered, and if included, the list would be very long indeed.

I humbly submit and thank God for the wisdom, encouragement and good health which He has lovingly bestowed upon me for the entire duration of my academic pursuit.

SPECIAL DEDICATION

To my beloved late Dad and Mum

Mr. Bernard Michael Jayasuriya
&
Mrs. Ignatia Gomes-Jayasuriya

To my beloved Wife

Mrs. Joanne Jayasuriya @ Song Poo Yong

To my beloved Sons

Joshua Jayasuriya & Melissa On
Grandson - Caleb Jayasuriya

Isaiah Jayasuriya

Ezra Jayasuriya

Giving thanks always for all things unto God and the Father in the name of our Lord Jesus Christ;

Ephesians 5:20, KJV

ABSTRACT

In the oil and gas industry, the onset of increased sand production due to aging fields has repercussions in the processing facilities. The erosive and corrosive nature of sand when present in the production fluids can cause detrimental damage to the facility. The early detection of presence of sand provides a useful tool so that oil and gas productions may be optimised, and unnecessary deferments averted, or in the worst case, the ultimate loss of revenue. However, field data on sand measurements is normally limited due to the unavailability of instrumentation, or if instrumented, there are insufficient samples in the measured process variables such as production flow, pressure of the flowline and sand production rates. The erosion of oil and gas wells poses a challenging task and can be surmounted by deploying a neural network in identifying the uncertainties in the system dynamics. Pre-processing of these limited process variables becomes an important and imperative part before the data is presented for the training of neural networks. Concerted efforts spent on data analysis have reaped benefits whereby models generated could accurately predict the imminent threat of sand production. A novel approach is undertaken in data pre-processing using the optimized Principal Component Regression (PCR) and Partial Least Squares Regression (PLSR) methodology has been implemented. The eigenvectors were selected to represent the parameters so that an almost universal validation data subset could be used in the pruning of the neural network. The coefficients of the PCR and PLSR respectively were automatically uploaded under different training scenarios through an expert system. The model was validated using residual analysis and the independence test of the cross-correlation between the inputs and the dependent variable. As a result, training of the neural network was more reliable with the PCR/PLSR validation dataset. Moreover, the performance index achieved on an independent test dataset was also invariably improved compared to that of the full dataset. The acceptable level of confidence attained in the approach adopted ensures that sand production could be detected in advance to avoid damage to oil and gas facilities. The reliable prediction of the onset of sand production ensures continuous production from the oil and gas facilities. More importantly, revenues from oil and gas production, and the safety of the workers in carrying out their tasks are assured.

TABLE OF CONTENTS

LIST OF SYMBOLS

Symbol	Description
δ_{ij}	Kronecker delta symbol
$\varepsilon(t,\theta_N)$	prediction error
Θ_N	estimated parameter
θ	weights vector
$\theta^{(i)}$	Specifies the current iterate
η	fluid viscosity
μ	viscosity in cP
$\mu^{(i)}$	Step size
Π	Covariance matrix
σ_h'	effective minor horizontal principal stress
σ_r	radial stress
τ	tortuosity
ϕ	porosity of the porous medium
$\varphi(t)$	is a vector containing the regressors
A_v	specific surface area
B	oil formation volume factor in RB/STB
C_0	uniaxial compressive strength (UCS)
$\nabla E(x)$	gradient
H	Hessian matrix
$F_i(.)$	i=1,2 activation function between hidden and output layers
J^*	productivity index (BOPD/psi)
K	is permeability
N	number of values in the data set.
R_c	pore pressure at the cavity wall with radius
V	loss function.
W_{ij}	weight matrix between hidden and output layers
d	number of estimated parameters.

Symbol	Description
$f_j(.)$	activation function between input and hidden layers
$f^{(i)}$	Search direction
f	function realized by the neural network
g_{pn}	normalized drawdown pressure gradient
g_{pn}^c	critical drawdown pressure gradient
h	formation thickness in ft
k_{ro}	permeability of oil in a two-phase reservoir
k_{rw}	permeability of water in a two-phase reservoir
k_s	is damage penetration
k	effective formation permeability in md
k	formation and damage permeability
k	rock compressibility
n_a	is number of past outputs used for determining the prediction
n_b	number of past inputs
n_k	time delay
p_b	Bubble pressure point
p_d	pressure conditions in the well
p_d^c	critical drawdown for sand production
p_e	constant reservoir pressure in psi
p_{f0}	pore pressure far from the well
p_{f0}	pore pressure far from the well
p_{fo}	far-field fluid pressure
$p_{w,min}$	lower well pressure limit
p_w	well pressure
p_{wf}	flowing bottomhole pressure in psi
p	overall reservoir pressure
$p(x,y)$	joint probability distribution of X and Y
$p(x)$	marginal probability density function of X

Symbol	Description
$p(y)$	marginal probability density function of Y
q	oil flow rate in Stock Tank Barrel/Day (STB/D)
q_b	oil flow rate in Stock Tank Barrel/Day (STB/D)
q_0	flow of oil
q_w	flow of oil
r_e	certain border distance in ft
r_e	reservoir radius
r_w	wellbore radius in ft
s	skin factor
$\vec{u}$	superficial velocity
$u(t)$	input
w_{ji}	weight matrix between input and hidden layers
x^n	Error in the vector
$\overline{x}$	Mean vector
x^n	Set of vectors
$\lvert x_i - y_j \rvert$	distance of two points x_i and y_i in the input space
$\hat{y}_i$	prediction at time t=i
$y(t)$	output
$\lvert y_i - y_j \rvert$	difference of $f(x_i)$ and $f(x_j)$.
z_i	input-output pair at time t=i

LIST OF TABLES

LIST OF FIGURES

LIST OF ABBREVIATIONS

Abbreviation	Description
AI	Artificial Intelligence
ANN	Artificial Neural Network
ARX	Auto Regressive Exogenous
BHFP	Bottom Hole Flowing Pressure
BHFP	Bottom Hole Flowing Pressure
BHP	Bottomhole Pressure
BHSP	Bottom Hole Static Pressure
CAPEX	Capital Expenditure
CFD	Computer Fluid Dynamics
CIU	Communication Interface Unit
COH	Cohesive Strength Of The Formation
CPP	Corporate Production Planning
CTD	Critical Total Drawdown
DCS	Distributed Control System
DD	Drawdown Pressure
DIN	German Standard On Terminal Mounting
E&P	Exploration And Production
EExd	Explosion Proof – Housing Equipment
EOVS	Effective Overburden Stress
FDP	Field Development Plan
FLP	Flow Line Pressure
GVF	Gas Volume Fraction
Hperf	Thickness Of Perforation Interval
HSE	Health Safety And Environment
HSSE	Health Safety Security And Environment
IEEE	Institution Of Electrical And Electronic Engineers
ILR	Initial Learning Rate
JIP	Joint Industry Project
LAN	Local Area Network

Abbreviation	Description
LGR	Liquid Gas Ratio
LMS	Least Mean Square
LWD	Logging While Drilling
MISO	Multiple Input Single Output
MLP	Multilayer Perceptron
MPSE	Mean Prediction Square Error
MTTR	Mean Time To Repair
MWD	Measurement While Drilling
NEL	National Electrical Laboratory
NN	Neural Network
NNARX	Neural Network Arx
NSSE	Normalized Sum Of Squared Error
OPEX	Operating Expenditure
PCA	Principle Component Analysis
PCR	Principle Component Regression
PLL	Potential Loss Of Life
PLSR	Partial Least Squares Regression
ProdLife	Production Life
Qg	Gas Production Rate
Qw	Water Production Rate (Liter/Day)
SAND	Sand Detected
SISO	Single Input Single Output
SPF	Shot Per Foot
THP	Tubing Head Pressure
TT	Transmit Time
TVD	Total Vertical Depth
UCS	Unconfined Compressive Strength
WGF	Wet Gas Flow
WHCP	Well Head Control Panel

CHAPTER 1

INTRODUCTION

1.1 Overview

1.1.1 Emerging Challenges

The global oil landscape continues to be promising and while there are two schools of thoughts on the depletion of the global oil reserves, amongst the technological community and those that presupposes that there is plentiful oil (Gorelick, 2010). The latter believes that oil production is only limited to the type of technology employed and the price of the commodity. Nevertheless, the demand for oil will continue to increase in the near future. Environmental legislations will continue to press for cleaner fuel, and there will be an increasing demand for gas.

With research funding cutbacks, the oil and gas industry will continue to see a widening gap between academia and industry. The key to the growth in the oil and gas reserves are technology and collaboration. If the frontiers of engineering are going to be pushed further, then new insights are required from the talented pool that have graduated from academia each year to link theoretical knowledge and industrial practitioners. The dire need for continuous improvement to meet the more difficult tasks of extracting oil and gas from fields is a reality.

It is expected that as oil and gas fields that produce hydrocarbons begin to age and approach at some stage in their lifetime, sand production becomes eminent. The onset of sand production becomes a threat to a producing oil or gas well and with obvious financial implications. The financial implications are due mainly to the intentional reduction in the production rates in order to reduce the resulting velocity of solids in the

fluid flow, which may consist of oil, gas and water in its respective composition. Fluid flow containing solids (sand) with high velocity would undeniably bring about the erosive and corrosive consequences to the facility. To complicate matters, the gas volume fraction (GVF) also plays a dominant role as to the transportation of solids in multiphase flow.

1.1.2 The Need for Continuous Production

The oil and gas industry with their aging fields has problems associated with sand production. Sand production is the phenomena where sand is produced simultaneously in the entrained fluids with oil and gas production.

In order for oil and gas to produce economically, well planning and economics play an important role. In terms of the drilling activities, a borehole is drilled normally into the ground into the rock strata that has enough porosity to allow the flow of hydrocarbons from the rock the reservoir below. Casing and tubing are installed with other completion equipment to direct the flow from one or more zones up through the completed well to the wellhead on the surface. In the well design phase, well engineers need to predict if solids in the form of sand particles will be expected. Core analysis needs to be carried to estimate the size of the sand particulates, so that suitable screens or filters can be installed in the completion formation. In the oil and gas industry, these screens are in the form of gravel packing and the size of the screen of "downhole" strainer depends on the anticipated sand size.

Fine sand particles, commonly referred as fines, are usually each about 25-100 μm in diameter. The screens of the gravel packing will need to be sized such that the fines can be adequately filtered. The sand particulates should remain in the reservoir and prevented from flowing up the well bore and up the surface. This is to ensure that the surface equipment will not be damaged due to the abrasive nature of the flowing sand particles. With gravel packing in installed downhole in the well, a flow

restriction is naturally introduced in the flowpath and therefore, the operating flow rates will always be lower than the design flowrates based on the wells bottom-hole pressure (BHP).

The onset of sand production could be due to the breaking down of the formation that will invariably lead to flow instability and formation damage. In such instances, the well sands-up and completely restricts any further flow from the well. It may not be economically viable to deploy a workover crew to "sand-out" the well, especially if it was an offshore platform, where the logistics and cost may outweigh the benefits of getting the well to start flowing again. On the other hand, it could be failure on the gravel packing screens, in which case the well needs to be immediately shut-in in view of the impending damage it can cause to the surface process and wellhead equipment. However, during the normal start-up of a well which has recently been drilled and have been closed for an extended period, solids are expected as debris comprising of drilling mud, perforation debris, gravel pack sand, scales, corrosion products, etc. Over time, it would eventually stabilise, and it is important that during this period, the production be at reduced flowrates.

Well gravel packing is a conventional oil field technique for screening or filtering formation sand and sediments from entering the well bore with the produced fluids. This is to avert production deferment because of fine sand, sometimes referred to as fines, blocking the continuous production of the hydrocarbon fluids. Gravel packing as shown in Figure 1-1 refers to the petroleum industry practice of surrounding with gravel or coarse sand, the perforated liner through the producing formation in an oil or gas well. When properly placed in the annular space between the wall of the well and the perforated liner, gravel supports the walls, prevents caving of loose material as shown in against the liner and serves to restrain sand from unconsolidated and disintegrating strata so that it may not enter the well.

Effective screening of sand diminishes the destructive influence of sand scouring on well equipment and tends to reduce maintenance costs.

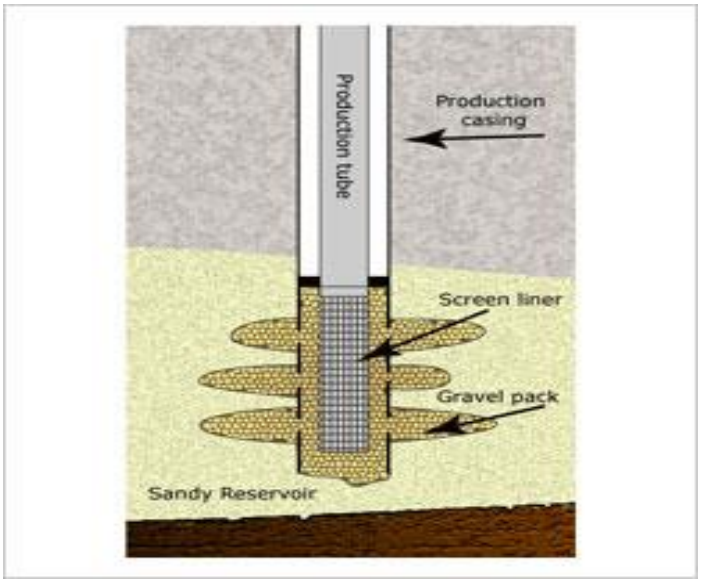

Figure 1-1: Gravel Packing to safeguard sand production in a well

Sand production will pose a couple of challenges to the oil and gas industry where there is already tough legislations in place to ensure that the industry continue to operate safely in the production of oil and gas. Moreover, the erosional problems associated with sand production manifest itself in bend ruptures as shown in Figure 1-2 should be managed in a systematic manner to prevent the release of hydrocarbon.

Figure 1-2: Erosive-corrosive effects on elbowsof flowlines

In the current mode of production of an oil well, the sand erosion rate is monitored and the opening of the production choke valve is adjusted as depicted in Figure 1-3. The production choke valve is sized for optimum performance and operates between an opening of 30% and 80%. If the erosion rate is acceptable, and the choke opening exceeds 80%, then it indicates the wellbore is plugged with formation sand as the oil can be produced at its optimum rate. Workover maintenance on the well is required to stimulate the flow in order to achieve its optimum production. On the other hand, if the erosion is not acceptable, and the choke opening is under 30%, then it indicates that formation sand has reached the surface of the wellbore and could cause erosional damage on the surface piping and equipment.

In both the scenarios above, the intervention by the production operator is of a reactive nature. Moreover, by the time the response is initiated erosional damage may have occurred and well needs to be shut-in for workover maintenance.

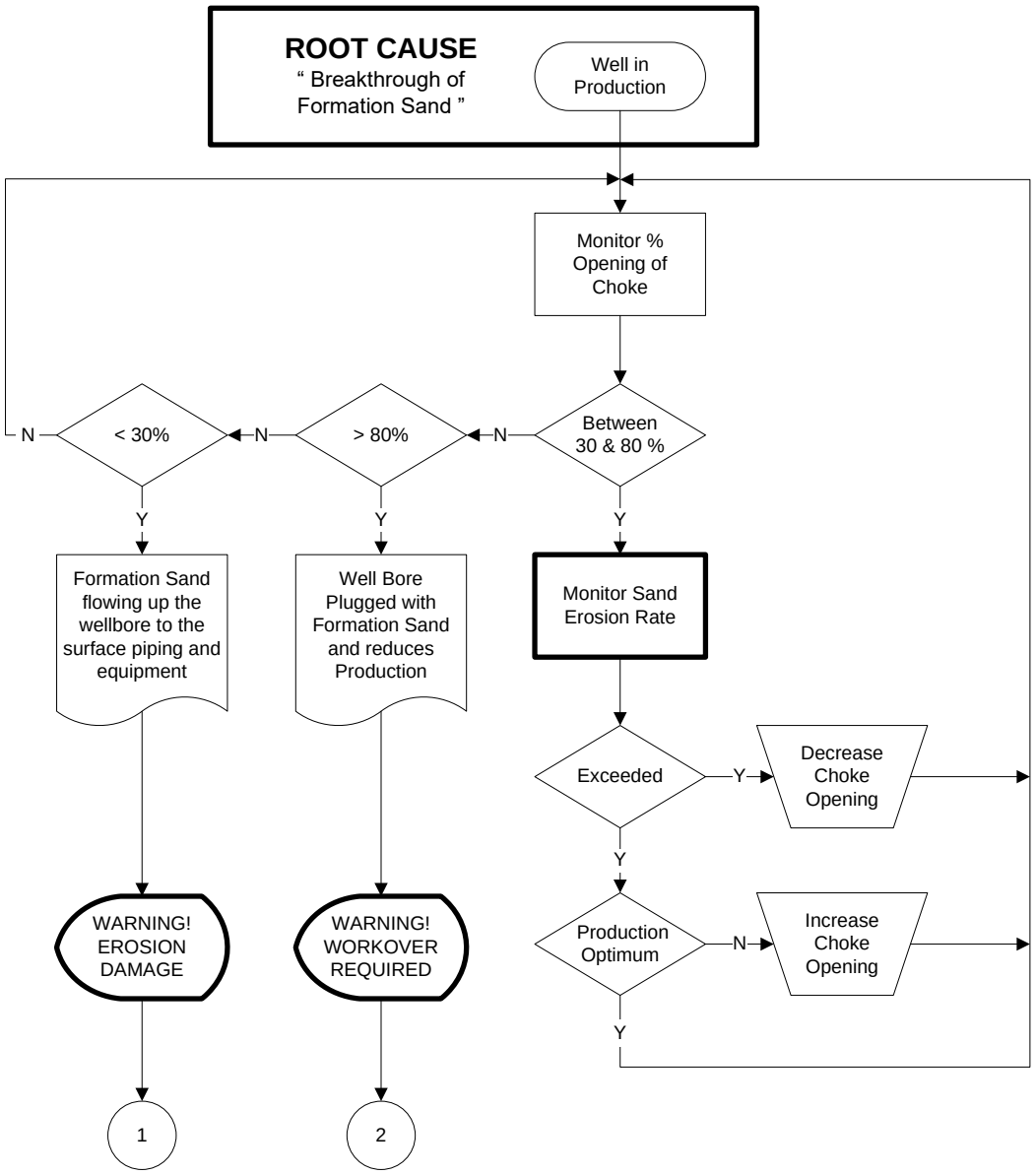

Figure 1-3: Formation Sand as root causes of oil production interruption

1.2 Problem Statement and its Significance

The problem with the current operations of oil wells is the way that the production operator responds to the onset of sand production in an oil well that occurs because of the decreasing forces in the reservoir causing formation sand to enter the wellbore as shown in Figure 1-4. In the event that formation sand accumulates at the entry to the well bore, then the well bore will begin to be plugged and production will be reduced. The operator will respond reactively by increasing the opening of the production

choke valve. However, depending on how quickly the wellbore is plugged, the oil can no longer flow out of the well bore, and production will eventually stop with economic implications resulting in production deferment.

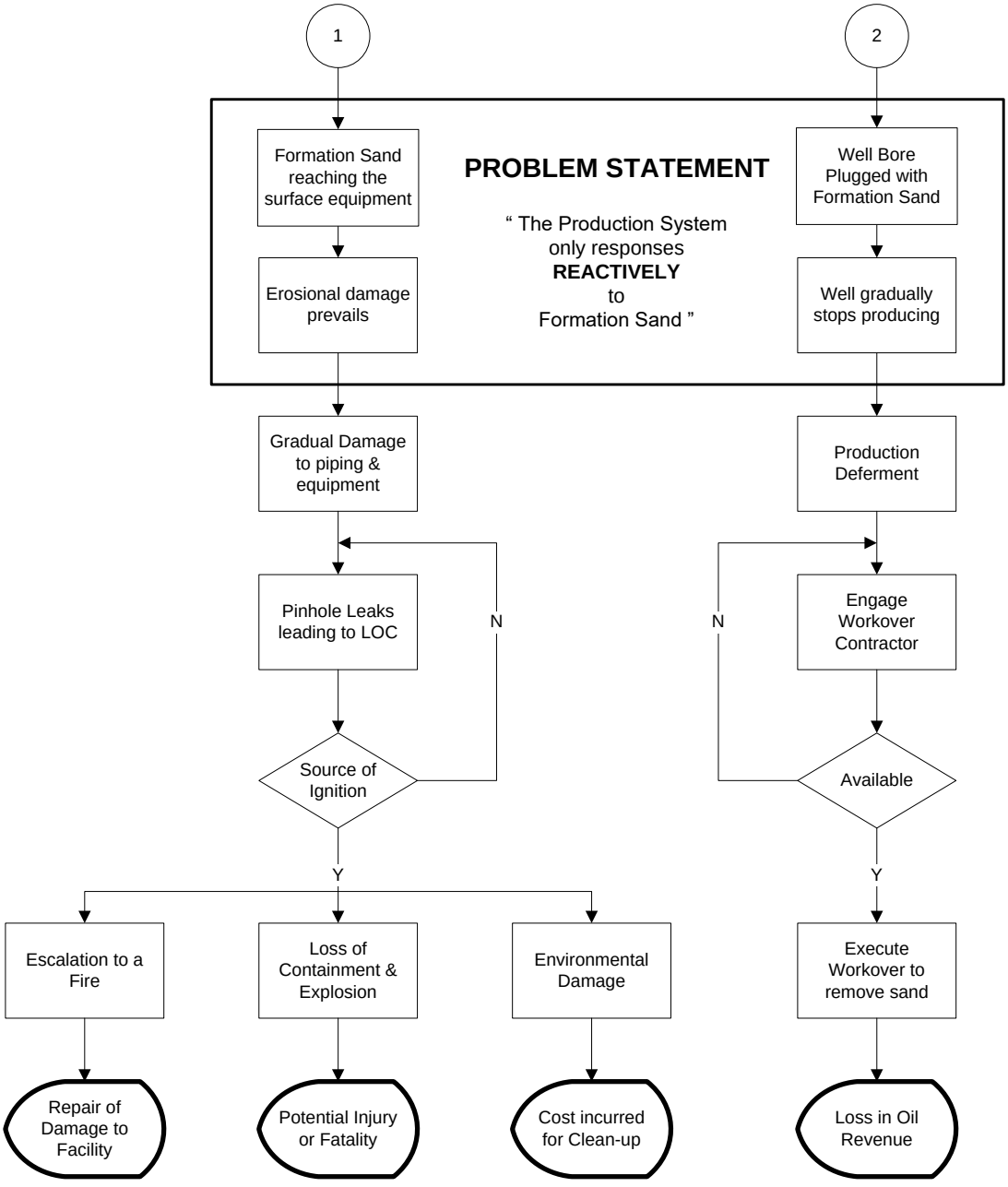

Figure 1-4: Reactive Response to the Sand Erosion Monitoring

On the other hand, in the event that formation sand does not accumulate at the entry to the well bore but reaches the surface of the well bore, the operator responds reactively by decreasing the opening of the production

choke valve. However, by then sand erosion could have caused detrimental damage to the surface piping and equipment with economic implications. Moreover, if there is a sudden onset of formation sand, pinhole leaks could develop at piping bends, resulting in a loss of containment of hydrocarbon in the flowlines. If there is a source of ignition present in such a hazardous area, this could result in an explosion and potential injury to personnel.

1.2.1 Erosion Problems

Sand production is one of the major problems faced in the oil and gas industry and is common to clastic or fragmented sedimentary basins throughout the world, affecting thousands of oil and gas fields. Erosion damage in oil and gas wells are problematic at high velocities due to the production of solid particles. In order to avoid damage, wells are made to flow at lower production traditionally based on guidelines governed by the American Petroleum Institute recommendations under API 14E. The downside of this approach is that there is a huge impact on the revenue actually generated as the fear of erosion damage dictates the high productivity of oil and gas wells. Sand production gives rise to entrained solids in the production fluids comprising of hydrocarbons particularly in high-capacity oil and gas production causing erosion damage and the importance of preventing damage to the subsurface location is given due consideration (Venkatesh, 1986).

One of the typical encountered problems in the production of formation sand is the sudden change of flowrate or high flowrate (Morita and Boyd, 1991). It emphasized the importance of a good completion of the reservoir formation during the drilling stage. An understanding of rock mechanics is also important so that the strategies to address the sand production problems could be adequately addressed.

In depleting oil and gas wells, sand production becomes an issue as the erosive-corrosive effects cause detrimental damage to pipelines,

flowlines, control valves, elbows and other fittings along the flowpath (Svedeman, 1994). There is a dire need to review the recommendations made in the API 14E on the erosional velocity criteria for the design of multiphase pipelines in these erosive-corrosive services. This is to ensure that flowrates in the presence of sand is not overly conservative, and further experiments were conducted for corrosive two-phase flow (Tronvoll, Dusseault, Sanfilippo, and Santarelli, 2000).

The ability to predict the onset of sand production proves to be an invaluable foresight as production flowrates of the problematic oil or gas well could be reduced in a timely manner. This will prevent sand particles travelling at such high velocities that could cause a loss of containment of the hydrocarbon, and consequently the potential for loss of life (DNV, 2010). In this way, working personnel can be forewarned and prevented from being exposed the released hydrocarbon in the vicinity.

1.2.2 Understanding the Hazards

The core activities of the oil and gas business is to explore and produce hydrocarbons in the most economical way, based on technical sound design and principles, while maintaining and safeguarding the safety of its personnel and the facilities or Assets. Asset integrity and operational excellence are corporate values and should be exercised at all levels of the business. In production optimisation initiatives, the wells are pushed to their limits in terms of the production flowrates. However, the operating flowrates must not exceed the designed flow rates such that formation sand is co-produced together with the hydrocarbon fluids. More specifically, the erosional velocities of the sand must not exceed the maximum allowable sand rate. These values are based on empirical experiments and recommended under API 14E of the American Petroleum Institute. The erosion limits stipulated under the recommended practice by API are conservative and the limits are being reviewed in recent years. This is

because there needs to be a trade-off between "producing to the well's capabilities" and the same time "producing within the erosional limits" so as not to incur damage to the process equipment.

When wells are produced at higher flowrates, the risk of erosion on the inner walls of the process piping is higher, and if it goes unnoticed, poses a hazard to process equipment and pipings. In the worst-case scenarios, gradual persistent erosion-corrosion effects will result in pinhole leaks in these flowpath components. For gas wells, where the hydrocarbon fluids are lighter, a gas cloud will form. If there is a source of ignition, and hence, completing the "fire-triangle" an explosion will occur. In the likelihood that there is presence of personnel in the vicinity, the outcome of the incident or event could result in potential loss of lives.

In conducting a HSSE study on fire protection analysis (FirePran), such facilities would require that the facility be installed with a fire, gas and smoke detection system approved to IEC 61508 requirements. The detectors would serve as mitigative or reactive hardware barriers, as they would be activated after the event has taken place. Likewise, preventive hardware barriers are required to prevent the event from happening. Like their mitigative counterparts, preventive barriers would also include other barriers in the form of procedures, amongst others, which are human-error prone. Hardware barriers in the form of instrumentation and other mechanical equipment would have to play their roles in ensuring the safety of, primarily, its personnel and then its assets.

1.2.3 Ensuring Continuous Production

From an economic and production standpoint, the demand for continuous operations of oil and gas production is expected. An optimum solution substantiated with a comprehensive economic evaluation model has been proposed for an effective sand management system (Benjing et al., 2008). With continuous operations, the integrity of oil and gas wells must be

ensured so that personnel safety is always of utmost importance in any esteemed organization. One of the problems underpinning the industry such as those with aging oil and gas fields is the onset of sand production together with the entrained fluid. This is a well-recognized issue facing the oil and gas industry and various countermeasures have been applied to overcome the impending problem.

With the advancement in the process control systems adopting the latest standards information technology, the industry today can monitor almost any measurements of any parameter or variable of interest (Abdelgawad and Bayoumi, 2011). With the colossal amount of data readily available if required, data-driven models take precedence and is the preferred choice as compared to mathematical modelling.

The application of neural networks in the areas of predicting diverse uncertainties is also an active area of research and has been in the petroleum industry (Ali, 1994; MY Kanj and Roegiers, 1998). Potential areas include, but not limited to, seismic pattern recognition, improvement of gas well production, prediction and optimisation of well performance amongst others. The uptake of the technology is gradually increasing in persuading decision makers on the ability of neural networks in solving problems in the petroleum industry. The deployment of neural networks in applications remains a challenge and it is anticipated with the passage of time, there will be a general acceptance of the technology.

In a multi-well field development, the success of a new well is determined by its physical location in the reservoir. The placement combinations for several wells can be carried out with a numeric reservoir simulator. Evaluation by a standard reservoir simulator is prohibitively time consuming and expensive, and the use of a fully-trained neural network has been successfully deployed as a fast prediction tool for optimising the new wells in the reservoir in the oil and gas industry with significant

reduction in efforts in computational processing (Centilmen, Ertekin, and Grader, 1999).

Models for predicting the onset of sanding co-production are used to forecast the production condition, e.g., pressure drawdown or flow rate, at which sand production occurs. The numerical and analytical sanding onset prediction models would need one or another rock mechanics input parameter or would demand extensive computations that employs Finite Element models.

A different approach requiring readily available rock mechanics data is not practical in cases when quick sand control decision is needed. In using these sanding onset prediction models it was reported that the sanding problems studied reached good agreement between predicted and field measured critical drawdown pressure (Lamorde, Somerville, and Hamilton, 2014; Yi, Valkó, and Russell, 2005).

Besides, in dealing with engineering problems that invariably affect an organization's productivity, profit and license to operate, any form of modelling should be efficient and could be rapidly deployed (Massie, Nygaard, and Morita, 1987).

1.3 Research Philosophy

The philosophy is that if the onset of the production of formation sand from the reservoir can be predicted, detrimental damage to surface piping and equipment can be avoided a result of sand erosion as shown in Figure 1-5. Moreover, injury to personnel can be mitigated and significant damage to facilities can be averted because of explosion and fire.

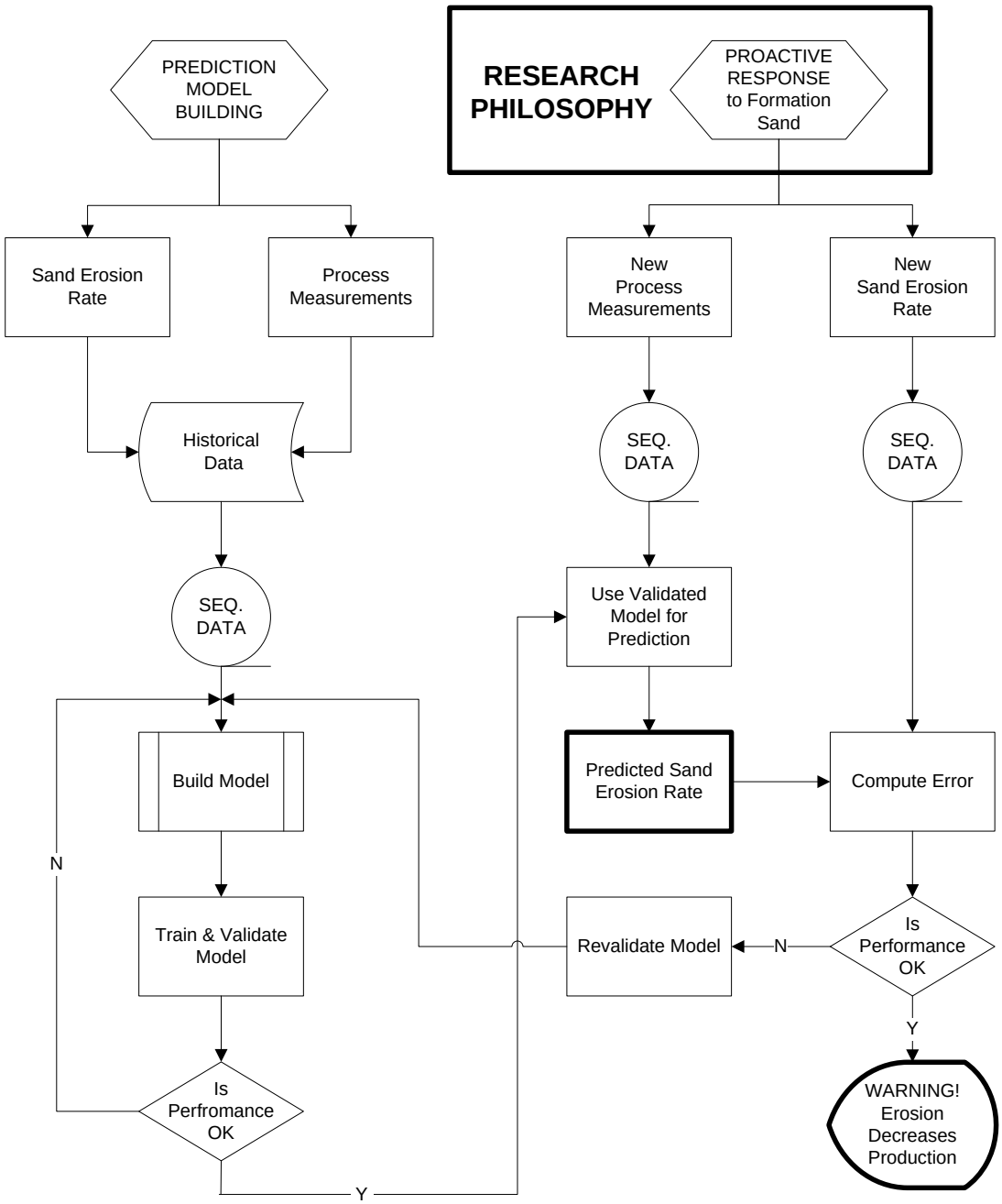

Figure 1-5: Predicting onset of the production of formation sand

1.4 Research Objectives

The motivation for this research work is to address the shortcomings of sand prediction models in the industry due to the high uncertainty of the nature of the reservoirs where oil or/and gas are usually found. The use of neural networks in prediction of systems with uncertainty is an established

methodology and the application of the methodology is a novel approach (Diebold, et al., 2005).

The objective of the thesis is to develop a sand production prediction model with a 95% confidence-level based-on available instrumentation installed on a typical oil and gas well by building a data-driven model based on a principal dataset by adopting a suitable and systematic approach.

1.5 Research Methodology

Datasets from historical records of episodes of sand erosion as a result of the onset of the production of formation sand were extracted. Subsequently, the corresponding datasets from historical records of surface process measurement covering the same period were extracted when sand erosion occurred. From both these datasets, there was a need to establish if a correlation exists between sand erosion and surface process measurements.

It is imperative to predict the onset of formation sand before it accumulates at the entry of the wellbore that could cause production deferment as a result of plugging. Eventually, the goal is to predict the onset of formation sand before it reaches the surface of the wellbore that could cause detrimental damage to surface piping and equipment as a result of sand erosion.

The research methodology adopted is that of an inductive and quantitative approach. The historical dataset for wells was obtained from the literature. The following steps were taken as shown in Table 1-1 to realise an artificial neural network-based sand prediction technique.

Table 1-1: Methodology **in Realising a Sand Prediction System**

Steps	Description of Steps
1	Scale the datasets so that they have a mean of zero and a variance of unity.
2	Assign sand dataset as dependent variable i.e., the output
3	Assign process measurement datasets as the independent variable i.e., the inputs
4	Design a Multiple-Input-Single-Output Neural Network with multiple inputs and one output.
5	Optimise the network for the number of neurons in hidden layer to obtain the desired performance.

The flowchart may be depicted as in Figure 1-6.

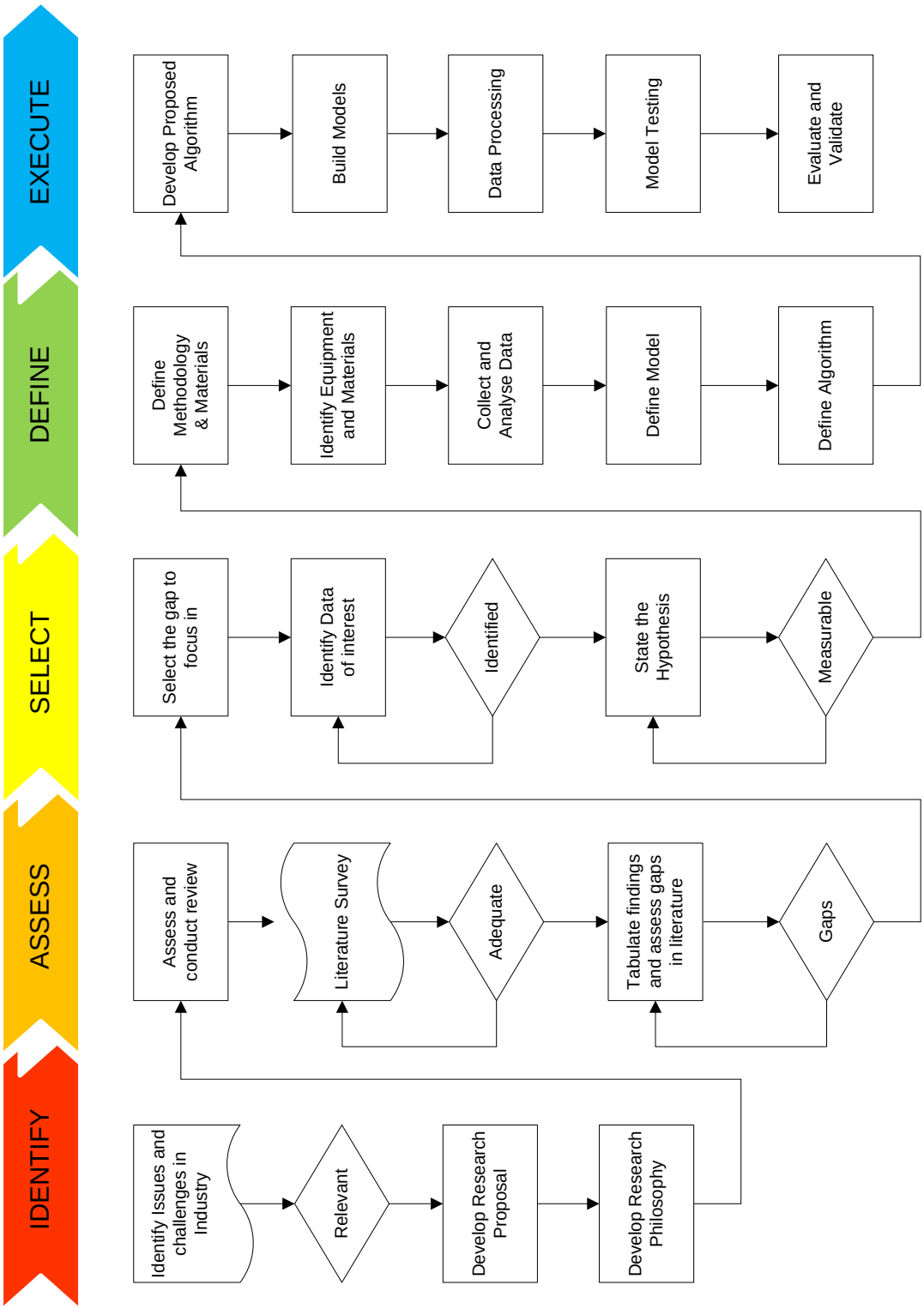

Figure 1-6: Flow Chart of the Methodology

1.6 Research Scope

The scope of the work is to address the uncertainties and assumptions of measurements required to build sand prediction models based on experimental, analytical, numerical and empirical analyses. It also assesses and evaluates the areas where artificial neural networks have also been employed in predicting parameters that are used as inputs into numerical models.

The scope of the thesis is limited to a data-driven model of an artificial neural-network to predict the onset of sand production in an oil /gas well based on data in the literature (Moricca, 1994). The onset of sand production is typically provided by measurements taken from a sand probe that is inserted in a flowline of an oil/gas well.

1.7 Thesis Organization

The thesis comprises six (6) main chapters. In Chapter 1, an introduction to the issues of sand production is underpinned with an explanation of an oil and gas production. The underlying physics and salient points pertaining to reservoir engineering and production optimisation for a typical oil and gas production system are introduced. The objectives are explicitly stated, and the scope of the work undertaken.

In Chapter 2, a literature survey of the vast amount of research that has spanned the last five decades in the field of sand production in term of the various models based on empirical, analytical experimental and numerical analysis. The use of artificial neural networks (ANN) is stipulated as a tool that would address the uncertainties and assumptions that were used in simplifying the mathematical analysis.

In Chapter 3, the methodology adopted in carrying out the work is explained in addressing the gaps existing in current research initiatives.

The materials that are required to realise the research endeavours are listed out.

In Chapter 4, the algorithm is described and developed underpins the importance of data pre-processing of the retrieved information. An appreciation of the statistical measures of the data and its corresponding probability distribution is analysed. Principal Component Analysis is introduced as a suitable data pre-processing and it is explored in detail, and the processed data is fed into a neural network autoregressive with exogenous inputs (NNARX).

In Chapter 5, the results are reported and discussed about the sand prediction system model when validated and tested with different inputs as determined by principal component analysis.

In Chapter 6, the thesis concludes and it precipitates areas of future work in the field of prediction and forecasting.

CHAPTER 2

LITERATURE REVIEW

2.1 Introduction

A current review of the integrity of the offshore facilities pertaining to erosion and corrosion problems, these being one of the root causes of major accident hazards, is picking up momentum as the oil and gas industry tightens up its realm on industrial and occupational safety (Jukes, Wittkower, and Poblete, 2009). Safety critical equipment is required to have performance standards to ensure that asset integrity is given its highest focus. Pragmatic solutions are required to address the problems in the facilities so as not to jeopardize continuous oil and gas production. Moreover, in order to prevent accidents and incidents in the oil and gas industry (Okstad, Jersin, and Tinmannsvik, 2012), there is a greater push from national regulators to ensure full compliance to health, safety and environment (HSE).

Advances in material science and engineering have undoubted brought more erosion and corrosion-resistance materials into the industry (Parsi et al., 2014). New facilities or greenfield projects will definitely benefit from the technology. However, existing and aging facilities under brownfield projects would need to invest in higher operating expenditure (OPEX) to ensure that fit-for-purpose monitoring systems (Speight, 2014) are put in place to ascertain the conditions of the piping, flowlines and pipelines connecting facilities within the oil and gas production system.

It is also recognized that sand is produced together with the oil and gas fluids in the process of producing oil and gas and is often referred to as sand production or solids production (Dehghani, 2010). Given that the erosive-corrosive effects are detrimental to the safe and continuous production of oil and gas, it is expedient that an understanding of the

underlying principles of sand production is fully comprehended. With newer methods of horizontal well drilling and completion, it is expected that there will be a higher probability of sand production. There are certain limits for the acceptable sand production, whereby, if these velocities are exceeded and allowed to continue for longer durations, further damage can be caused to not only the reservoir formation and downhole equipment, but more importantly on the surface equipment, flowlines, fittings and pipings. Sand-related failures can be of significant cost, which result in downtime and production deferment. To ensure that the financial payback period is optimised with larger profit margins, oil and gas are produced at higher production rates, resulting in higher velocities and thereby, causing damage to equipment. It is also recognized that erosion and corrosion problems due to sand production in aging assets have been overlooked (Popoola, Grema, Latinwo, Gutti, and Balogun, 2013), and hence, due attention required at higher management levels.

There is a whole range of monitoring systems available in the market offered to the oil and gas industry, and their effectiveness, limitations and advantages need to be understood (Brown and Davies, 2000). The release of hydrocarbon into the atmosphere as a result of a loss of containment (LOC) due to erosion, corrosion or their combined effects will expose a facility to high risk of fire that could escalate to an explosion. Early detection of these adverse effects is instrumental to an effective monitoring system to ensure that oil and gas facilities are safe to operate and produce (Rahman, Khaksar, and Kayes, 2010). Prediction of the onset of sanding and the amount of sand produced under a given set of conditions do not have models that currently exist in the industry (Addis, Gunningham, and Brassart, 2008).

As oil and gas fields that have been producing hydrocarbons begin to age and approach the end stage in their lifetime, sand production becomes eminent. The onset of sand production becomes a threat to a producing oil

or gas well with obvious financial implications. The financial implications are due to the intentional reduction in the production rates in order to lower the resulting velocity of solids in the fluid flow comprising oil, gas and water in their respective composition. Fluid flow containing solids (sand) with high velocity would undeniably bring about the erosive and corrosive consequences to the facility. To complicate matters the gas volume fraction (GVF) also plays a dominant role as to the transportation of solids in multiphase flow (Bello, Oyeneyin, and Oluyemi, 2011).

Petroleum production engineering is associated with activities concerned with the ability of a well to produce or inject at a flowrate against differential pressure drop in the near wellbore region i.e., the productivity or injectivity index. Reservoir engineering on the other hand, deals with the reservoir-at-large and the lifecycle of hydrocarbon recovery. Production engineering often deals with production optimisation to accelerate the production by increasing the well production or injection rate, but more importantly the reduction in the well drawdown, i.e., the difference between the driving reservoir pressure, and the flowing bottomhole pressure (FTBH). Although it is economically attractive to lower the FBHP to increase the production rate, it is not always desirable as there may be adverse effects associated with solids production, and in particular the risk of sand production (Bai, Santana, and Shen, 2011). One of the common objectives of reservoir engineering is to reduce the risk so that oil and gas wells can produce continuously, reliably and safely. Numerical reservoir simulation ensures that solids production in terms of sand, wax, scale, paraffin and asphaltene deposition are adequately understood, studied, analysed and engineered (Guo, 2007).

Figure 2-1 shows the different components in a complex interaction of reservoir inflow, flow through perforations and tubing outflow, well choke, surface pipelines and separators.

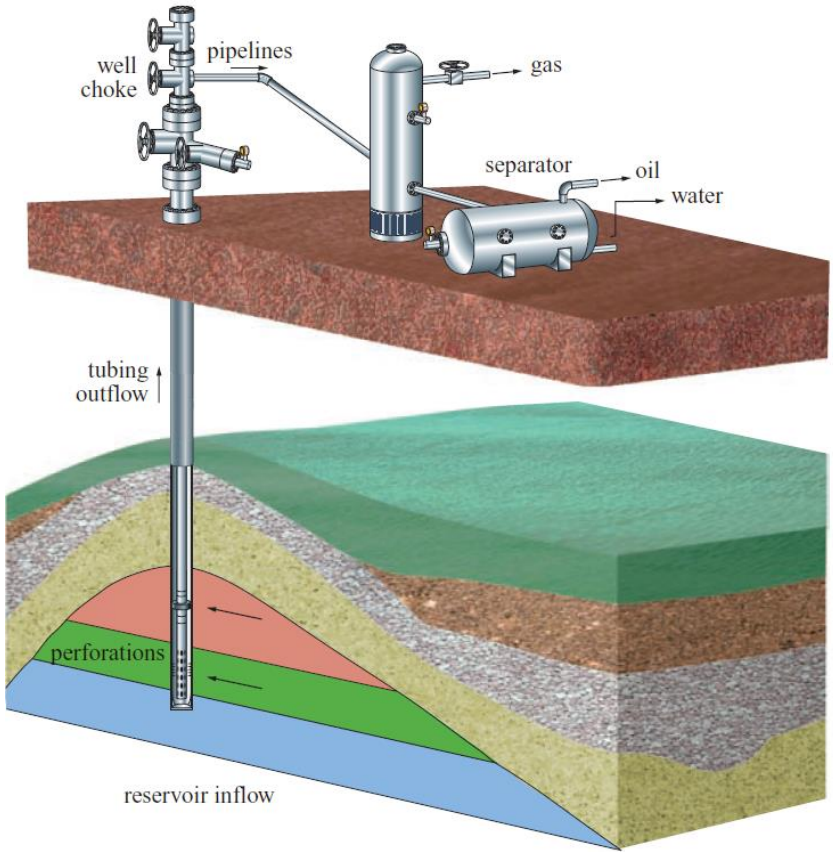

Figure 2-1: Petroleum production system: elements affecting well productivity- Source (Guo, 2007)

The pressure losses near the wellbore of an oil or gas well, due to formation damage has a reduced permeability and the zone with the altered permeability is known as skin (Van Everdingen, 1953). Skin effect accounts as in Figure 2-2 for the additional pressure drop necessary to overcome the flow resistance of the reduced permeability zone caused by drilling mud invasion, the effect of partial penetration or the effect of the penetrating contact angle of the well architecture.

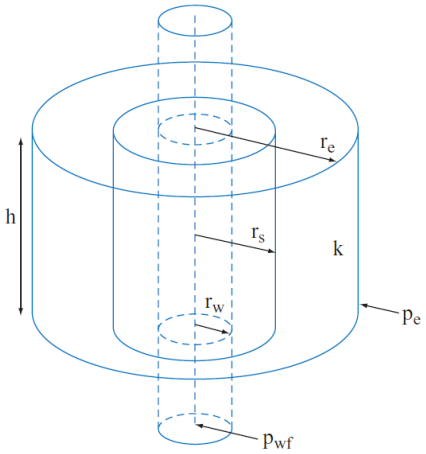

Figure 2-2: Skin radius r_s of the zone characterized by the skin with respect to the drainage radius - Source (Guo, 2007)

The single steady-state inflow performance of a reservoir for the oil flow rate **q** assuming under-saturated conditions (gas in solution) is given by,

$$q = \frac{kh(p_e - p_{wf})}{141.2B\mu\left[In\left(\frac{r_e}{r_w}\right) + s\right]} \tag{2-1}$$

where,
- q is the oil flow rate in Stock Tank Barrel/Day (STB/D)
- k is the effective formation permeability in md
- h is the formation thickness in ft
- p_e is the constant reservoir pressure in psi
- p_{wf} is the flowing bottomhole pressure in psi
- B is the oil formation volume factor in RB/STB
- μ is the viscosity in cP
- r_e is the certain border distance in ft
- r_w is the wellbore radius in ft
- s is the skin factor

Assuming that reservoir and near-the-wellbore pressures are above the bubble point, the expressions for the flow of oil q_0 and water q_w should consider the relative permeability reduction due to the effect of their respective phase's saturation,

$$q_0 = \frac{kk_{ro}h\left(p_e - p_{wf}\right)_0}{141.2B_0\mu_0\left[In\left(\frac{r_e}{r_w}\right) + s\right]} \quad (2\text{-}2)$$

$$q_w = \frac{kk_{rw}h\left(p_e - p_{wf}\right)_w}{141.2B_w\mu_w\left[In\left(\frac{r_e}{r_w}\right) + s\right]} \quad (2\text{-}3)$$

where $\mathbf{k_{rw}}$ and $\mathbf{k_{ro}}$ are the respective permeability of water and oil in a two-phase reservoir. Water saturation near the wellbore will invariably lower the oil flow (Guo, 2007).

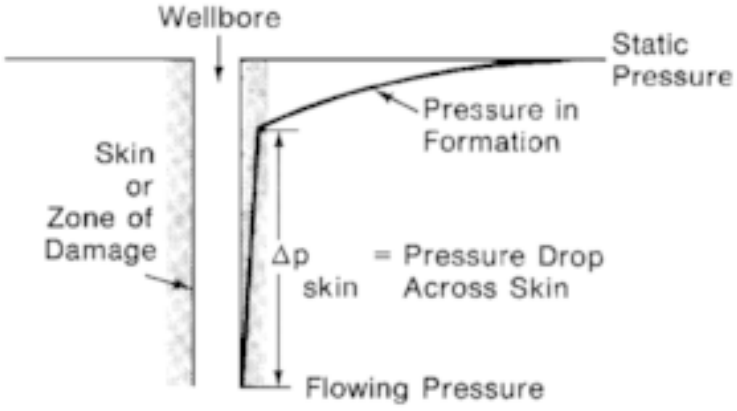

Figure 2-3: Damage wellbore

The skin factor s can be related to formation and damage permeability k, damage penetration k_s and well radius r_w for a given r_e by (Hawkins Jr., 1956)

$$s = \left(\frac{k}{k_s} - 1\right).In\left(\frac{r_e}{r_w}\right) \quad (2\text{-}4)$$

where, k is the formation and damage permeability
k_s is damage penetration
s the skin factor
r_e is the reservoir radius
r_w is the wellbore radius
s the skin factor

2.1.1 Productivity Index

The productivity index J^* (BOPD/psi) above the bubble point pressure p_b, when there is no water production, is the ratio between the oil flow rate q_b and the pressure drawdown is given by (Dake, 1998).

$$J^* = \frac{q_b}{p_e - p_{wf}} \frac{7.08kh}{(p_D) + s}\left(\frac{k_{ro}}{\mu_0 B_0}\right) \;\; ; \;\; for\; p_{wf} < p_b \tag{2-5}$$

where,

J^*	is the productivity index (BOPD/psi)
q_b	is the oil flow rate in Stock Tank Barrel/Day (STB/D)
k	is the effective formation permeability in md
h	is the formation thickness in ft
p_b	is the bubble pressure point
p_e	is the constant reservoir pressure in psi
p_{wf}	is the flowing bottomhole pressure in psi
B	is the oil formation volume factor in RB/STB
μ	is the viscosity in cP
r_e	is the certain border distance in ft
r_w	is the wellbore radius in ft
s	is the skin factor

2.1.2 Inflow Performance Relationship

The objectives of production optimization may be to enhance reservoir inflow performance or to reduce outflow performance. The results could be more production with less pressure drawdown. The understanding of reservoir inflow, wellbore vertical lift and surface facilities pressure constraint is necessary to optimize the field production performance and should be considered when addressing issues associated to sand production.

The Inflow Performance Relationship (IPR) and its corresponding graph of flow rate against the downhole flowing bottomhole pressure that typically characterizes the well performance is depicted in Figure 2-4.

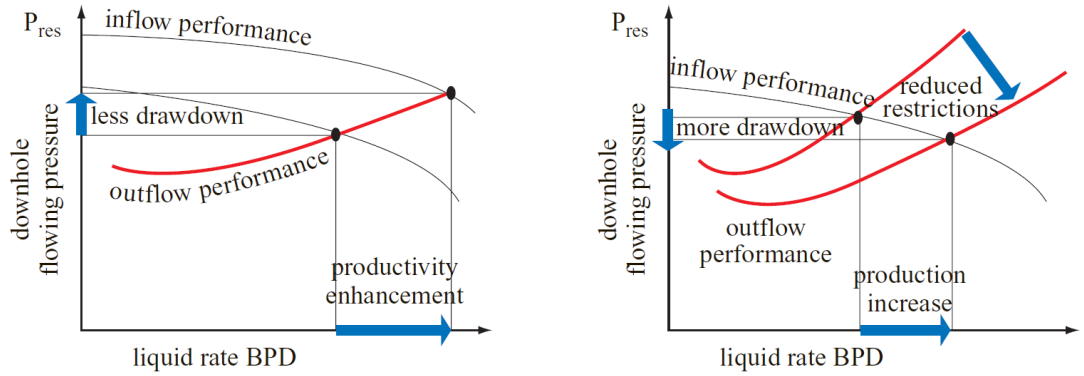

Figure 2-4: IPR and the effects of drawdown to production - Source: (Guo, 2007)

2.2 Multiphase flow with Sand

The main flowpath components after a wellhead are the following; production choke, elbows, tee-caps, valves, and other instrumentation. These flowpath components are "hot spots" with a high likelihood of erosion affecting these components when sand is produced in the entrained fluid from an oil or gas production well. The combined effects of the erosive/corrosive nature of sand produced will result in pinhole leaks at these hot spots if sand production is excessive. Pinhole leaks, if undetected for a considerable time will lead to a gas cloud being formed, that could potentially result in an explosive mixture and eventually an explosion. Sand erosion probes when deployed primarily for this purpose are also known as pressure trigger probes because a shutdown on the wellhead control panel (WHCP) is triggered by a pressure transducer when the pressure-contained tube in the probe is breached or penetrated by the high velocity sand particulates in the produced fluids. In the recent decade or so, sand erosion probes have been designed for continuous monitoring.

Fluid dynamics in terms of velocity limits are also an integral part of an understanding of the erosive and corrosive effects of sand production. It is these effects, more than any other that has driven oil and gas operating companies to take the necessary measures to ensure that the

safety of its people and assets are given the utmost priority so that the Health Safety and Environment (HSE) issues are adequately and strictly in compliance. Bends in flowlines commonly referred to as elbows are highly vulnerable for oil and gas wells that produce fluids with entrained solids (Mazumder, Shirazi, and McLaury, 2008). Gradual metal loss occurs from the inner walls of process equipment and fitting because of repeated impact of suspended solids in entrained fluids of oil and gas production. The thinning of walls of elbows due to erosion results in the process equipment not being able to withstand the original design pressure. Sand erosion in single-phase flow is difficult to predict due to the different interacting parameters.

The new DNV Recommended Practice O501 provides valuable tools for dimensioning of piping systems and components, optimisation of production, and inspection and maintenance planning (Veritas, 1996). The DNV erosion model calculates erosion rates using real time data such as sand signal, flow, temperature and pressure and additional information based on statistical and historical data. Data from both intrusive and non-intrusive sand probes, depending on the principle of operation, has to be fed into a sand erosion prediction for sand and erosion rates to be calculated.

2.2.1 Single-Phase and Multiphase Flow

The single steady-state inflow performance of a reservoir for the oil flow rate $\mathbf{q}$ assuming under-saturated conditions (gas in solution) is given by,

$$q = \frac{kh(p_e - p_{wf})}{141.2B\mu\left[In\left(\frac{r_e}{r_w}\right) + s\right]} \tag{2-6}$$

where, q is the oil flow rate in Stock Tank Barrel/Day (STB/D)
k is the effective formation permeability in md
h is the formation thickness in ft
p_e is the constant reservoir pressure in psi

p_{wf} is the flowing bottomhole pressure in psi
B is the oil formation volume factor in RB/STB
μ is the viscosity in cP
r_e is the certain border distance in ft
r_w is the wellbore radius in ft
s is the skin factor

Generally, water produced with the oil exists partly as free water and partly as water-in-oil emulsion. In some cases, however, when the water–oil ratio is very high, oil-in-water rather than water-in-oil emulsion will form. Along with the water and oil, gas will always be present and, therefore, must be separated from the liquid. The volume of gas depends largely on the producing and separation conditions.

Assuming that reservoir and near-the-wellbore pressures are above the bubble point, the expressions for the flow of oil q_0 and water q_w should take into account the relative permeability reduction due to the effect of their respective phase's saturation,

$$q_0 = \frac{kk_{ro}h\left(p_e - p_{wf}\right)_0}{141.2B_0\mu_0\left[In\left(\frac{r_e}{r_w}\right) + s\right]} \quad (2\text{-}7)$$

$$q_w = \frac{kk_{rw}h\left(p_e - p_{wf}\right)_w}{141.2B_w\mu_w\left[In\left(\frac{r_e}{r_w}\right) + s\right]} \quad (2\text{-}8)$$

where, q_0 is the flow of oil
q_w is the flow of oil
k_{rw} is the permeability of water in a two-phase reservoir
k_{ro} is the permeability of oil in a two-phase reservoir

Water saturation near the wellbore will invariably lower the oil flow (Guo, 2007).

2.2.2 Sand Erosion in Multiphase Flow

Sand erosion in multiphase flow is a different phenomenon altogether and various regimes have been investigated in depth (McLaury, Shirazi, and

Rybicki, 2010). In the past, prediction of multi-phase flow models was empirical and was heavily dependent on the accuracy of flow experiments. Mechanistic models were developed to predict multiphase flow comprising oil, gas and sand particles upstream of elbows flowing under different flow regimes for annular and slug flow. Annular flow experiments were primarily performed in the vertical run, while slug flow was carried out on the horizontal piping run. The mechanistic models were improved to predict sand erosion under the different flow regimes based on the gas-liquid flow.

A comprehensive review on the erosion of elbows of hydrocarbon production has been produced in this respect by the National Engineering Laboratory (NEL) on behalf of the UK Health and Safety pertaining to the hydrocarbon production (Osu, 2004). An overview is given of different erosion mechanisms and the factors that influence them. The report looks at particulate erosion in more detail, particularly erosion on elbows in terms of its corresponding mathematical equations and physics constraints. The undetected release of hydrocarbon gases from pinhole leaks from elbows could result in a loss of containment with a gas cloud forming near the leak. If the gas release remains unnoticed or undetected, the likelihood of an explosion is high in the event that a source of ignition is present.

2.2.3 Tool for Flow Modeling

Various modelling techniques have been developed with the aid of computational fluid dynamics (CFD) and have in recent past, being increasingly used to understand the dynamics of flow profiles with entrained solids in the production fluid in flow geometries such as elbows, valves, reducers, enlargers, etc (Wallace, Dempster, Scanlon, Peters, and McCulloch, 2004). A number of equations are derived for the particular flow profile and the dynamics of the flow is modelled using commercially available software.

CFDs have helped engineers to understand flow profiles visually (Zhang, McLaury, and Shirazi, 2009). The turbulent velocity profile in the near-wall region and the effect on particle impact velocity was investigated and simulation results showed that the particle impact velocity is affected significantly when near-wall velocity profile is implemented. In addition, the effects of particle size were investigated in the near-wall region of a turbulent flow in elbows with smaller radius. CFD software would have otherwise required minicomputers a decade or two ago, which was not commercially attractive and affordable by individuals or small-scale research, while today desktop PC's and laptops are readily available to the engineering community. The governing equations are of prime importance as in the case for any mathematical-base modelling techniques. Other parameters such as sand particle size, flowline diameter and velocity are but a few of the parameters that are required for a successful CFD model to be visualized.

The study of sand erosion on process piping and components was carried out using CFD, to assess the behaviour of sand erosion on both standard pipe components and complex geometries (Huser and Kvernvold, 1998). This led to new Det Norske Veritas (DNV) procedures based on CFD to predict sand erosion in typical pipe components such as pipe bends, blinded Tee bends, straight pipes, welds and reducers (DNV, 2007). The standard provides valuable tools for dimensioning of piping systems and components, optimisation of production, and inspection and maintenance planning.

2.3 Equipment and Measurement Technology

Different sand monitoring that are commercially available in the oil and gas industry are evaluated for multiphase flow (Shirazi, Ali, and McLaury, 2000). Data collected from these sand monitoring devices were analysed and evaluated against models that calculate particle impact velocities and

erosion rates. The important finding was that there is a correlation between the outputs from the sand detectors and the erosion model, thereby allowing results from sand detectors to be interpreted using the erosion model.

Both intrusive-type sand probes and the extrusive or non-invasive acoustic sensors as shown in Figure 2-5 have their strengths depending on their applications and purpose of their installations (Salama, 2000).

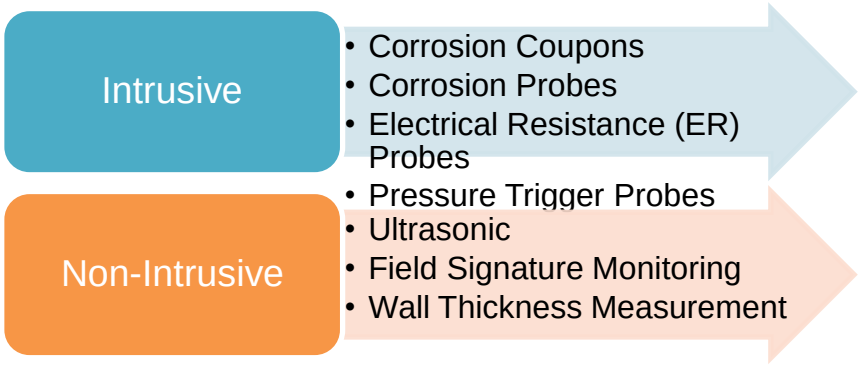

Figure 2-5: Erosion and Corrosion Measurement technologies

Each of the technologies employed have their advantages and disadvantages and their usage in the different applications warrants some discussions.

2.3.1 Performance Analysis of Measurement Technology

The various technologies in Table 2-1 deployed in the oil and gas industry for monitoring the erosive-corrosive effects of sand are assessed and compared.

Table 2-1: Comparison table for sand monitoring tools

Measurement Technology	Advantages	Disadvantages
Intrusive Monitoring:		
Corrosion Coupons	Simple measurement of loss in weight of coupon because of corrosion for pipelines in general.	Corrosion is pre-dominantly due to water and presence of corrosive products and not by sand production.

Measurement Technology	Advantages	Disadvantages
Electrical Resistance-based Erosion probe	Real-time and direct measurement of metal loss on the probe is correlated with the wall thickness loss of the flowline.	When elements on the probe are depleted, replacement required with a well to shut down. Economic implications associated with production deferment. Functionality depends on where the probe is located on the flowline for it to be reliable.
Pressure-trigger Probe	Erosion due to sand particles will eventually breach the tip of the probe, and hence preventing further erosion to the equipment, by triggering an automatic shutdown of the well.	Reactive as it does not provide proactive monitoring of sand production. Performs reliably if it is placed at the correct location in the flowline.
Non-Intrusive Monitoring:		
Acoustic measurement	Device is clamped onto the flowline, and there is no need for dedicated access fitting on the flowline for installation.	As it is acoustic, device calibration equipment is required to inject sand into the flowline to eliminate the background.
Wall-thickness measurement	Mats are can easily be installed at elbows and piping bends at locations that have been determined.	Wall thickness loss is pre-dominantly due to corrosion rather than sand production.
Field signature method	Provides information about erosion and corrosion due to metal loss.	Bulky and expensive and are pre-dominantly used for subsea pipelines.

From Table 2-1, a sand monitoring device that calculates metal loss and provides real-time measurement to a system is desirable. The electrical resistance-based erosion probe provides a direct measurement of metal loss and was selected for the monitoring of sand production. Upon

depletion of the elements on the probe, the probe needs to be replaced once the threshold is reached. The installation of the probe is crucial to ensure its effectiveness in the measurement of metal loss. The sand erosion probe is selected to monitor the onset of sand production.

2.3.2 Typical Instrumentation of Oil or Gas Well

In order to control and optimise production of oil and gas wells, it is important that these wells are adequately provided with at least transmitters to measure pressure and flow parameters. More importantly, the co-production of sand as a by-product in some cases needs to be monitored. If sub-surface gravel packing is installed at the onset of the design of the oil and gas well, then the likelihood of sand production is slim. Failures of downhole sand control is common and the risk needs to be managed accordingly to ensure that wells could produce that do not require intervention due to downhole sand screen failures (Guinot, Duncan, Douglass, Orrell, and Stenger, 2009). However, given the uncertainty of sand production, most wells are equipped for monitoring sand. This is to ensure that the equipment on the surface facilities is not subjected to excessive effects of erosion and corrosion.

A typical oil or gas well is instrumented with the following instrumentation as depicted in Figure 2-6. The tubing head pressure (THP) transmitter is located between the wellhead and the choke valve and measures the pressure of the tubing of the well up to the wellhead. Transmitters for the flowline pressure (FLP) and wet gas flow (WGF) of the unstabilised fluid are measured after or downstream of the choke valve. Annuli pressure management requires that the casing head pressure (CHP) be being monitored for well integrity. A typical oil or gas well that is likely to co-produce sand will normally be designed with erosion (EL) and corrosion (CL) probes that measure metal loss due to erosion and corrosion, respectively.

Getting these process measurements from the remote fields is a challenging task. However, with cost justifications, remote telemetry units (RTU's) can be deployed to these fields in order to obtain real-time process measurements.

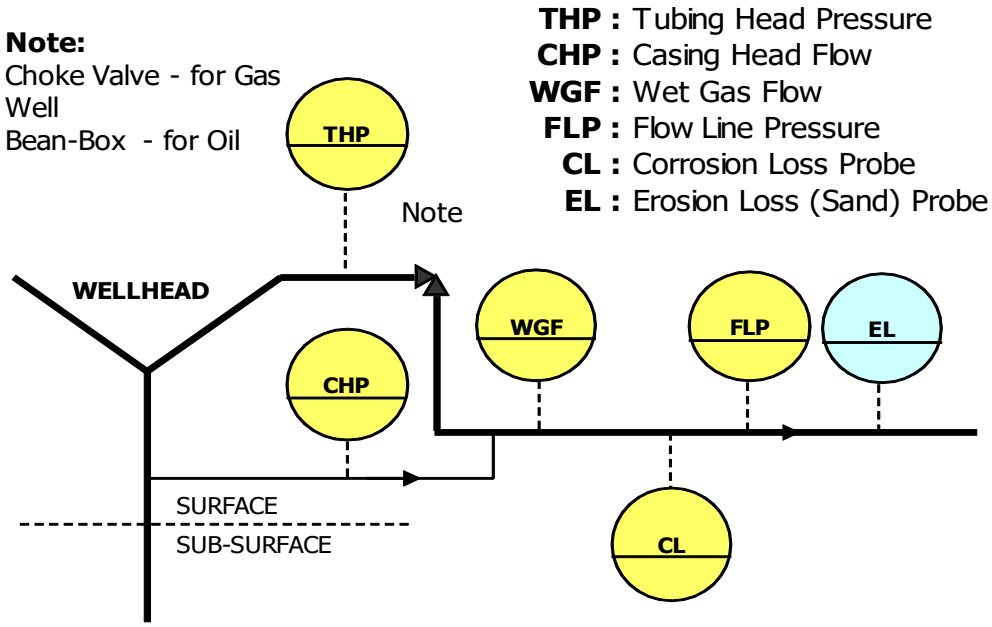

Figure 2-6: Instrumentation and equipment of a typical oil or gas well

2.3.3 Feasibility and Costing of Current Approach

In the current approach, sand production rates are deduced from process parameters that are normally available on a typical oil or gas well. A typical oil or gas well is usually provided with instrumentation to measure process parameters such flow, pressure, temperature, etc, as deemed required. In a typical smart field approach, remote monitoring and control are the basic requirements of these process parameters so that oil and gas production could be optimized. A data communication infrastructure would normally be available to facilitate the polling of these process parameters and therefore, it is highly feasible as these data are required for other purposes. The incremental cost associated with the current approach would be

minimal and would be related to building a model of the facility, the efforts on data pre-processing, training of the neural nets, implementation on the Operator DCS, etc.

2.4 Solids Production from Formation Sand

The pressures that are built-up in the sub-surface region of the producing well drive sand production. Solid particles produced with hydrocarbons from a reservoir sometimes follow the reservoir fluid into the wellbore and appear at the surface as sand. The amount of solids produced can vary from miniature to catastrophic amounts that could possibly lead to a complete filling of the borehole. It is estimated that seventy percent of the world's hydrocarbon reserves are contained in reservoirs where solids production is likely to become a problem at some point in time (Penberthy, WL and Shaughnessy, 1992). The modelling of sand production requires the coupling of two basic mechanisms (Rahmati et al., 2013).

- Mechanical instability and degradation around the wellbore
- Hydromechanical instability due to flow-induced pressure gradient on degraded material surrounding the cavity i.e., the perforation and open hole.

The phenomenon of sand production involves processes that can be broken into three main stages (Detournay, Tan, and Wu, 2005).

- Tensile or compressive failure within the vicinity of the perforation or open hole and its progression further into the formation
- Dislodgment or disaggregation of sand particles from the failed section of the formation
- Movement of those particles into the wellbore, and then to the surface if settlement does not occur.

The relatively simple analytical models for the onset of sand production show that two groups of data are required for sand prediction:

- rock properties (primarily strength)

- conditions of the formation (in situ stresses and pore pressure)

Stress changes induced during depletion of oil or gas wells are usually difficult to predict but it is of vital importance for the prediction of reservoir compaction and permeability alterations, and conventional assumptions of constant overburden and the absence of lateral deformation may be highly inaccurate (Papamichos, Vardoulakis, Tronvoll, and Skjaerstein, 2001).

Observations of sand production can be classified in three types (Fjær, Holt, Horsrud, Raaen, and Risnes, 2011).

- Transient sand production, where a burst of sand is followed by a continuous production of sand with declining rate under constant conditions.
- Continuous sand production, where sand is continuously produced at a relatively constant rate.
- Catastrophic sand production, where sand is produced at such a high rate that the well is choked.

There is insufficient force to pull sand grains out of rock that is intact by the flowing fluid in the wellbore. However, sand production may only occur if the rock near the producing cavity is unconsolidated or has been damaged. The onset of sand production is therefore, closely related to stress-induced damage of the rock (Tronvoll and Fjær, 1994).

Monitoring of sand production is usually based on measurements or observations at the surface. However, the produced sand will only reach the surface if the well flow is sufficiently strong to carry the sand grains all the way up through the well. Thus, sand transport in the well is also a significant part of the sand production problem.

2.5 Modelling of Rock Properties

Rocks are generally composite materials, and hence inhomogeneous on a microscopic scale. The behaviour of rocks in terms of their elastic response

and failure stresses etc., depend on the void space is essential for oil to be produced from a reservoir. The approach based on the macroscopic description of porous and permeable media, allows the study of both static and dynamic mechanical properties (Biot, 1941).

2.5.1 Porosity, ϕ

The porosity, ϕ of a porous medium is defined as the fraction of the bulk volume that is occupied by void space, which means that $0 \leq \phi < 1$. Likewise, $1-\phi$ is the fraction occupied by solid material (rock matrix). The void space generally consists of two parts; the interconnected pore space that is available to fluid flow, and disconnected pores that is unavailable to flow and it is therefore common to introduce the so-called "effective porosity" that measures the fraction of connected void space to bulk volume (Lie, 2014).

For non-rigid rocks, the porosity is usually modelled as a pressure-dependent parameter and hence, it is compressible, having a rock compressibility defined by:

$$k = \frac{1}{\phi}\frac{d\phi}{dp} = \frac{dln(\phi)}{dp} \tag{2-9}$$

where, k is the rock compressibility
ϕ is the porosity of the porous medium
p is the overall reservoir pressure

2.5.2 Permeability, K

The permeability is the basic flow property of a porous medium and measures its ability to transmit a single fluid when the void space is completely filled with this fluid. The precise definition of the permeability K is the proportionality factor between the flow rate and an applied pressure or potential gradient.

$$\vec{u} = -\frac{K}{\eta}\nabla\phi \tag{2-10}$$

where η is the fluid viscosity and $\vec{u}$ is the superficial velocity, i.e., the flow rate divided by the cross-sectional area perpendicular to the flow.

The permeability is a function of porosity and assuming a laminar flow (low Reynolds numbers) in a set of capillary tubes, one can derive the Carman–Kozeny relation,

$$K = \frac{1}{8\tau A_v^2}\frac{\phi^3}{(1-\phi)^2} \tag{2-11}$$

which relates permeability to porosity φ, but also shows that the permeability depends on local rock texture described by tortuosity τ and specific surface area A_v. The tortuosity is defined as the squared ratio of the mean arc-chord length of flow paths, i.e., the ratio between the length of a flow path and the distance between its ends (Lie, 2014).

2.5.3 Critical drawdown for Cylindrical Cavities

A necessary condition for sand production is that the rock is unconsolidated or has been damaged by some other mechanism caused by the effective stresses in the vicinity of the producing cavity. The effective stresses depend on several factors, in particular the far-field in situ stresses, the pore pressure, the geometry of the producing cavity and the rock properties. A criterion for sand failure around a producing opening, caused by the in-situ stresses.

Drawdown, p_d, is used to describe the pressure conditions in the well and is defined as the difference between the pore pressure p_{f0} far from the well and well pressure p_w is given by.

$$p_d = p_{fo} - p_w \tag{2-12}$$

When the well pressure has been reduced such that the well starts to produce sand, critical drawdown p_d^c for sand production in the well has been reached (Fjær et al., 2011).

The condition for shear failure at the wall of a cylindrical hole can be derived from expressions for the stresses at the cavity wall combined with a failure criterion. Consider first the simple case where the effective minor horizontal principal stress (σ_h') is isotropic i.e., principal axes of stress and the principal axis of strain coincides. During production, the pore pressure at the cavity wall with radius, R_c is $p_f(R_c) = p_w$, and the smallest principal stress is,

$$\sigma_\theta(R_c) = 2\sigma_h - p_w - \frac{1 - 2\nu_{fr}}{1 - \nu_{fr}}\alpha\left(p_{f0} - p_f(R_c)\right) \tag{2-13}$$

Failure according to the Mohr–Coulomb failure criterion, requires that,

$$\sigma_\theta(R_c) - p_f(R_c) = C_0 - \left[\!\left[(\sigma]\!\right]_r(R_c) - p_f(R_c)\right) tan^2\beta \tag{2-14}$$

Solution of these equations in terms of p_w gives the lower well pressure limit $p_{w,min}$ failure is initiated. Critical drawdown p_d^c for the cavity is defined as,

$$p_d^c = p_{fo} - p_{w,min} \tag{2-15}$$

Assuming that the rock is sufficiently soft so that the Biot constant α ~ 1, the solution of Eqs. (2-13) and (2-14) can be expressed as:

$$p_d^c = \left(1 - \nu_{fr}\right)(C_0 - 2\sigma_h') \tag{2-16}$$

Figure 2-7 illustrates the shear failure criterion Equation (2-15) graphically of a characteristic relationship between critical drawdown p_d^c and uniaxial compressive strength C_0 for a cylindrical cavity.

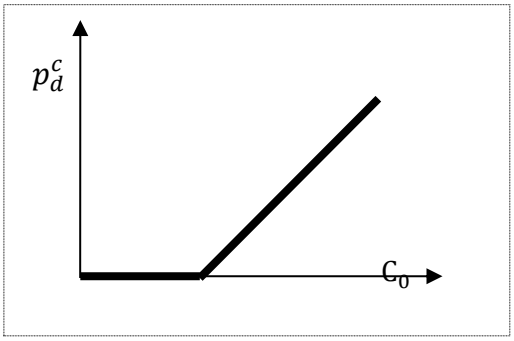

Figure 2-7: Characteristic relationship for a cylindrical cavity

The simplistic model shows that minimum formation strength is required in order to prevent rock failure during production. It also shows that the critical drawdown depends on the effective stresses far from the well, such a way when the reservoir depletes, the far-field fluid pressure p_{fo} is reduced. The implication is the probability for sand production increases as the reservoir is produces under constant drawdown.

Apart from shear failure, another failure mechanism to be considered is tensile failure. At the cavity wall, the radial stress, σ_r and the pore pressure, p_p are both equal to the well pressure, p_w implying that the effective radial stress is zero at the cavity wall (Fjær et al., 2011).

An increasing pore pressure gradient becoming larger than the radial stress gradient at the cavity wall, will cause the effective radial stress to be negative and provides a precursor for a minimum criterion for tensile failure inside the cavity wall.

$$\left.\frac{\partial p_f}{\partial r}\right|_{r=R_c} > \left.\frac{\partial \sigma_r}{\partial r}\right|_{r=R_c} \tag{2-17}$$

If the tensile strength is larger than zero, this criterion may not be sufficient for tensile failure to occur (N Morita and Whitfill, 1989). The normalized drawdown pressure gradient g_{pn} is defined as,

$$g_{pn} = R_c \left.\frac{\partial p_f}{\partial r}\right|_{r=R_c} \tag{2-18}$$

where R_c is the radius of the cavity. The critical drawdown pressure gradient g_{pn}^c is the largest possible normalized drawdown pressure gradient without sand failure.

$$g_{pn}^c = R_c \frac{\partial \sigma_r}{\partial r}\bigg|_{r=R_c} \tag{2-19}$$

Consider the simple case of a cylindrical cavity in a formation where the stress is isotropic. Assuming $R_o \gg R_w$ and $\sigma_{ro} \gg \sigma_h$ the radial stress equation simplifies to

$$\sigma_r = \left(1 - \frac{R_w^2}{r^2}\right)\sigma_h + \frac{R_w^2}{r^2} p_w + \frac{2\eta}{r^2}\int_{R_W}^{r} r' \, \Delta p_f(r') dr' \tag{2-20}$$

Taking the derivative with respect to r we find that the critical drawdown pressure gradient is given as,

$$g_{pn}^c = 2\left[\sigma_h - p_w - (p_{fo} - p_w)\alpha \frac{1 - 2v_{fr}}{2(1 - v_{fr})}\right] \tag{2-21}$$

Drawdown and pore pressure gradient are the two criteria which limit the range for sand free production. The conditions illustrated graphically in Figure 2-8 is the elementary version of a sand production stability diagram (N Morita and Whitfill, 1989).

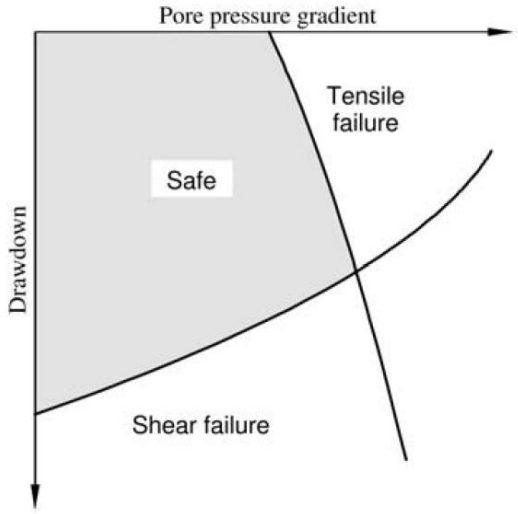

Figure 2-8: Stability diagram for production cavities.

2.5.4 Sand Arches

Sand production has been associated with a phenomenon known as sand arching. Granular grains such as those from the well's formation material grains become interlocked through friction and cohesive forces that creates an arch shaped structure as depicted in Figure 2-9 and is able that to provide enough resistance to withhold forces due to mechanical and hydrodynamic stresses.

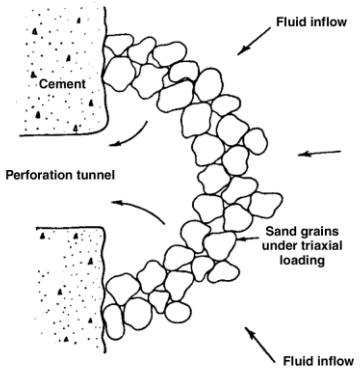

Figure 2-9: Establishment of sand arch at the wellbore

Sand arching experiments were conducted with unconsolidated sand which provided the underlying principles of sand arch formation, stabilization, and failure where it was observed the possibility of maintaining sand arches (Bratli and Risnes, 1981; Hall and Harrisberger, 1970). Sand arches may be formed when damaged rock or loose sand is pushed towards the small, perforated holes in the casing. Moreover, rocks that have been severely damaged can form a sand arch around a cavity assisted by capillary forces. The collapse and reforming of sand arches in the perforation cavity under increasing fluid gradient were studied and observed (Bratli and Risnes, 1981). Sand arch failure can occur due to a different mechanism driven by tensile failure on the face of the cavity. The only parameter that depends on the fluid flow is the pore pressure gradient. If permeability reduction occurs due to fines migration, the pore pressure gradient increases and tensile failure is more likely to happen.

Although unconsolidated or damaged rock is a necessary condition, but it is not necessarily a sufficient condition for sand production. Damaged rock could form stable sand arches that allow for sand free production at significantly higher drawdowns contrary to that determined by rock failure conditions. However, on exceeding the stability limit for the sand arches, sand will be produced into the well through the perforation tunnel into the wellbore (Fjær et al., 2011).

2.6 Sand Production Prediction Techniques

2.6.1 Rock Mechanics Parameters

It is important that the parameters pertaining to rock mechanics are identified so that the interactive nature amongst the parameters can be studied and results can be correlated to the onset of sand production and in the relative and absolute quantification of volumetric sand rates. Table 2-2 list a summary of the work that has been carried out on the various parameter to substantiate the underlying modelling techniques that have been adopted in the production of formation sand (Khamehchi, Kivi, and Akbari, 2014).

Table 2-2: Parameters causing breakaway of formation sand

Rock Mechanics Parameters	Literature
In-situ stresses, drawdown pressure, flow rate of different fluids from reservoir to the well, strength and mechanical properties of the reservoir rock, perforation density, fluid density and reservoir pressure.	Veeken et al., 1991; Ghalambor and Asadi, 2002; Weissenburger et al.,1987.
Reservoir permeability	Veeken et al., 1991; Morita et al., 1989.
Perforation depth	Veeken et al., 1991; Ghalambor and Asadi, 2002.
Reservoir thickness	Veeken et al., 1991; Han et al., 2011.

Rock Mechanics Parameters	Literature
Wellbore inclination	Veeken et al., 1991; Weissenburger et al., 1987.
Shale volume and porosity	Ghalambor and Asadi, 2002.
With sufficiently large flowrate, tensile net stresses can be induced in the surrounding formation and cause sand tensile failure	(Nouri et al., 2006; Weingarten and Perkins, 1995).
Increase in in-situ stress and drawdown causes increase in shear stresses. If the shear stress increases to the point that the formation generally fails in shear (i.e., a function of the reservoir rock properties), weakly cemented rock may become disaggregated	Morrica et al., 1994; Weingarten and Perkins, 1995.
Compaction effect of the net overburden stress	Morrica et al., 1994.
Presence of large volume of low permeability shales in the bulk rock may increase rock strength and decrease flow rates which consequently lowers the probability of sand production in shaly sands	Ghalambor and Asadi, 2002.
Water inflow into a hydrocarbon bearing may cause changes in relative permeability or weakening the overall strength of the rock	Nouri et al., 2006.
Chemical interactions may also occur between the water and the rock cementation and affect the sand production	Weingarten and Perkins, 1995.
Destruction of capillary induced cohesion between the grains due to increase of water saturation	Nouri et al., 2006; Han and Dusseault, 2002.
Presence of water enhances the sand production severity if sand production is already underway.	Morrica et al., 1994.

Fundamental research work has been carried out by various researchers on the key parameters in the field of rock mechanics. The outcome of the research is to predict if sand production will occur in the early life of a well and it is primarily used in the field development planning stage. Based on these parameters, well design would include downhole

sand control in which case gravel packs and screens will be part of the well design. Key risk decisions are made on these assumptions of these rock mechanics parameters and carry a high degree of uncertainty and will invariably increase the cost of the well design.

2.6.2 Sanding Criteria

The criteria for sand production is based on the premise that sand arches are formed in the cavity closed to the well bore, and that these arches can collapse and when subjected to axial and radial stresses and strains. The sanding criteria in Table 2-3 provides a summary of the work in the literature (Azad, Zargar, Arabjamaloei, Hamzei, and Ekramzadeh, 2011).

Table 2-3: Sanding criteria resposible for release of fomation sand

Sanding Criteria	Literature
Shear and tensile failure	(Antheunis et al., 1976; Bratli and Risnes, 1981; Perkins and Weingarten, 1988; Morita, Whitfill, Fedde, et al., 1989; Morita, Whitfille, Massie, et al., 1989; Van den Hoek et al., 1996)
Critical pressure gradient criteria	(Risnes et al., 1982; Morita, Whitfill, Fedde, et al., 1989; Morita, Whitfille, Massie, et al., 1989; Weingarten and Perkins, 1992)
Critical plastic deformation	(Morita and Fuh, 1998)
Erosion base	(Philips and Whitt, 1986; Tronvoll et al., 1992, 1997; Papamichos and Malmanger, 1999)
Mechanisms include drawdown, draw-down rate (ramp-up strategy), depletion, flow rate, water-cut, completion strategy (e.g., size, phasing, and orientation of	(Nouri, Vaziri, Kuru, and Islam, 2006)

Sanding Criteria	Literature
perforations) and frequency of shut-downs and start-ups.	
Effect of water breakthrough	(Han and Dusseaut, 2002; Vaziri et al., 2002, 2004)

Based on the understanding of rock mechanics parameters, various models were built and the criteria for formation sand to be released into the well bore were carried out. Shear and tensile stresses within the reservoir lend themselves in the understanding of the sand production. The effect of water breakthrough in the later life of the well, drawdown, flowrate, amongst other criteria were better understood. However, all these are based on experimental, numerical and analytical methods with assumptions made for the parameters based on rock mechanics.

2.7 Sand Erosion Prediction Tool

The new DNV Recommended Practice O501 (DNV, 1999) provides valuable tools for dimensioning of piping systems and components, optimisation of production, and inspection and maintenance planning. The DNV erosion model calculates erosion rates using real time data such as sand signal, flow, temperature and pressure and additional information based on statistical and historical data. Data from both intrusive and non-intrusive sand probes, depending on the principle of operation, has to be fed into a sand erosion prediction for sand and erosion rates to be calculated.

Feedforward back-propagation network (BPN) and the generalized regression neural network (GRNN) architectures to predict important sanding indication parameters for gas wells (Kanj & Abousleiman, 1999) was carried out using data available in the public domain data has been devised and validated. The neural network system took the following inputs for the wells; total vertical depth, transit time, formation cohesive strength,

water and gas rates, drawdown pressure, original static reservoir pressure, effective overburden stress, interval length, and perforation density.

Neural networks have been applied to obtain real-time and well-specific grain-size distributions to improve gravel-pack design and achieve optimum sand control (Faga and Oyeneyin, 2000). Neural networks have been applied with success to predict grain-size distributions from well logs.

An intelligent sand management strategy (Oyeneyin, Macleod, Oluyemi, & Onukwu, 2005) is a key enabler to reliable sand prediction. The work provided a straightforward way of integrating real-time data into a reservoir-management process, and its methodology implies how to gain value from the information provided by a continuous data stream. Sand production could be a transient phenomenon, and needs to be given constant attention, to detect catastrophic downhole sand failures that would have adverse economic effects on the production of oil and gas.

The need to optimise production is no longer an option and oil companies invest hugely to ensure that continuous and real-time data from the wells are being transmitted from intelligent wells and sensors. Neural network learns from the data gathered and detects underlying relationships, and once this has been established the neural networks can be used for predictive data mining such as predicting sand production (Oberwinkler & Stundner, 2005) to prevent equipment from being damaged to avert production deferment. Early detection of the onset of sand production through the predictive data mining give operators ample time to cut-back production which effectively reduces the velocities of the abrasive sand particles.

Sand production prediction has traditionally been looked at the design stage by well and reservoir engineers in deciding as to the requirements of application of the appropriate sand control technology. In this respect, it belongs to the realm of the sub-surface engineering community. Rock mechanics is the theoretical and applied science of the mechanical

behaviour of rock and rock masses; it is that branch of mechanics concerned with the response of rock and rock masses to the force fields of their physical environment (Jaeger, Cook, and Zimmerman, 2009).

A predictive tool that forecasts the drawdown associated with the onset of sanding as well as it predicts the sanding rate in real time in which the model simulated the interaction between fluid flow and mechanical deformation of the medium in predicting sand production (Nouri, Vaziri, Belhaj, and Islam, 2004).

In a recent work (Oluyemi, Oyeneyin, & Macleod, 2010), unconfined compressive strength (UCS) was identified as a key parameter required for the evaluation and analysis of sanding potential of any reservoir formation and the choice of neural network was due to its ability to better resolve the widely known complex relationship between petrophysical, textural and geo-mechanical strength parameters. Field-life sanding potential evaluation and analysis of reservoir formations throughout the life cycle of the well is therefore necessary so that important reservoir/field management decisions regarding sand control deployment can be made. The real-time functionality of the model data was assured by the real-time data gathering via logging while drilling (LWD) and other was measurement while drilling (MWD) tools.

2.8 Performance Comparison of Sand Production Prediction Techniques

When dealing with sand production, there are essentially two approaches that are adopted. A pro-active event-driven approach is to predict when the sand arch collapses causing formation sand to leave the wellbore into the tubing before it causes detrimental damage to the equipment on the surface facilities. The other approach is what follows after the sanding threshold has been surpassed, and formation sand is produced with the entrained fluid into the production facilities. The volumetric sand rate is of concern so as to ensure that the production separators are not filled with

sand and cause detrimental damage to equipment. Table 2-4 shows the limitations associated with sand quantification (Azad et al., 2011).

Table 2-4: Two general approaches adopted with sand productions

Approach	Literature	Benefit	Limitations
Onset Prediction: Predict the onset of sand production or sanding	Risnes et al., 1982; Morita, Whitfill, Fedde, et al., 1989; Morita, Whitfill, Massie, et al., 1989; Veeken et al., 1991; Weingarten and Perkins, 1992; Kessler et al., 1993; Sanfilippo et al., 1995; Wang and Dusseault, 1996.	Reduce damages associated with sand production	Simplicity of sanding criteria used in these models reduce their efficiency and accuracy
Quantification: Quantify volumetric sand production in terms of rate and cumulative amount of produced sand after threshold of sanding is surpassed	Papamichos and Malmanger, 1999; Papamichos, 2002; Vaziri et al., 2002; Willson et al., 2002; Nouri et al., 2003, 2004; Van den Hoek and Geilikman, 2003, 2005.	Ability to determine if sand production can be handled at the surface. Decide on application of sand control.	# Lack of dedicated sand production field data such as sand influx tests, discrepancies in production-related field data, experimental laboratory tests performed on relatively small samples. # uncertainty in the calculation of the cumulative amount and concentration of produced sand # scarcity of data regarding the amount of produced sand

2.8.1 Review of Sand Production Prediction Models

Most of these models are based on the continuum assumption, while a few have recently been developed based on discrete element model. Some models are only capable of assessing the conditions that lead to the onset of sanding, while others are capable of making volumetric predictions. Some models use analytical formulae, particularly those for estimating the onset of sanding while others use numerical models, particularly in calculating sanding rate. Although major improvements have been achieved in the past decade, sanding tools are still unable to predict the sand mass and the rate of sanding for all field problems in a reliable form.

The new DNV Recommended Practice O501 (DNV, 1999) provides valuable tools for dimensioning of piping systems and components, optimisation of production, and inspection and maintenance planning. The DNV erosion model calculates erosion rates using real time data such as sand signal, flow, temperature and pressure and additional information based on statistical and historical data. Data from both intrusive and non-intrusive sand probes, depending on the principle of operation, has to be fed into a sand erosion prediction for sand and erosion rates to be calculated.

A predictive tool that forecasts the drawdown associated with the onset of sanding as well as it predicts the sanding rate in real time in which the model simulated the interaction between fluid flow and mechanical deformation of the medium in predicting sand production (Nouri et al., 2004).

An intelligent sand management strategy (Oyeneyin, Macleod, Oluyemi, & Onukwu, 2005) is a key enabler to reliable sand prediction. The work provided a straightforward way of integrating real-time data into a reservoir-management process, and its methodology implies how to gain value from the information provided by a continuous data stream. Sand

production could be a transient phenomenon, and needs to be given constant attention, to detect catastrophic downhole sand failures that would have adverse economic effects on the production of oil and gas.

Sand production prediction has traditionally been looked at the design stage by well and reservoir engineers in deciding as to the requirements of application of the appropriate sand control technology. In this respect, it belongs to the realm of the sub-surface engineering community. Rock mechanics is the theoretical and applied science of the mechanical behaviour of rock and rock masses; it is that branch of mechanics concerned with the response of rock and rock masses to the force fields of their physical environment (Jaeger et al., 2009).

Numerical models are by far the most powerful tools for predicting sand production. Numerical methods in the mechanical modeling are categorized under continuum, discontinuum and a combination of the two or hybrid approaches. Several mechanisms are recognized as responsible for sand production. They are mainly based on shear and tensile failure, critical pressure gradient, critical drawdown pressure, critical plastic strain, and erosion criteria (Rahmati et al., 2013).

Different models have used and are representative of the work that has been carried out to address the two general approaches to production of formation sand from the wellbore. Table 2-5 summarises the key benefits and limitations of the different techniques that have widely used (Khamehchi et al., 2014).

Table 2-5: Benefits/limitations of techniques of sanding models

Technique	Literature	Benefits	Limitations
Field observation Methods: One-parameter, two-parameter,	(Nobuo Morita, 1994; Veeken, Davies, Kenter, and Kooijman, 1991)	Increase in the resolution of determining the possibility of sand production.	Comprehensive field data required and may not respond in all cases.

Technique	Literature	Benefits	Limitations
and multi-parameter correlations are three categories			
Physical model testing:	(Nouri et al., 2006; Papamichos, Cerasi, and Stenebråten, 2010; Rodrigues, Cobbold, and Løseth, 2009; Vaziri, Phillips, and Hurley, 1997; Xiao and Vaziri, 2011)	# Able to predict the onset of sand production. # Complicated models can quantify sand rates.	# Time consuming and expensive. #Limitation of size of laboratories and results are influenced by boundary effects.
Numerical methods:	(Ashoori, Abdideh, Hayavi, and Branch, 2014; Climent, Arroyo, Gens, and Sullivan, 2014; Han, 2014; Ju, 2014; N Morita and Whitfill, 1989; Solnordal, Wong, and Boulanger, 2015; Wang, Wan, Settari, and Walters, 2005)	# Capability of handling complex situations with different boundary conditions, different constitutive laws and materials, and time-dependent parameters. # Models provide comprehensive tools for determining the impact of different factors in sanding to provide a deeper insight. # Powerful and exact approaches.	# Computationally demanding and complexity in setting-up and running simulations, high costs and demands for input data that are not routinely measured. # Calibration of these models demands a complete series of laboratory experiments to increase the exactness of the methods. # Requires a complete set of data incorporating the massive experiments.
Theoretical	(Biot, 1941; Hoek et	Simple and	Less efficient

Technique	Literature	Benefits	Limitations
sanding onset prediction methods:	al., 2000; Tengattini and Einav, 2015)	easy-to-use and are the most beneficial methods for quick sand control decision is necessary.	and accurate due to simplicity of sanding criteria.
Analytical models:	(Al-Shaaibi, Al-Ajmi, and Al-Wahaibi, 2013; Araujo Guerrero et al., 2014; Hoek et al., 2000; Horsrud, Risnes, and Bratli, 1982; Jo and Gray, 2010; N Morita, Whitfill, Fedde, and Levik, 1989; Ranjith, Perera, Perera, Wu, and Choi, 2013; Younessi, Rasouli, and Wu, 2013)	Same set of governing equations. Models based on shear failure criteria and models based on tensile failure criteria.	Single mechanism of sanding and under over-simplified geometrical and boundary conditions of the actual complicated field-scale problems.
Artificial Neural Networks:	(Adibifard, Tabatabaei-Nejad, and Khodapanah, 2014; Aifa, 2014; Aïfa, 2014; Azad et al., 2011; Chaki, Verma, Routray, Mohanty, and Jenamani, 2014; Irani and Nasimi, 2011; Jahanandish, Salimifard, and Jalalifar, 2011; Kamari, Bahadori, Mohammadi, and Zendehboudi, 2014; Mazen Kanj and Abousleiman, 1999; MY Kanj and Roegiers, 1998; Khamehchi et al., 2014; Oluyemi, Oyeneyin, and Macleod, 2010; Shokooh Saljooghi and Hezarkhani,	# Easiness of analytical models and the exactness of numerical methods. # Reduced complexity and hardship accompanied by numerical methods. # Simplicity associated with analytical methods. # ANN can simulate highly non-linear functions and can be trained to accurately predict new	# Need for real, precise, and illustrative main parameters affecting sand as inputs to the network. # Possibility of getting trapped in local minimas, leading to unreliable predictions.

Technique	Literature	Benefits	Limitations
	2015; YIlmaz and Yuksek, 2008)	data. # Data-driven model and more flexibility for self-adjustment to adapt various ranges of data. #Does not require any previous assumption about complex mechanical behavior of the rock and failure mechanisms.	

From Table 2-5, the benefits of employing neural networks for the purposes of prediction of reservoir properties, sand production, etc far outweighs the limitations associated with the technique.

2.8.2 Review of Neural Networks in Sand Production Predictions

The notion of Artificial Neural Networks (ANN) first appeared in the work of McCulloch and Pitts (McCulloch and Pitts, 1943). As a psychiatrist, McCulloch developed logical representations of the nervous system. From biology, they concluded that difficult computational tasks could be performed with only simple structural components, known as neurons. For example, the human brain can perform complex information processing such as speech and pattern recognition much faster than ordinary serial computers. Since the brain's biochemical connections are a lot slower than the computer's electronic circuits, it must mean that a neural network such as the human brain is a nonlinear and parallel computer. A neuron consists of a cell that will process synaptic inputs and produce an output that in turn can be used as input to other neurons. Each neuron performs only the

simple task of a weighted summation of the inputs and outputs the sum transformed by an activation function. The interconnections between neurons, the synapses, are subject to modification through learning processes. Neural networks, both biological and artificial, adapts through learning processes. Through interaction with the environment, the neural network adapts its synaptic strengths to perform a specific task. This is referred to as learning. Various methods for learning have been proposed; the first from studies of the learning of biological neural networks. Hebb postulates what was later to be known as Hebbian learning, based on the observation that the connection between two neurons is strengthened if the two neurons are activated simultaneously (White, 1992). Many different structures of neural networks were developed in the following period, some more applicable to engineering problems than others. Associative memories and self-organizing maps are two examples.

A synopsis was written of the areas of petroleum technology in which neural networks have been used with success, and other potential areas of application including examples on seismic pattern recognition, permeability predictions, identification of sandstone lithofacies, drill bit diagnosis and analysis and improvement of gas well production (Ali, 1994). There is undeniably a learning curve of a purely practical nature, involved in understanding what neural networks are, its operations and their benefits. The synopsis reflects a practical focus on the application of neural networks in the petroleum industry.

A prototype feedforward neural net structure with five elements characterizing the particular well, its formation, and the reservoir namely; porosity, clay content, formation age and condition, oil API gravity and drawdown pressure to predict the tendency of the well to produce sand with a robust performance. The use of the neural approach to predicts sanding onset is a good example of the multi parameter correlations,

although establishing such correlations requires a comprehensive field data base (MY Kanj and Roegiers, 1998).

Feedforward back-propagation network (BPN) and the generalized regression neural network (GRNN) architectures to predict important sanding indication parameters for gas wells was carried out using data available in the public domain data has been devised and validated (MY Kanj and Abousleiman, 1999). The neural network system took the following inputs for the wells; total vertical depth, transit time, formation cohesive strength, water and gas rates, drawdown pressure, original static reservoir pressure, effective overburden stress, interval length, and perforation density.

Feedforward back-propagation network (BPN) and the generalized regression neural network (GRNN) architectures to predict important sanding indication parameters for gas wells (Kanj & Abousleiman, 1999) was carried out using data available in the public domain data has been devised and validated. The neural network system took the following inputs for the wells; total vertical depth, transit time, formation cohesive strength, water and gas rates, drawdown pressure, original static reservoir pressure, effective overburden stress, interval length, and perforation density.

Accuracy of artificial neural network has been used to determine functional relationships between reservoir parameters and seismic data. The accuracy of ANN was carried by dimensionally reducing the input data and estimated by the k-fold estimation method (Aminzadeh, Barhen, Glover, and Toomarian, 2000).

Neural networks have been applied to obtain real-time and well-specific grain-size distributions to improve gravel-pack design and achieve optimum sand control (Faga and Oyeneyin, 2000). Neural networks have been applied with success to predict grain-size distributions from well logs.

An artificial neural network (ANN) has been developed as a tool to evaluate and optimize stimulation methods and to develop a prediction model for enhancing the production opportunities of the oil and gas (McNichol, Getzlaf, and Protz, 2001). It further re-iterates the point that although vast amount of data is available within the industry, the need to analyze data to enhance the ability to improve well economics and to predict well formation.

Modular artificial neural network system has been implemented successfully in predicting directly from well logs the partial saturation hydrocarbon fluids (oil, water, gas). Density, sonic, resistivity and neutron porosity logs were used as inputs with an optimal 4-4-1 Neural Network architecture (Helle and Bhatt, 2002).

Neural network learns from the data gathered and detects underlying relationships, and once this has been established the neural networks can be used for predictive data mining such as predicting sand production to prevent equipment from being damaged to avert production deferment (Oberwinkler and Stundner, 2004). Early detection of the onset of sand production through the predictive data mining give operators ample time to cut-back production which effectively reduces the velocities of the abrasive sand particles.

An intelligent sand management strategy is a key enabler to reliable sand prediction (Oyeneyin, Macleod, Oluyemi, and Onukwu, 2005). The work provided a straightforward way of integrating real-time data into a reservoir-management process, and its methodology implies how to gain value from the information provided by a continuous data stream. Sand production could be a transient phenomenon, and needs to be given the constant attention, to detect catastrophic sand failures in the well that would have adverse economic effects on the production of oil and gas.

The need to optimise production is no longer an option and oil companies invest hugely to ensure that continuous and real-time data from the wells are being transmitted from intelligent wells and sensors.

Vast amount of data is readily available and the need to translate data into valuable and quality information to manage depleting oil and gas fields. The need to make value-of-information (VOI) analysis more accessible and useful by discussing its past, present, and future is highlighted and how such decision-making may be deployed in the oil and gas industry (Bratvold, Bickel, and Lohne, 2007).

A neural network system approach was adopted in assessing the probability of a casing collapse and the expected collapse depth for a field that have experienced severe casing collapses. The five input parameters to the neural net were latitude and longitude of the well, total depth of the well, corrosion weight factor, failure time factor and zone factor. It was seen an decision making tool in dictating which fields should be developed in the future (Salehi, Hareland, Dehkordi, Ganji, and Abdollahi, 2009).

Sand production in the entrained fluid is a natural consequence of fluid flow into a wellbore from the reservoir. For fields with high reservoir pressures, the onset of sand production is of little concern. However, the effect of sand transport on pressure drop becomes more pronounced in the late life of reservoir. A model was developed that analysed the significant effect of sand on pressure drop during early and late life of a well that was not previously accurately predicted in existing models (Olufemi & Darlington, 2010). Poorly consolidated reservoirs are susceptible to sand production and tend to increase the pressure drawdown along the well length. It is difficult to measure flow rate for each phase along a wellbore for downhole condition, especially for real time applications. Instead, the measurable parameters such as downhole temperature and pressure are collected and are important information to help in the understanding of the bottom-hole flow condition.

Unconfined compressive strength (UCS) was identified as a key parameter required for the evaluation and analysis of sanding potential of any reservoir formation and the choice of neural network was due to its ability to better resolve the widely known complex relationship between petrophysical, textural and geo-mechanical strength parameters (Oluyemi et al., 2010). Field-life sanding potential evaluation and analysis of reservoir formations throughout the life cycle of the well is therefore necessary so that important reservoir/field management decisions regarding sand control deployment can be made. The real-time functionality of the model data was assured by the real-time data gathering via logging while drilling (LWD) and other was measurement while drilling (MWD) tools.

Artificial neural networks were deployed to assess the strength of the intact rock that were under uni-axial tension to tri-axial compression by predicting the value of major principal stress at failure from uni-axial compressive stress and minor principal stress. Prediction errors were lower compared with empirical techniques and also were more flexible in the predicting major principal stress at failure in the brittle and ductile regimes (Rafiai and Jafari, 2011).

Artificial neural networks could be a technique could be used that has the added benefit of numerical and experimental methods in terms of the accuracy and the simplicity of analytical ones and has been used to predict critical bottomhole flowing pressure that prevent the onset of sand production. The main parameters that were responsible for causing sand production were investigated from field data. To simplify the model, only factors pertaining to production and reservoir characters, and formation and strength characters were considered while the completion characters were omitted. Inputs to the model included unconfined compressive strength, overburden and horizontal stresses, critical depths, transit time and reservoir pressure to predict a critical drawdown pressure The model

was subsequently evaluated against credible analytical models and it is reported that it has a high degree of accuracy in predicting the onset of sand production (Azad et al., 2011).

A neural network workflow, which provides a systematic approach for tackling various problems in reservoir engineering where an ANN model was developed for water saturation prediction in a petroleum field based on wireline logs. The ANN established the complex nonlinear relationship between wireline logs and core saturation data (Al-Bulushi, King, Blunt, and Kraaijveld, 2012).

A novel method using ANN was reported for sand production prediction. Sand prediction techniques based on field experiences rely on establishing a correlation between sand production well data and field/operational parameters. The immediate advantage of applying ANN as it eliminates the necessity of assumption about complex mechanical behaviour of the rock and failure mechanisms in order to construct reliable and accurate models. Subsequent study developed ANN in a three-stage process to simulate the complex relation between parameters critical total drawdown and all technical as an indication of the onset of sand production. The technical parameters identified were total vertical depth, effective overburden vertical stress, transit time and cohesive strength. (Khamehchi et al., 2014).

Porosity is one of the most important parameters of the hydrocarbon reservoirs, the accurate knowledge of which allows petroleum engineers to have adequate tools to evaluate and minimize the risk and uncertainty in the exploration and production of oil and gas reservoirs. Applying an efficient method that can model porosity is important and ANN has been explored in this field. Changes in relative permeability or weakening of the overall strength of the rock as a result of water flow into the hydrocarbon bearing rocks may cause chemical interactions to occur between water and rock cementation and may affect the sand production (Aïfa, 2014).

In a recent comprehensive study on sand production, a practical sand production model was developed to estimate amount and rate of sand produced was conducted. In the study, a sand production quantification model was developed by correlating the critical plastic volume obtained from the numerical modelling with the cumulative amount of sand produced from sanding experiments. It was found that in weakly-consolidated and consolidated sandstones, sanding rate decreased rapidly with time and would cease once the failed materials transportable by fluid flow had been produced under given drawdown and stress condition (Wu et al., 2016).

In a recent study, least square support machine (LSSVM) classification approach was published as a novel technique and was applied to identify the conditions under which sand production occurs. The model used the following parameters; true vertical depth, transmit time, cohesive strength of the formation, water and gas flow rates, bottom hole flowing pressure, drawdown pressure, effective overburden stress, shut per foot, and the perforation interval. A mathematical non-linear relationship between the available data considered as the input parameters and the output was an indication that sanding production may occur (Gharagheizi, Mohammadi, Arabloo, and Shokrollahi, 2016).

2.9 Summary

The chapter looked at single and multiphase flow and more specifically at sand erosion in multiphase flow and the use CFD's in modelling of flow profiles. It reviews the equipment and measurement technologies that have been employed in industry for the monitoring and detection of sand production that is caused by formation sand in the reservoir. It looks at the traditional and more conservative methods in the prediction of sand production from an oil and gas reservoir. It also gives an overview of the research activities that have taken place in the industry. A review of the

various techniques was highlighted of current technologies based on physical measurement of the corrosive and erosive effects of sand. An understanding of rock properties is important to appreciate the underlying of critical drawdown pressure and the stability of sand arches in the mechanics of sand production. Prediction techniques of sand production based on the assumptions made around the parameters associated with rock mechanics taking into account the sanding criteria for sand to be produced from the reservoir. Various sand prediction tools are reviewed in the literature and their performance are compared. The chapter concludes with the benefits of neural network-based sand prediction techniques that are not based on rock mechanics parameters and their many assumptions.

These technologies are deployed in a reactive manner at best but more importantly, it requires manual human intervention of the oil and gas wells that have experienced the onset of sand co-production. There is an economical consequence, as these wells need to be shutdown to prevent further damage to the flowlines and their associated flow path components. In the event that the instrumentation fails to detect sand, these wells will continue to produce causing detrimental damage that could result in injury to personnel who are not aware of the hazard. As a result, there is a potential loss of life (PLL) or multiple injuries. It is therefore, expedient that industry take a more proactive approach to monitoring sand production in a more proactive and predictable manner so as to avert production deferment from an economic standpoint, and to avoid catastrophic failures of sand detectors that could potentially injure or take the lives of personnel working in these facilities.

CHAPTER 3

RESEARCH METHODOLOGY & MATERIALS

3.1 Introduction

Most oil and gas wells have measurements of process parameters such as flow and pressure and complex non-linear equations represent the relational change amongst these parameters. The resultant change amongst these parameters indicates the production of formation sand entrained in the production fluids from a particular oil or gas well and will cause sand to be produced or a phenomenon more commonly known as sand production. Sand production has caused detrimental damage to equipment in the oil and gas industry. Sand monitoring devices installed at strategic locations on oil and gas flowlines enable monitoring of the onset of sand production. Due to the highly complex nature of an oil and gas well, and the uncertainties associated with these parameters, the field of artificial intelligence has been successfully employed in the prediction of sand production (Oluyemi et al., 2010). The use of artificial neural networks (ANN) in particular has shown accurate predictions with a high level of confidence. The results from the predictions drive important decision as to reduce the flow of the well by "beaning-back" the well. The more severe cases require that the well be completely closed in. The reduction in flow of an oil and gas well has drastic economic repercussions. A decision tool that can help substantiate in this critical decision-making process is highly invaluable from a business perspective. These process parameters together with a sand monitoring system provide the basis of measurements in realizing a neural network-based sand prediction tool.

The overall research philosophy is depicted in Figure 3-1.

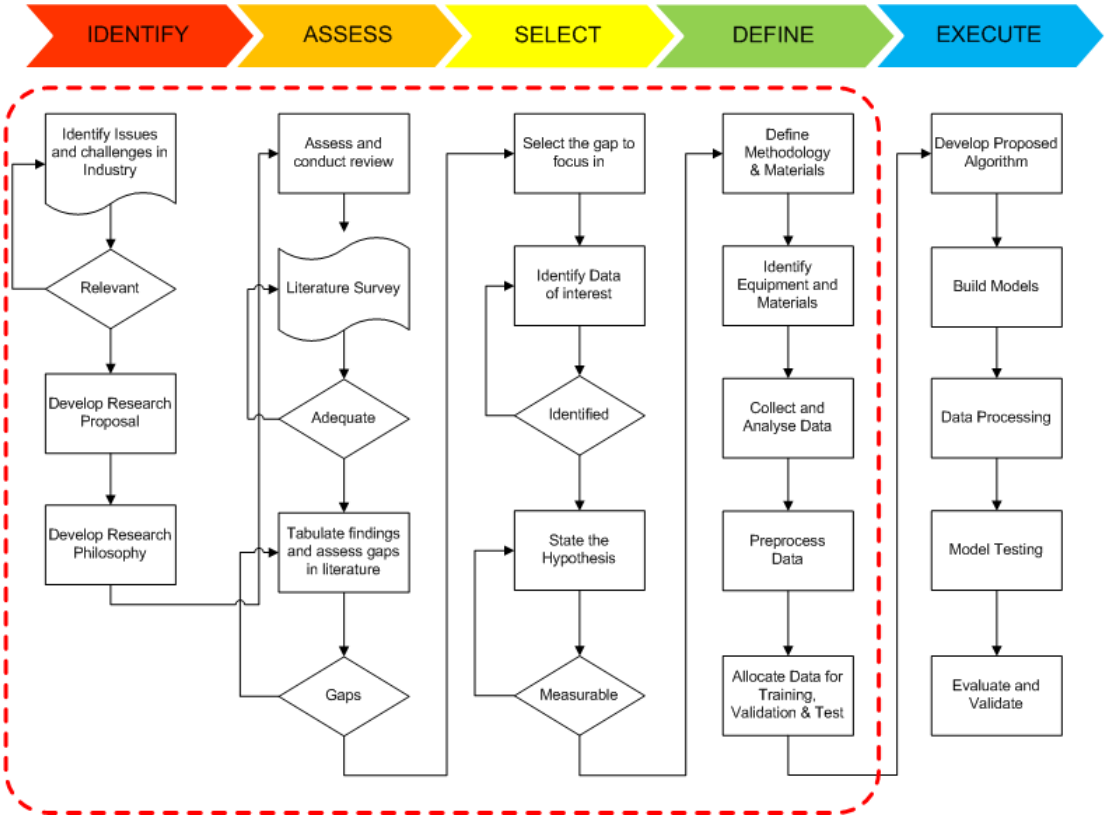

Figure 3-1: Overall Methodology – Relevant Phases within Red Dotted Lines, and without the Execute Phase

3.2 Identify Phase

3.2.1 Identify Area of Increasing Challenges

The issues and challenges facing the oil and gas industry are wide and varied and an area that has been economically impacted is production deferment. Continuous oil and gas production will be heavily interrupted due to reliability of compressors, erosion of valves, corrosion of production tubings, etc. However, an area where production deferment of oil and gas production is an increasing challenge to the industry is the interruption to continual and safe production that is attributed to sand. It continues to be a challenge due to the uncertainties associated with the reservoir of an oil and gas field. Sand production is a result of the collapse of the sand arches. The ability to predict these underlying causes of sand production by

addressing the effects on the flowing bottomhole pressure and the detection of sand by implementing suitable sand measurement technologies contributes towards averting the production deferment. The challenges and approaches in developing the research philosophy is summarised in Table 3-1 below.

Table 3-1: Identify - Approaches to Sand Production Prediction

Item	Description of Item
Causes	Effective stresses in the reservoir contributes towards the collapse of sand arches causing sand to be produced at the surface.
Effects	Flowing bottomhole pressure or the wellbore pressure drops and hence, causing the critical flowing bottomhole pressure (CFBHP) to be reached.
Challenge #1	Measurement of CFBHP is not readily available.
Approach	Derive drawdown from correlated measurement at the surface from available process parameters.
Challenge #2	Various measurement technologies for the monitoring of sand production is available but are reactive in nature, and by then equipment damage would have occurred
Approach	Adopt a suitable measurement technology and assess the suitability for the installation of the sand probe on the flowline

3.3 Assess Phase

3.3.1 Literature Review

Having identified the underlying causes for sand production, the literature is reviewed in the terms of the drawdown aspects for a specific reservoir. The attributes of porosity and permeability of rocks in the reservoir contributes largely to the flow of hydrocarbon fluids towards the wellbore. At the perforations, formation sand in the reservoir gradually builds up to form a sand arch as hydrocarbons flow into the porous medium. With an increase in the stresses and strains in the reservoir, the stable sand arch

will gradually collapse at an unknown time. Upon collapse of the sand arch, disaggregated sand flows through the perforations. Depending on the depth of the perforating zones, the hydrostatic head of the wellbore needs to be exceeded for formation sand to reach the surface at the wellhead. Suitable measurement technologies will detect the sand on the surface. Operator intervention would be required to reduce the flow of the well. The effect of reducing the production flow is to increase the flowing bottomhole pressure (FBHP) which invariably causes the drawdown to reduce. Different sand prediction technologies and techniques are reviewed for the suitability of a sand production prediction system. The gaps are assessed for a reliable prediction system to be realised and how these gaps can be addressed. The literature review structure is shown in Table 3-2.

Table 3-2: Assess - Structure of Literature Review

Review	Description of Review
Drawdown	Production of oil and gas is a result of drawdown which is the differential pressure between the reservoir and the wellbore, for rocks of a given porosity and permeability.
Effect of Formation Sand	Formation sand gradually builds a sand arch near the wellbore as oil flows through the porous medium.
Collapse of Sand Arch	As a result of the increase in stresses and strains in the reservoir, the sand arch collapses and the disaggregated sand flows through the perforations.
Sand Transport	Sand is transported to the surface if it can overcome the hydrostatic head of the wellbore.
Sand Detection	When sand is detected at the surface, the well is beaned back so as to reduce the flow, such that the FBHP increases, causing drawdown to reduce.
Sand prediction system	Reliability of a prediction system for the onset of sand production.
Assess gaps	Findings tabulated and gaps are assessed.

3.4 Select Phase

3.4.1 Gaps Selected

Based on the literature survey, there was no reported work on the prediction of sand production from an oil and gas well based on process measurements on the surface facilities. Furthermore, rigorous modeling efforts have been carried out on the prediction of sand during the design of an oil and gas well. It is appreciated that this is an important aspect of addressing the inherent uncertainties of a reservoir. However, once the well is in its production phase, there were efforts carried out to model the well with parameters based on the reservoir properties. Efforts in model building for sand production prediction in these areas suffer from the assumptions made of these parameters of reservoir properties. The uncertainties attributed to change in reservoir temperature, change in rock properties due to increase in mechanical stresses and strains, etc will affect these mechanistic models. On the other hand, data-driven models using real-time production data do not suffer from those that are based on rock mechanics.

3.4.2 Hypothesis Formulation

In the literature reviewed, the approach undertaken in this Thesis was not reported in any other work to date. There is an anticipated relationship amongst the variables from the correlation of process measurements at the surface at the wellhead and flowlines of oil and gas wells and the critical flowing bottom hole pressure (CFBHP). This has a direct relationship with the drawdown of the well.

An increase in the drawdown of the well will cause disaggregated sand due to untimely collapse of the sand arch to flow to the surface. Disaggregated sand in the entrained fluid will into the flowlines. Sand probes installed in suitable and correct locations along the flowlines will

detect sand in the entrained fluid. The hypothesis is that from the correlations amongst the process measurements at the wellhead, an artificial neural network can predict the onset of sand production in the well bore.

3.4.3 Variables

The presence of variables other than the independent variables will significantly contribute to the causes in predicting the dependent variable. Moreover, the presence or absence of the intervening variable can affect the reliability of the outcome as depicted in Figure 3-2.

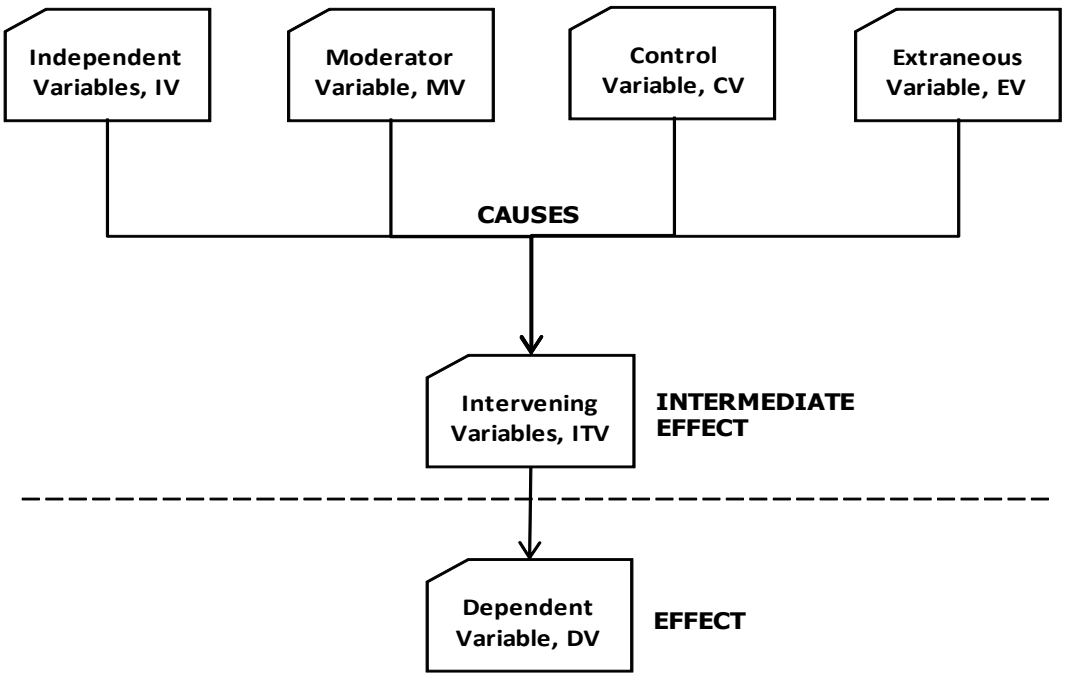

Figure 3-2: Intervening variables affecting the dependent variable

The hypothesis is made testable by providing operational definitions for the variables of the hypothesis in Table 3-3.

Table 3-3: Operarional Definitions for the variables identified

Variable	Measurements	Operational Definitions
Independent variable (IV):	Process Parameters:	Production of oil and gas is a result of drawdown which is the differential pressure

Variable	Measurements	Operational Definitions
		between the reservoir and the wellbore, for rocks of a given porosity and permeability.
Control Variable (CV):	Reservoir/Pore Pressure	Formation damage causing formation sand to gradually builds a sand arch near the wellbore as oil flows through the porous medium.
Extraneous Variable (EV):	Stresses/Strains	Increase in stresses and strains in the reservoir causes the sand arch to collapse and the disaggregated sand flows through the perforations.
Moderator Variable (MV):	FBHP/Well Pressure	Sand flows to the surface if it can overcome the hydrostatic head of the wellbore.
Intervening Variable (IVT):	Rock mechanics parameters COH	Uncontrolled disturbances in the rock structure.
Dependent Variable (DV):	Sand	Sand erosion depletes the sensing elements causing metal loss of a sand erosion probe. Whenever sand is detected at the surface, the well is beaned-back to reduce the flow. The FBHP will increase and cause drawdown to reduce.

It was necessary to extract datasets of the dependent variable from historical records of episodes of sand erosion of the onset of the production of formation sand. Subsequently, the corresponding datasets of the independent variables were extracted from historical records of measurements of process parameters covering the same period when these sand erosion episodes occurred. These corresponding datasets will

establish if a correlation exists between sand erosion/corrosion and measurements of the process parameters.

3.5 Define Phase

3.5.1 Equipment and Materials

In order to obtain the sand measurements from a remote offshore location, a communication infrastructure needs to be in place. This was to ensure that real-time sand measurement is continuously available for the model. Data from the sand probe is stored on the sand logger that is an integral part of the sand probe assembly. The sand logger is connected to the field junction box and data is sent to the field interface unit (FIU) that is located in a non-hazardous area. Depending on the oil and gas platform's communications system, data will be sent through the distributed control system (DCS), remote telemetry unit (RTU) or a modem to the onshore sand monitoring system server.

Information is then sent to the Plant Information (PI) System that populates the historical database. Historical data from PI will be used to build the artificial neural network model. The block diagram of the communication infrastructure is shown in Figure 3-3. Every component along the communication path is monitored to ensure that the system is healthy as indicated by the green boxes.

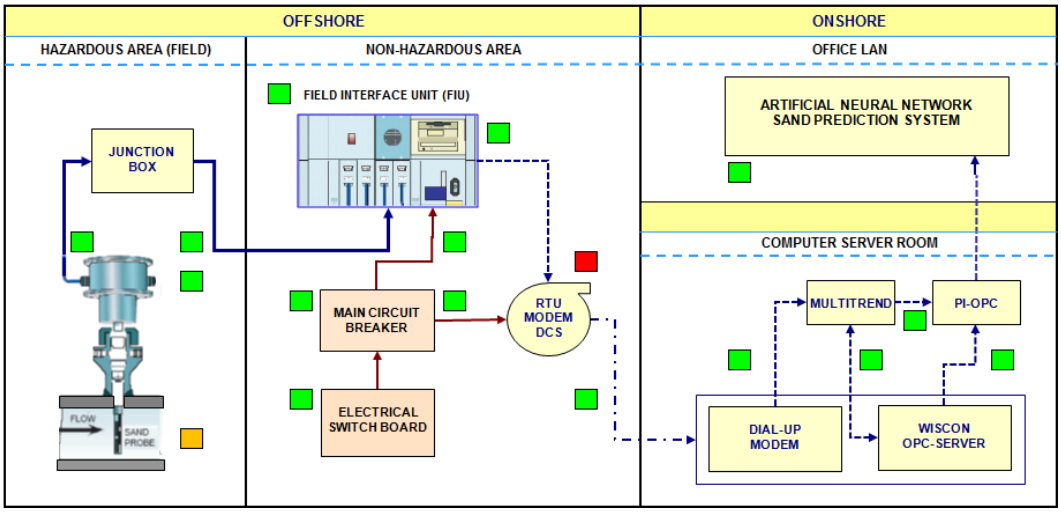

Figure 3-3: Communication flow of sand measurement into the ANN-based Sand Prediction System

3.5.2 Candidate well

The candidate wells were selected based on its historical events of the onset of sand production that have caused detrimental damage to equipment or flowlines. Sand erosion has predominantly caused damage to gas wells rather than oil wells. This is partly due to the higher velocities associated with gas wells. The selection is also based on level of real-time instrumentation that has been installed on the well and the facilities.

3.5.3 Sampling Rate

Erosion is a slow and intermittent process, and the sampling period needs to be determined based on typically between one and two hours. If the sampling period is too frequent, then there will be too much data without any significant change. On the other hand, if the sampling period is less frequent, then a short episode of sand erosion may not be recorded.

3.5.4 Process Measurements

Process parameters of the selected variables need to be measured by suitable and certified process transmitters that are suitable for the oil and

gas industry. These transmitters are typically connected on the Wellhead and Christmas Tree Equipment. Pressure gauges are visible for pressure monitoring. However, real-time measurements are required to be continuously fed into a supervisory control and data acquisition (SCADA) system.

The flowchart may be depicted as in Figure 3-4 for the conceptual aspect of the methodology.

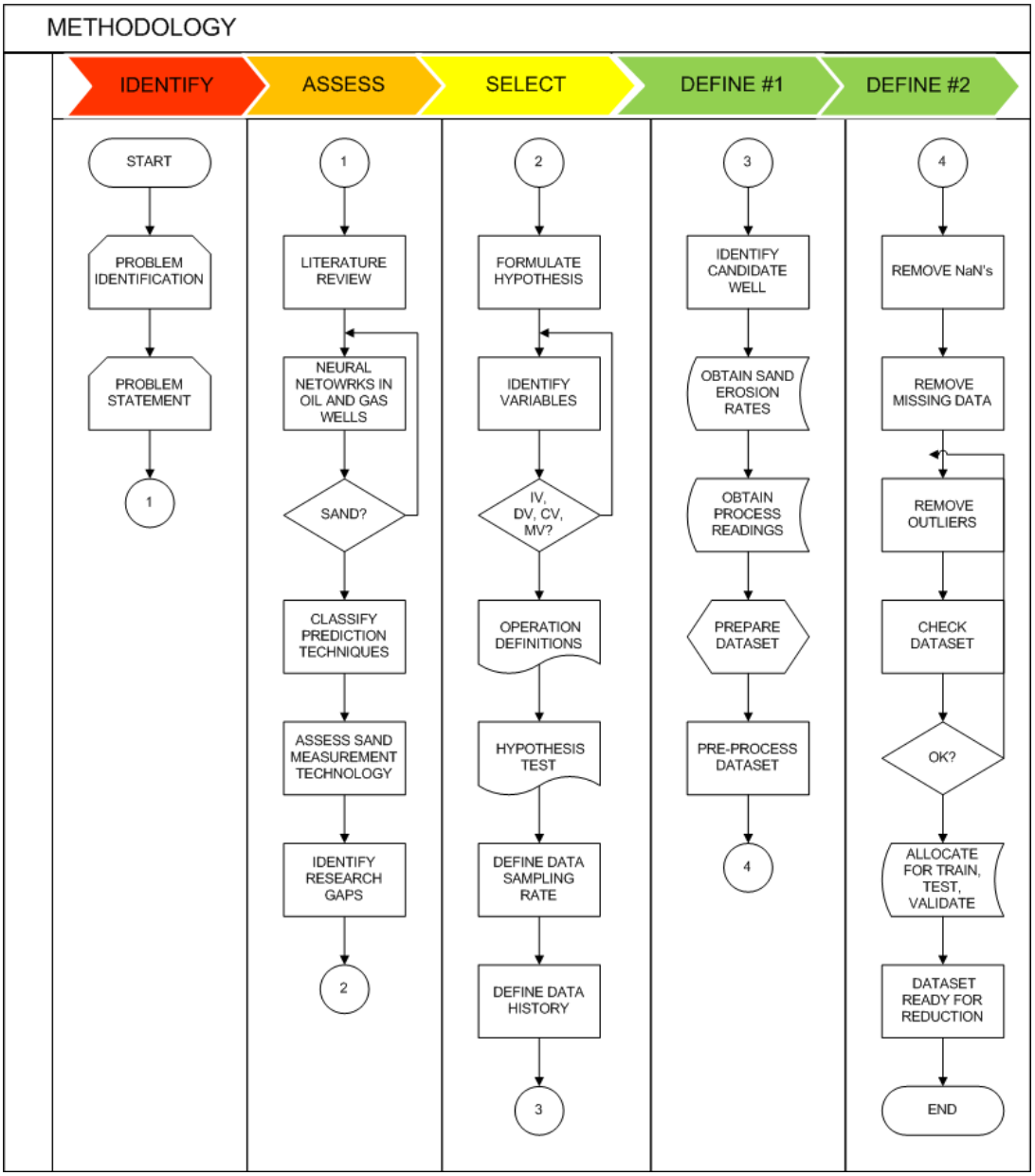

Figure 3-4: Flow Chart of the Methodology - Conceptual

3.6 Summary

In this chapter, the key areas of challenges in the prediction of sand production are identified in terms of the drawdown aspects for a specific reservoir. Based on the literature survey gaps are selected for the research and a hypothesis is formulated on the anticipated relationship amongst the different process variables and the onset of sand production. In order to obtain data from a particular well, a data communication infrastructure for a data-acquisition system needs to be realised to provide real-time process parameters and sand production data. A sampling rate is determined based on the on the historical data available for a specific candidate well. Process measurements from instrumentation from a typical well are recorded and provides the historical information that is required to build a neural network-based sand production prediction model. The thesis has formulated the hypothesis that the onset of sand production can be predicted by a neural network model based on the combination of the measurement of process parameters at the wellhead of a typical oil and gas well. The operational definitions for the identified variables are qualified, while the intervening variable(s) with intermediate effects can significantly affect the accuracy and reliability of the prediction.

CHAPTER 4

PROPOSED ALGORITHM AND DEVELOPMENT

4.1 Introduction

It is expedient that there is a suitable dataset of sufficient size and excitation for neural networks to be adequately trained. Data pre-processing play an important role on any given dataset. Depending on the availability of the data, there is the option of dividing the dataset for training, validation and test subsets. In order to obtain the optimum performance of the neural network, it is necessary that the network be trained by a dataset of optimum size. This will also ensure that the time taken to train the network is optimised.

Neural network training is made more efficient when pre-processing steps are performed on the network inputs and targets. Data obtained from instrumentation in real time will have instances of outliers. There will be instances of unreliable communications that give zero values, and these undesirable data needs to be processed. In some cases, there will be slight changes in the data, and it is prudent to capture information that is suitable for the neural network.

4.2 Execute Phase

In the execute phase, the algorithm is developed and described to realise a sand prediction system. The pre-processed data was further reduced due to their high correlation. The model was selected with neural network architecture defined. The testing of the model and the approach to validate the model were defined to ensure that the model can be improved to overcome overfitting. This is shown in the last stage of the overall methodology in Figure 4-1.

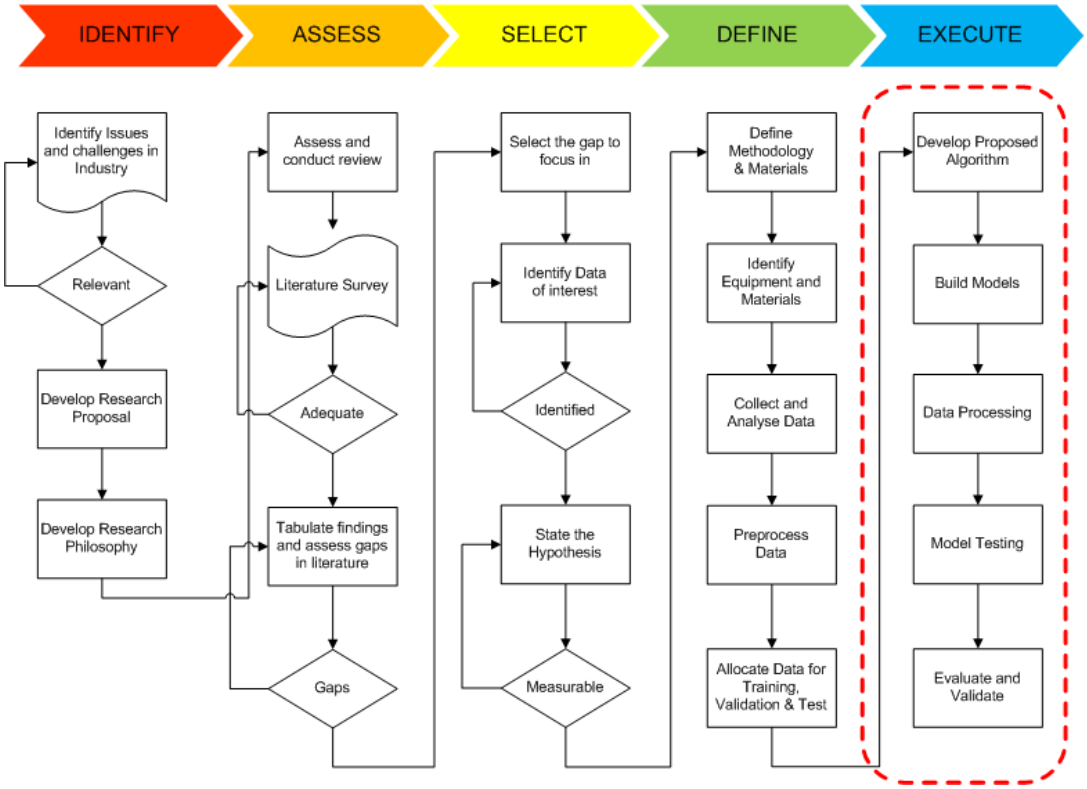

Figure 4-1: Overall Methodology - Execute Phase to Develop the Algorithm

4.2.1 Proposed Algorithm and Description

The process parameters were flow and pressure measurements for a well and these parameters were highly correlated. Hence, the main principal components that are orthogonal to one another will be extracted from the data using principal component analysis. The coefficients of the principal components were used to determine and select process variables that largely contributed to the data.

Based on the hypothesis formulation in the previous chapter, a relationship between the critical flowing bottomhole pressure (CFBHP) and the selected variables will be established. This is associated with the drawdown of the well and invariably contributes towards the production of sand. Given the uncertainties that give rise to the production of sand, any model representing the process will be highly non-linear. Regression analysis that is typically used in linear systems was used to exhibit the highly non-linear nature of the process of the production of sand in the

entrained fluids during the normal production of oil and gas from the reservoir. Principal component regression (PCR) and partial least squares regression were both employed to test for correlation. A suitable neural network was employed to establish the non-linear relationship.

It is not sufficient that the error margin be small in prediction, but it is also important that the predictions fall within an acceptable level of confidence. Statistically, a 95% level of confidence is generally accepted and was adopted in the validation of the prediction. Overfitting is a phenomenon whereby a neural network has memorised the data and it is not able to perform when introduced with new data. A neural network-based auto-regressive with exogenous inputs (NNARX) will typically have past inputs and outputs that are fed into the regression vector. With only three to four input variables, the regression vector with four past inputs [e.g., u(t-1),……u(t-4)] and four past outputs [e.g., y(t-1),……y(t-4)], the NNARX model would be required to accommodate 16 inputs to 20 inputs, respectively. Therefore, in order to overcome the overfitting issue, pruning was deployed to reduce the number of weights connecting to and from the neurons in the hidden layer. The approach adopted is shown in Table 4-1 below.

Table 4-1: Algorithm Development

Approach	Description of Approach
1	Since the measurements were highly correlated, apply principal component analysis.
2	Carry out a correlation between the derived drawdown from the process measurements and the sand erosion loss to indicate the onset of sand production.
3	Carry out regression analysis to describe the correlations between the variables and a neural network was employed.
4	Deploy a Neural Network-based auto-regressive with exogenous inputs (NNARX) model to establish a correlation.

Approach	Description of Approach
5	Determine the number of regressors in the NNARX structure for the past inputs and past outputs based on the Lipschitz Quotient.
6	Determine the number of neurons in the hidden layer are based on rules of thumb i.e., size of input layer, 2x's size of input layer, etc
7	Employ pruning was employed to improve the performance of the prediction within the 95% confidence limit.

The proposed algorithm is depicted as in Figure 4-2.

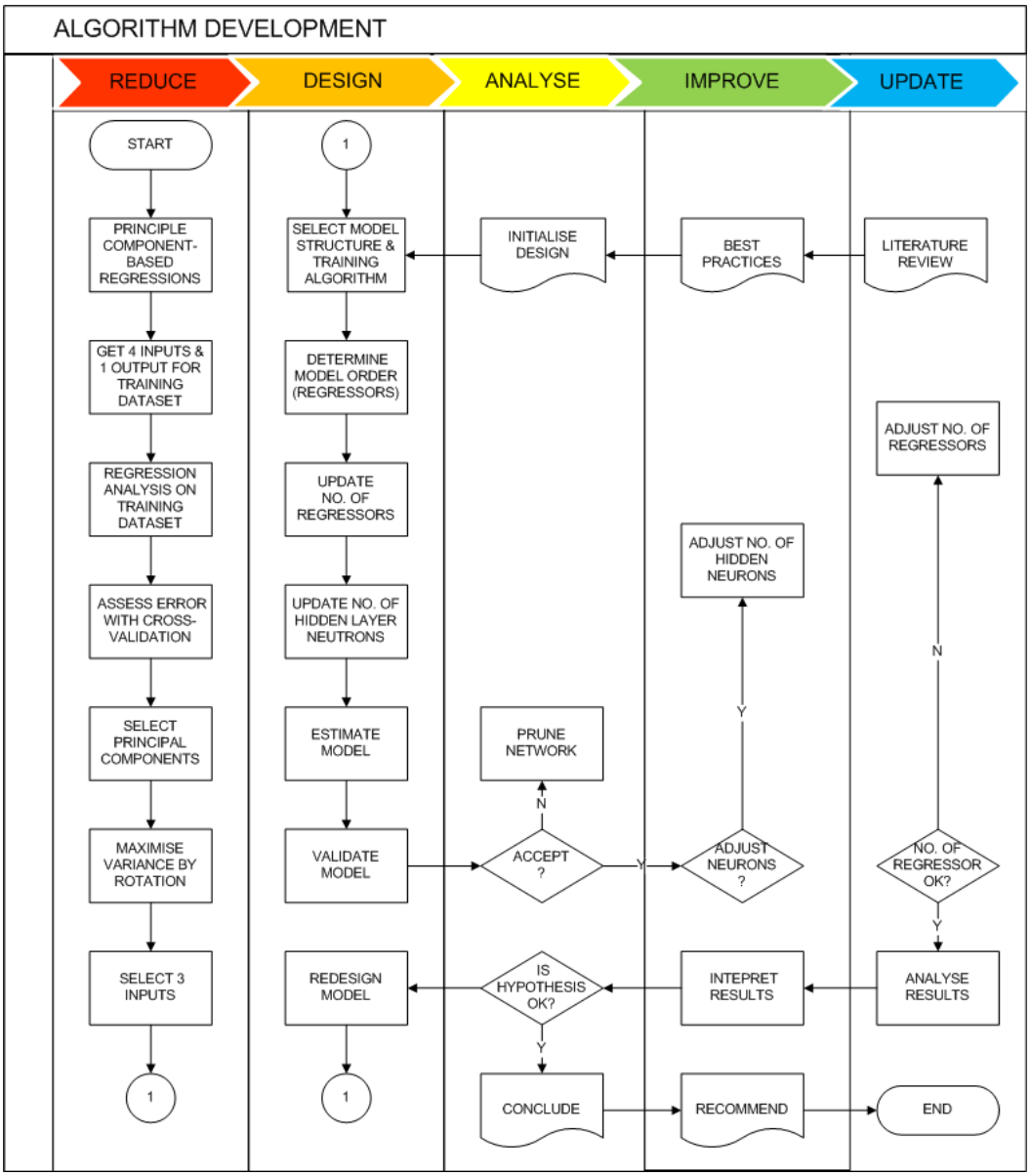

Figure 4-2: Flow Chart of the Methodology - Execute

4.3 Principal Component Analysis

In some situations, the dimension of the input vector is not necessarily large, but the components of the vectors are highly correlated or redundant. It is useful in this situation to reduce the dimension of the input vectors. An effective procedure for performing this operation can be realized by applying principal component analysis (PCA) (Bishop, 1995). The technique orthogonalizes the components of the input vectors so that they are uncorrelated with each other. It orders the resulting orthogonal components (i.e., principal components) so that those with the largest variation come first. It eliminates those components that contribute the least to the variation in the data set.

With multivariate statistics, the problem of visualizing data and their relationships that has more than three variables becomes a problem (The MathWorks, 2013). However, in datasets with many variables, groups of variables often move together and the reason for this is that more than one variable might be measuring the same driving principle governing the behaviour of the system. In many systems, there are only a few such driving forces, but measurement of various system variables can be easily realised with readily available instrumentation. With the redundancy of information, measurement of a large group of variables can be replaced with a smaller group of new variables.

PCA is a quantitatively rigorous method for achieving this simplification (Jolliffe, 2002). The method generates a new set of variables, called principal components. Each principal component is a linear combination of the original variables. All the principal components are orthogonal to each other, so there is no redundant information. The principal components as a whole form an orthogonal basis for the space of the data. The first principal component is a single axis in space. Upon projecting each observation on that axis, the resulting values form a new variable. However, the variance of this variable is the maximum among all

possible choices of the first axis. The second principal component is another axis in space, perpendicular to the first. Likewise, projecting the observations on this axis generates another new variable, and the variance of this variable is the maximum among all possible choices of this second axis. The full set of principal components is as large as the original set of variables. Usually, the sum of the variances of the first few principal components would exceed 80% of the total variance of the original data (Jolliffe, 2002). By examining plots of these few new variables, a deeper and better understanding of the driving forces that generated the original data may be attained.

4.3.1 Orthogonality of variables

Although a dataset is not large, potential improvements can be achieved by first mapping the data into a space of lower dimensionality. In general, a reduction in the dimensionality of the input space will be accompanied by a loss of some of the information, which discriminates between different classes (Bishop, 1995). The goal in dimensionality reduction is therefore, to preserve as much of the relevant information as possible. Another approach to dimensionality reduction is based on the selection of a subset of a given set of features or inputs known as feature selection. However, the principal component analysis technique involves feature transformations where inputs are combined, without reference to a corresponding target data, to make a set of features.

The goal of PCA is to map vectors z^n in a d-dimensional space $(x_1, \ldots\ldots, x_d)$ onto vectors $\mathbf{z^n}$ in an M-dimensional space $(z_1, \ldots\ldots, z_M)$ where M < d (Bishop, 1995). The vector x can be represented, without loss of generality, as a linear combination of a set of orthonormal vectors u_i such that,

$$x = \sum_{i=1}^{d} z_i \, u_i \qquad (4\text{-}1)$$

where the vectors $\mathbf{u_i}$ satisfy the orthonormality relation in which $\boldsymbol{\delta_{ij}}$ is the Kronecker delta symbol, defined as $\boldsymbol{\delta_{ij}} = \mathbf{1}$ if $\mathbf{i} = \mathbf{j}$ and $\boldsymbol{\delta_{ij}} = \mathbf{0}$, as in equation (4-2),

$$u_i^T u_j = \delta_{ij} \tag{4-2}$$

Explicit expressions for the coefficients $\mathbf{z_i}$ in equation (4-1) can be found by using equation (4-2) to give equation (4-3)

$$z_i = u_i^T x \tag{4-3}$$

which can be regarded as a simple rotation of the coordinate system from the original $\mathbf{x's}$ to a new set of coordinates given by the $\mathbf{z's}$. If only a subset M < d of the basis vectors u_i are retained such that only M coefficients of $\mathbf{z_i}$ are used, the remaining coefficients will be replaced by constants b_i so that each vector x is approximated by an expression of the form shown in equation (4-4)

$$\tilde{x} = \sum_{i=1}^{M} z_i u_i + \sum_{i=M+1}^{d} b_i u_i \tag{4-4}$$

A form of dimensionality reduction has taken place since the vector x which originally contained $\mathbf{d}$ degrees of freedom must now be approximated by a new vector $\mathbf{z}$ which has $\mathbf{M}$ degrees $(\mathbf{M < x})$ of freedom. Considering a dataset of N vectors, $\mathbf{x^n}$ where $\mathbf{n = 1, \ldots . N}$. The basis vectors $\mathbf{u_i}$ and the coefficients $\mathbf{b_i}$ are chosen such that the approximation given by equation (4-4) with the values of $\mathbf{z_i}$ determined by equation (4-3) gives the best approximation to the original vector $\mathbf{x}$ on average for the whole data set.

The error in the vector $\mathbf{x^n}$ introduced by the dimensionality reduction is given by equation (4-5),

$$x^n - \tilde{x}^n = \sum_{i=M+1}^{d} (z_i^n - b_i) u_i \tag{4-5}$$

The best approximation is defined to be that which minimizes the sum of the squares of the errors (SSE) over the whole dataset which may be written as,

$$E_M = \frac{1}{2}\sum_{n=1}^{N}\|x^n - \tilde{x}^n\|^2 = \frac{1}{2}\sum_{n=1}^{N}\sum_{i=M+1}^{d}(z_i^n - b_i)^2 \tag{4-6}$$

where the orthonormality relation of equation (4-7) is being used. Setting the derivative of E_M with respect to b_i = 0, yields,

$$b_i = \frac{1}{N}\sum_{n=1}^{N} z_i^n = u_i^T \bar{x} \tag{4-7}$$

where the mean vector $\bar{x}$ is defined as,

$$\bar{x} = \frac{1}{N}\sum_{n=1}^{N} x^n \tag{4-8}$$

Using equations (4-3) and (4-7), the sum-of-squares error (SSE) can be written as equation (4-9),

$$E_M = \frac{1}{2}\sum_{i=M+1}^{d}\sum_{n=1}^{N}\{u_i^T(x^n - \bar{x})\}^2 = \frac{1}{2}\sum_{i=M+1}^{d} u_i^T \Pi u_i \tag{4-9}$$

where $\mathbf{\Pi}$ is the covariance matrix of the set of vectors $\mathbf{x^n}$ and is given in equation (4-10),

$$\Pi = \sum_{n}(x^n - \bar{x})(x^n - \bar{x})^T \tag{4-10}$$

Minimizing $\mathbf{\Pi}$ in equation (4-10) with respect to the choice of basis vectors $\mathbf{u_i}$ it can be shown that the minimum occurs when the basis vectors satisfy equation (4-11),

$$\sum_{u_i} = \lambda_i u_i \tag{4-11}$$

so that they are the eigenvectors of the covariance matrix. Since the covariance matrix is real and symmetric, its eigenvectors can indeed be

chosen to be orthonormal as assumed. The value of the error criterion at the minimum can be obtained as,

$$E_M = \frac{1}{2} \sum_{i=M+1}^{d} \lambda_i \tag{4-12}$$

Thus, the minimum error is obtained by choosing the $\mathbf{d}—\mathbf{M}$ smallest eigenvalues, and their corresponding eigenvectors, as the ones to be discarded.

The linear dimensionality reduction procedure derived above is called the Karhunen-Loeve transformation and is discussed at length in (Jolliffe, 2002). Each of the eigenvectors u_i is called a principal component. The error introduced by a dimensionality reduction using principal component analysis can be evaluated using equation (4-12). In some applications, the original data has a very high dimensionality and only the first few principal components are retained. In such cases, use can be made of efficient algorithms that allow only the required eigenvectors, corresponding to the largest few eigenvalues, to be evaluated.

4.3.2 Regression Analysis

Regression analysis is a statistical process for estimating the relationships among variables including techniques for modeling and analysing several variables. The focus is on the relationship between a dependent variable (DV) and one or more independent variables (IV). More specifically, regression analysis looks at how the dependent variable changes when any independent variable is varied, while the other independent variables are fixed. Regression analysis is widely used for prediction and forecasting, where its use has substantial overlap with the field of artificial intelligence. Regression analysis is also used to understand which amongst the independent variables are related to the dependent variable, and to explore the forms of these relationships.

Two techniques of regressions namely, principal component regression (PCR) and Partial Least Squares Regression (PLSR) were employed to select suitable inputs to be fed into the neural network based on the number of principal components identified. Both methods construct new predictor variables, and hence, the use of the term components, which essentially are linear combinations of the original predictor variables, but are, constructed orthogonally in different ways. PCR is a regression analysis that uses principal component analysis when estimating regression coefficients. In PCR, the dependent variable is regressed on a subset of the principal components of the independent variables and effectively imposing some form of regularization. In the case with neural networks, regularization is introduced in the form of a penalty to prevent over fitting. Only the principal components with the highest variance are selected, but not discrediting the ones of lower variance depending on the parsimony of the model. PCR creates components to explain the observed variability in the predictor variables, without giving due consideration to the response variable. On the other hand, PLSR models a response variable when there are a number of predictor variables that are highly correlated or even collinear. PLSR take the response variable into account, and therefore often leads to models that are able to fit the response variable with fewer components.

Cross-validation is a statistically sound method for choosing the number of components in PLSR or PCR (Mevik and Cederkvist, 2004). It avoids overfitting data by not reusing the same data to both fit a model and to estimate the mean squared prediction error (MSPE) and the error is not biased.

4.4 Maximal Information Coefficient

Maximal information coefficient (MIC) is a technique that measures of the strength of the linear or non-linear association between two variables. The

MIC belongs to the maximal information-based nonparametric exploration (MINE) of data analysis. It is a class of statistics and identifies pair-wise associations for further analysis while filtering out weaker ones. The measure of dependence on all possible variable pairs is computed and the highest-scoring pairs are examined (D. N. Reshef, Reshef, and May, 2015). Events or measurements are termed probabilistically independent if they do not contribute to the probabilities of the others. By convention, any measure of association, referred to as measures of dependence between two variables must be zero if the variables are independent.

The entropy of a single random variable that is a fundamental role in information theory provides the basis of mutual information, MI, of a pair of random variables. Mutual information seems to solve the problem of equitably quantifying statistical associations between pairs of variables. Unfortunately, reliably estimating mutual information from finite continuous data remains a significant and unresolved problem (Kinney and Atwal, 2014). Improved estimators for mutual information from samples of random points distributed according to some joint probability density based on entropy estimates from k-nearest neighbour distances have been employed (Kraskov, Stogbauer, and Grassberger, 2004).

For two continuous random variables X and Y whose joint probability distribution is $p(x,y)$, and $p(x)$ and $p(y)$ are the marginal probability density functions of X and Y respectively, the mutual information between them, denoted by $I(X;Y)$

$$I[X;Y] = \int_X \int_Y p(x,y)\, log_2 \frac{p(x,y)}{p(x)p(y)}\, dxdy \tag{4-13}$$

Mutual information can be equivalently expressed as

$$\begin{aligned} I[X;Y] &= H(X) - H(X|Y) \\ &= H(Y) - H(Y|X) \\ &= H(X) - H(Y) - H(X|Y) \\ &= H(X,Y) - H(X|Y) - H(Y|X) \end{aligned} \tag{4-14}$$

where $H(X)$ and $H(Y)$ are the marginal entropies, $H(X|Y)$ and $H(Y|X)$ are the conditional entropies, and $H(X,Y)$ is the joint entropy of X and Y.

It can be shown from (4-13) and (4-14), $I(X;Y)$ is non-negative and consequently, $H(X) \geq H(X|Y)$ using Jensen's Operator Inequality based on the definition of Mutual information (Hansen and Pedersen, 2003).

MIC is a univariate method that is based on the information entropy concept and can detect all forms of associations between any pair of variables (pairwise relationship ((Simon and Tibshirani, 2011). The maximal information coefficient uses a methodology of binning by selecting the number of bins and picking a maximum over many possible grids as a means to apply mutual information on continuous random variables. Bins for both variables should be selected in such a way that the mutual information between the variables be maximal whenever,

$$H(X_b) = H(Y_b) - H(X_b, Y_b) \tag{4-15}$$

For a dataset D containing n observations on two variables X and Y, the values in X and Y can be partitioned into x-bins and y-bins, respectively, to create x by y grid (D. Reshef, Reshef, Mitzenmacher, and Sabeti, 2013) . Let $D|G$ be the distribution of observations in D on the cells of a certain gird G, and $I(D|G)$ denotes the mutual information of $D|G$. For a fixed D, different grids G results in different distributions $D|G$ and the characteristic matrix of

$$M(D)_{x,y} = \frac{I*(D,x,y)}{log_2 min\{x,y\}} \tag{4-16}$$

where $I*(D,x,\ y) = \max(ID|G)$ over all grids G in x columns and y rows.

The characteristic matrix is then used in the calculation of MIC as

$$MIC(D) = \max_{xy<B(D)} \frac{I*(D,x,y)}{log_2 min\{x,y\}} \tag{4-17}$$

where $B(n)$ is the upper bound on the grid size.

4.5 Neural Network Design

4.5.1 System Modeling

System modelling is a challenging field as there could be no or little physical insight and typically, mathematical models were derived to understand the behaviour of a complex system such as an oil and gas well. With increasing uncertainties and complexities, the use of a data-driven model becomes more appropriate in realizing prediction systems. Many processes in practice are continuous and their models are commonly derived from basic principles like mass and energy balances resulting in nonlinear continuous time models. A proper assumption, as normally done in identification, is that a discrete time nonlinear system with a fixed unknown structure and constant unknown parameters exists (Chen and Billings, 1992). This assumption was applied throughout this work and assumed that an originally continuous time process is discretizable where the continuous time system was modelled with a discrete time nonlinear model. It is well known that a nonlinear system can be described by a nonlinear time series model involving nonlinear regression of past data. A general model of a discrete time noise process can be mathematically modelled (Priestley, 1988).

Causal modelling attempts to resolve questions about possible causes to provide explanations of phenomena (effects) because of previous phenomena (causes). Without loss of generality, a causal model (structure) consists of a representation of the phenomena along with indicating the cause-and-effect relationships amongst the phenomena. A causal system, also known as a physical or non-anticipative system is a system where the output depends on past and current inputs but not future inputs i.e., the output $\mathbf{y}(\mathbf{t_0})$ only depends on the input $\mathbf{u}(\mathbf{t})$ for values of $\mathbf{t} < \mathbf{t_0}$. Through a procedure known as systems identification, causal neural networks may be modelled. Causal neural networks seek to isolate variables that represent

the "cause" phenomena and those, which represent the "effect" phenomena, and to determine the magnitude and direction of change in the effects corresponding to a change in the cause. Identified variables in conjunction with their functional relationships can serve as a useful computational model for making inferences (Pearl, 1987).

4.5.2 Linear System Identification

The field of system identification is well developed for linear systems (Ljung, 1987). However, a linear model is only useful if the underlying physical process exhibits qualitatively similar dynamic behaviour to the linear model in the operating region of interest. All physical systems are nonlinear to a certain extent. As a result, much research is dedicated to the development of approaches for modelling and analysis of nonlinear systems. Nonlinear systems usually exhibit a variety of complex dynamic behaviours. This complex behaviour of nonlinear systems and the fact that it is usually not possible to incorporate any a priori knowledge about the system dynamics in the identification procedure makes it almost impossible to estimate the “true” nonlinear model of a physical process.

The primary aim is to construct networks that allow modelling of the global system dynamics devoid of the need for physical insight or an extensive prior knowledge. Approximating a parameterized model in this fashion is known as Black Box Modelling, while one that is created purely from physical insight of the system is termed White Box Modelling. Prediction with neural networks uses models that require extensive analysis of the system under study. It is important that the data is analysed before being fed into the model. This somewhere-in-between approach is commonly referred to as Grey Box Models and the challenge is to develop structures that allow models that are inclined towards the black box modelling approach.

Systems identification is a field that has been given prominence due to its ability to identify the transfer functions of linear systems based on a given set of inputs and outputs. This serves as a powerful tool as real systems may be modelled using the black box approach (Ljung, 2001). Systems identification is the process of finding a model of a physical system given the input-output measurements. Nonlinear system identification is a much more recent discipline than linear system identification and the theory for the nonlinear case is often an extension of the linear one. For linear systems, system identification and control are well-developed disciplines with decades of research. The use of mathematical modelling is limited in the sense that for many complex non-linear systems, the equations may not be available or sufficiently formulated. An area of recent interest is the use of neural networks in carrying out systems identification. This is especially so in the identification of complex non-linear systems. Like the linear case, non-linear system identification is an extension for non-linear time invariant complex systems. There are many model structures used in the linear case and one that has been particularly explored is that of the Auto Regression with Exogenous (ARX) inputs. For nonlinear systems, however the theory is significantly less well founded. Properties such as observability, stability and controllability are not straightforward in the nonlinear case. Nevertheless, neural networks despite the challenges, have been incorporated in system identification and control problems with much success (Norgaard, Ravn, Poulsen, and Hansen, 2000).

4.5.3 Linear Model Estimation

Dynamic models are mathematical relationships between the system's inputs $\mathbf{u}(\mathbf{t})$ and outputs $\mathbf{y}(\mathbf{t})$ that can be used to compute the current output from previous inputs and outputs. The general form of a model in discrete time is given by.

$$y(t) = f\big(y(t-1), \dots y(t-na), u(t-nk), \dots u(t-nk-nb+1)\big) \qquad (4\text{-}18)$$

where the function f depends on a finite number of previous inputs u and outputs y. na is the number of past output terms and nb is the number of past input terms used to predict the current output. nk is the delay from the input to the output, specified as the number of samples (The MathWorks Inc, 2014).

Generally, all systems are nonlinear, and the output is a nonlinear function of the input variables. However, a linear model is often sufficient to accurately describe the system dynamics and therefore, it is customary that a linear model is initially fitted during the identification exercise. The additional flexibility of nonlinear models may be sought after under varying situations. The linear model may provide a poor fit to the measured output signals and little or no improvement by changing the model structure or order. In this case, nonlinear models become suitable candidates as they have more flexibility in capturing complex phenomena than their linear counterparts of similar orders. Based on physical insight or data analysis, the system may be deemed weakly nonlinear. The approach would be to initially estimate a linear model and then use this estimated linear model as an initial model for nonlinear estimation. In this way, the fit of the nonlinear estimation can be improved by using nonlinear components of the model structure to capture the dynamics. The physical insight of the system may exhibit nonlinear characteristic, in which case the system can represented as a nonlinear grey box model. Before fitting a nonlinear model, transformation of the input and output variables should be carried out such that the relationship between the transformed variables becomes linear.

The Final Prediction Error (FPE) criterion provides a measure of model quality by simulating the situation where the model is tested on a different data set (Ljung, 2011). According to Akaike, the most accurate model has

the smallest FPE (Pan, 2008). The Final Prediction Error (FPE) is defined by,

$$FPE = V\left(\frac{1+\frac{d}{N}}{1-\frac{d}{N}}\right) \tag{4-19}$$

where $\mathbf{V}$ is the loss function, $\mathbf{d}$ is the number of estimated parameters, and $\mathbf{N}$ is the number of values in the data set.

Assuming that final prediction error is asymptotic for $\mathbf{d} << \mathbf{N}$ the following approximation may be made to compute FPE,

$$FPE = V\left(1+\frac{2d}{N}\right) \tag{4-20}$$

The loss function $\mathbf{V}$ is defined by the following equation:

$$V = det\left(\frac{1}{N}\sum_{1}^{N}\varepsilon\,(t,\theta_N)\big(\varepsilon(t,\theta_N)\big)^T\right) \tag{4-21}$$

where $\varepsilon(\mathbf{t},\boldsymbol{\theta}_\mathbf{N})$ is the prediction error and $\boldsymbol{\theta}_\mathbf{N}$ represents the estimated parameters.

Akaike's Information Criterion (AIC) is defined by the following equation,

$$AIC = log\,V + \frac{2d}{N} \tag{4-22}$$

where V is the loss function, $\mathbf{d}$ is the number of estimated parameters, and N is the number of values in the estimation data set (Bozdogan, 1987).

For $\mathbf{d} << \mathbf{N}$:

$$AIC = log\left(V\left(1+\frac{2d}{N}\right)\right) \tag{4-23}$$

A linear ARX model is checked based on the linear model order estimated to provide some insight on the dataset. The Final Prediction Error (FPE) criterion provides a measure of model quality by simulating the

situation where the model is tested on a different training dataset (Akaike, 1969).

4.5.4 Nonlinear ARX Models

Nonlinear ARX models extend the linear ARX models to the nonlinear case with the following structure:

$$y(t) = f\big(y(t-1), \dots, y(t-na), u(t-nk), \dots, u(t-nk-nb+1)\big) \quad (4\text{-}24)$$

A nonlinear ARX model can be understood as an extension of a linear model. A linear SISO ARX model has this structure:

$$\begin{aligned} y(t) + a_1 y(t-1) + a_2 y(t-2) + \dots + a_{na} y(t-na) \\ = b_1 u(t) + b_2 u(t-1) + \dots + b_{nb} u(t-nb+1) + e(t) \end{aligned} \quad (4\text{-}25)$$

where the input delay nk is zero to simplify the notation.

The current output $\mathbf{y(t)}$ is predicted as a weighted sum of past output values and current and past input values. Rewriting the equation as a product:

$$\begin{aligned} y_p(t) = [-a_1, -a_2, \dots, -a_{na}, b_1, b_2, \dots, b_{nb}] \\ * [y(t-1), y(t-2), \dots, y(t-na), u(t), u(t \\ -1), \dots, u(t-nb-1)]^T \end{aligned} \quad (4\text{-}26)$$

where $[y(t-1), y(t-2), \dots\dots, y(t-na), u(t), u(t-1), 1, u(t-nb-1)]$ are delayed input and output variables known as regressors. The linear ARX model thus predicts the current output y_p as a weighted sum of its regressors.

This structure can be extended to create a nonlinear form as:

$$y_p(t) = f\begin{pmatrix} y(t-1), y(t-2), y(t-3), \dots, u(t), u(t-1), \\ u(t-2), \dots \end{pmatrix} \quad (4\text{-}27)$$

Instead of the weighted sum that represents a linear mapping, the nonlinear ARX model has a more flexible nonlinear mapping function where f is a nonlinear function. In addition, the inputs to f are model regressors. Several nonlinear mapping functions such as wavelet network, one-layer

sigmoid network, multilayered neural network, etc are amongst the most common non-linear estimators. Nonlinear ARX regressors can be both of delayed input-output variables with more complex nonlinear expressions of delayed input and output variables. In the simplest case, regressors are delayed inputs and outputs, such as $u(t-1)$ and $y(t-1)$ and are called standard regressors.

By default, all regressors are inputs to both the linear and the nonlinear function blocks of the nonlinearity estimator as depicted in Figure 4-3.

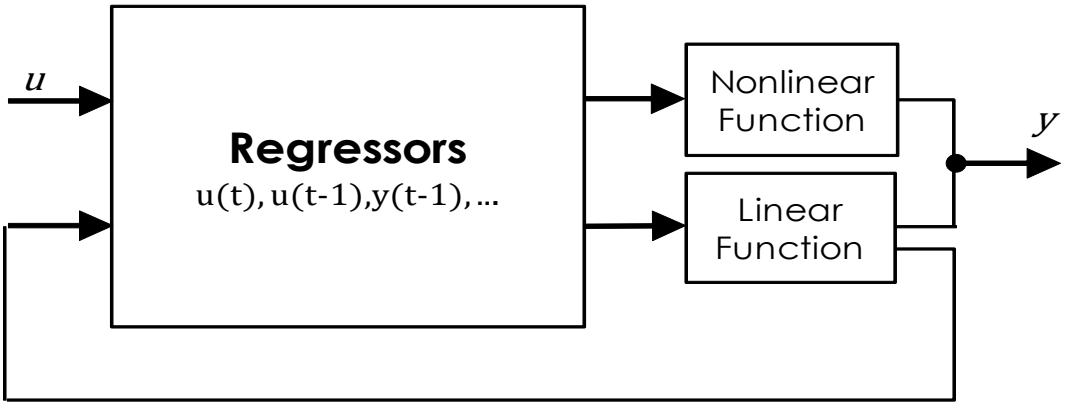

Figure 4-3: Non-linear ARX Model Block Diagram

The nonlinearity estimator block maps the regressors to the model output using a combination of nonlinear and linear functions. The nonlinearity estimator block can include linear and nonlinear blocks in parallel.

4.5.5 Artificial Neural Networks

Neural networks have been used to model single-input-single-output (SISO) systems where a high level of confidence was obtained, and demonstrated by the good one-ahead prediction of the output (Tant and Cauwenberghe, 1996).

The field of artificial intelligence (AI) is not new, but with advancing computing capabilities readily available on desktop computers, the methodology is increasingly being used in addressing problems in industry. Artificial Neural Networks (ANN's) are the most commonly deployed form of artificial intelligence today and have found applications across both industry and commerce. ANN's are able to approximate any non-linear system quite easily based on relevant data pertaining to the system of interest. There are also other sand prediction tools based on rigorous mathematics around the understanding of rock mechanics. The complexities and intricacies of multiphase flow presents an enormous challenge in the oil and gas industry and have gained momentum in academic research laboratories with major oil companies under various Joint Industry Projects (Falcone, Teodoriu, Reinicke, and Bello, 2007). Nevertheless, the use of AI and particularly in the area of neural networks in the oil and gas industry has been slow. Its novelty is yet to be fully realized for the obvious benefits and eminent profitability that ANN promises. The next section will focus on a commonly used network structure, the perceptron.

One widely used application of ANN in engineering is pattern classification based on of carefully chosen independent variables. Rosenblatt wrote the first paper on the network structure called the perceptron. Perceptrons are also used extensively as adaptive filters (Rosenblatt, 1958). Limitations of these so-called single layer perceptrons led to the development of Multilayered Perceptrons (MLP) that included a hidden layer of nonlinear neurons. The MLP's ability to approximate nonlinear functions is summarized in the following theorem, known as the universal approximation theorem (Cybenko, 1989), which states that "A feed forward neural network with a sufficiently large number of hidden neurons with continuous and differentiable transfer functions can approximate any continuous function over a closed interval"

It was subsequently shown that it was not the specific choice of the sigmoid activation function, but rather the multilayer feedforward architecture itself that gives neural networks the potential of being universal approximators (Hornik, Stinchcombe, and White, 1989). The use of neural networks as a generic model structure for the identification of nonlinear dynamic systems is an area of current research actively pursued. The Multilayer Perceptron (MLP) network is a very common member of the neural network family due to its ability to model simple as well as complex functions (Kim and Adali, 2003). In its simplest form, the perceptron consists of a single neuron with multiple input synapses. The neuron is presented with training patterns and the corresponding target classes. Rosenblatt proved that if two classes were linearly separable the perceptron would converge to a configuration of parameters that classifies each pattern correctly (Rosenblatt, 1961). For the case of a single neuron, this is equivalent to placing a dividing hyperplane in the weight space. This form of training is called supervised learning or learning with a teacher. Limitations of these so-called single layer perceptrons led to the development of Multilayered Perceptrons (MLP) that included a hidden layer of nonlinear neurons.

The class of MLP-networks, shown in Figure 4-4 is those confined to having only one hidden layer with hyperbolic tangent and linear activation functions (Norgaard, Ravn, and Poulsen, 2002).

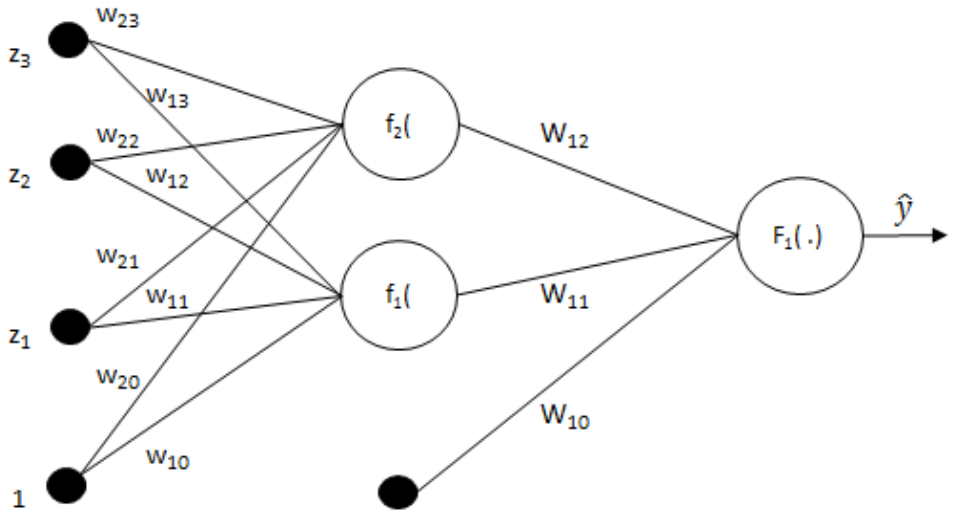

Figure 4-4: MLP with hidden layer of nonlinear neurons - Source: (Norgaard et al., 2002)

where,

$\hat{y}_i$	is the prediction at time t=i
z_i	is the input-output pair at time t=i
w_{ji}	is the weight matrix between input and hidden layers
W_{ij}	is the weight matrix between hidden and output layers
$f_j(.)$	j=1,2 is the activation function between input and hidden layers
$F_i(.)$	i=1,2 is the activation function between hidden and output layers

The function is described in (Norgaard et al., 2000) and is given by the following,

$$\begin{aligned} \hat{y}_i(w, W) &= F\left(\sum_{j=1}^{q} W_{ij}\, h_j(w) + W_{i0}\right) \\ &= F_i\left(\sum_{j=0}^{q} W_{ij} f_j\left(\sum_{l=1}^{m} w_{ji}\, z_i + w_{j0}\right) + W_{i0}\right) \end{aligned} \tag{4-28}$$

The weights vector, θ, are the adjustable parameters of the network determined through a process called training.

$$Z^N = \{[x(t), y(t)]t = 1, \ldots . . N\} \tag{4-29}$$

The objective of training is then to determine a mapping from the set of training data to the set of possible weights.

$$Z^N \rightarrow \hat{\theta} \tag{4-30}$$

so that the network will produce predictions $\hat{y}_i$, which in some sense are "close" to the true outputs $y(t)$.

The prediction error approach is based on the introduction of a measure of closeness in terms of a mean square error criterion.

$$V_N(\theta, Z^N) = \frac{1}{2N}\sum_{t=1}^{N}[y(t) - \hat{y}(t|\theta)]^T\,[y(t) - \hat{y}(t|\theta)] \tag{4-31}$$

The weights are then found as:

$$\hat{\theta} = argmin\, V_N(\theta, Z^N) \tag{4-32}$$

by some kind of iterative minimization scheme:

$$\theta^{(i+1)} = \theta^{(i)} + \mu^{(i)} f^{(i)} \tag{4-33}$$

where $\theta^{(i)}$ specifies the current iterate, $f^{(i)}$ is the search direction, and $\mu^{(i)}$ is the step size.

4.6 Model

4.6.1 Network Architecture and Order

The arrangements of neurons in the different layers and the pattern of connection within the neural network are generally called the architecture of the net. Essentially, there are feedforward and feedback or recurrent networks. Multi-layered perceptron (MLP) are strictly feed-forward (one directional), i.e., a node from one layer can only have connections to a node of the next layer and all layers are fully connected.

The simplest and most widely used approach for modelling nonlinear dynamics using neural networks is extending the linear ARX model with a neural network to form the Neural Network Auto Regressive with Exogenous inputs (NNARX) model. For MISO systems, the NNARX model has been used to train and validate application specific data with a high degree of level of confidence (Chen and Billings, 1992). The network as depicted in Figure 4-5 is trained based on the NNARX model structure. Let $\boldsymbol{\varphi}(\mathbf{t})$ be a vector containing the regressors, and θ be a vector containing the weights and the function, $\mathbf{f}$ realized by the neural network.

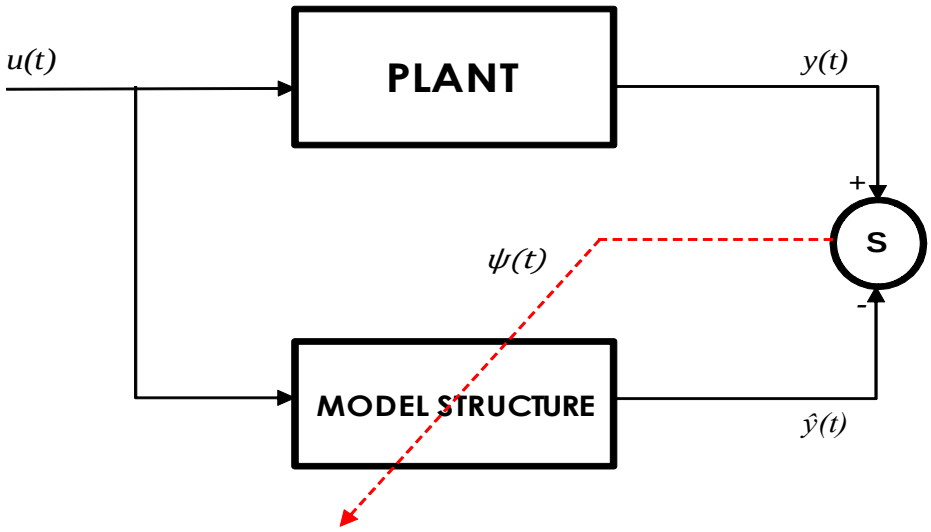

Figure 4-5: Model NNARX Structure

Due to the complexity, uncertainty and nonlinearity of a large class of systems, it is difficult to derive accurate and complete equations of appropriate models for input-state-output representations of the systems from first principles. Input-output models based on input-output data are employed to represent the unknown nonlinear systems. The identification from sampled input and output signals involves two tasks; identification of model orders and nonlinear function approximation. In order to obtain a valid neural network model based on the prediction error principle, the model orders and the number of hidden units must be adjusted.

For the NNARX model structure, the number of past signals (i.e., model order) that were used as regressors has to be determined. Various functions can be used to estimate the order to observe a reasonable performance and in this case, the Lipschitz function is employed that is based on the Lipschitz condition (He and Asada, 1993). The approach is based on the continuity property of the nonlinear functions, which represents input-output models of continuous dynamic system. The input output model representing nonlinear dynamical systems described by differential or difference equations relating input and output of the systems as in,

$$y(t) = f\big(y(t-\tau), \dots, y(t-m\tau), u(t-\tau), \dots, u(t-l\tau)\big) \tag{4-34}$$

Parameters m and l in (4-34) are orders of the input-output model.

$$y = f(x) = f(x_1, x_2, \dots \dots, x_n) \tag{4-35}$$

The non-linear function $f(x)$ can be re-constructed from input-output data pairs (x_i , y_i). The Lipschitz quotient, q_{ij} can be defined as given.

$$q_{ij} = \frac{|y_i - y_j|}{|x_i - y_j|}, (i \neq j) \tag{4-36}$$

$|\mathrm{x_i} - \mathrm{y_j}|$ is the distance of two parts x_i and y_i in the input space and $|\mathrm{y_i} - \mathrm{y_j}|$ is the difference of $f(x_i)$ and $f(x_j)$.

If the function $f(x)$ is continuous, Lipschitz condition states that Lipschitz quotient must be bounded for any input-output data pairs where L is a bounded value.

$$0 \leq q_{ij} \leq L \tag{4-37}$$

From (4-35) and (4-36), a large Lipschitz quotient only occurs for data points i and j with a small distance $|x_i - y_j|$. The bound of Lipschitz quotient, q_{ij} is obtained using the Schwartz inequality and is given by,

$$q_{ij}^{(n)} \leq \sqrt{n}\, M \tag{4-38}$$

The following index is used to identify the optimal number of input variables.

$$q^{(n)} = \left(\prod_{k=1}^{p} \sqrt{n}\, q^{(n)}[(k)) \right)^{1/p}] \tag{4-39}$$

where $q^{(n)}(k)$ is the k-largest Lipschitz quotient among all $q_{ij}^{(n)}$ with n input variables. In plotting a curve of $q^{(n)}$ against n, $q^{(n)}$wil reach some saturated value when $n = n_0$. Then, n_0 is the optimal number of optimal input variables. p is generally selected to be $0.01 \sim 0.02N$.

Given a set of corresponding inputs and outputs of an input-output model, the Lipschitz function calculates a matrix of indices to determine a proper lag space structure before identifying a model of a dynamic system. An insufficient lag space structure leads to a large index. While increasing the lag space, the index will decrease until a sufficiently large lag space structure is reached. Increasing the lag space beyond this will not reduce the index significantly.

The regression vector for the NNARX model structure is an expression given by equation ((4-40),

$$\varphi(t) = [y(t-1) \ldots y(t-n_a) \ldots . u(t-n_b - n_k + 1)]^T \tag{4-40}$$

where, $\varphi(t)$ is a vector containing the regressors,
$y(t)$ is the output
$u(t)$ is the input
n_a is number of past outputs used for determining the prediction
n_b is the number of past inputs
n_k is the time delay

and the predictor $\hat{y}(t|\theta)$ is expressed by equation ((4-41),

$$\hat{y}(t|\theta) = \hat{y}(t|t-1,\theta) = f(\varphi(t),\theta) \tag{4-41}$$

where, $\boldsymbol{\varphi}(\mathbf{t})$ is a vector containing the regressors, $\boldsymbol{\theta}$ is a vector containing the weights and f is the function realized by the neural network.

The NNARX model has a predictor without feedback. Other model types have feedback through the choice of regressors, which means that the networks become recurrent whereby future inputs will depend on present and past network outputs. This might lead to instability in certain regimes of the network operating range and it can be very difficult to determine the stability of the predictor (Norgaard et al., 2000).

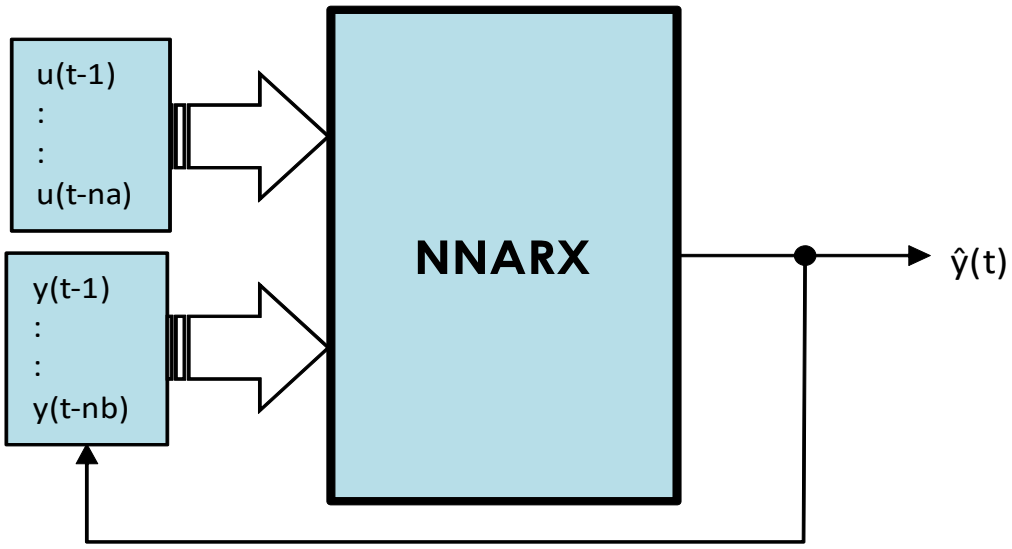

Figure 4-6: Neural Network ARX Model Structure with past inputs and outputs

4.6.2 Activation Function

Activation functions in the hidden units introduce nonlinearity into the multilayer network. The capability to represent nonlinear functions makes multilayer networks so powerful. Moreover, back propagation learning, requires that the activation function must be differentiable and bounded. The sigmoidal functions such as logistic and tanh and the Gaussian function are the most common choices are S-curved functions. It should be noted that functions that produce both positive and negative values tend to yield faster training than functions that produce only positive due to better numerical conditioning. Numerical condition affects the speed and accuracy of most numerical algorithms.

For hidden units, sigmoid activation functions are usually preferable to threshold activation functions. The fast hyperbolic tangent function was used as the activation for the hidden layer and the function is given below.

$$\begin{aligned} tanh\, x &= \frac{e^{x} - e^{-x}}{e^{x} - e^{-x}} \\ &= \frac{e^{2x} - 1}{e^{2x} + 1} \\ &= 1 - \frac{2}{e^{2x} + 1} \end{aligned} \tag{4-42}$$

Since there is only single output, the output layer is a single linear neuron.

4.6.3 Learning Rate

The rate at which ANN learns depends upon several controllable factors. A slower learning rate means a more time significantly is spent in accomplishing the off-line learning to realise an adequately and satisfactory trained system (Anderson and Mcneill, 1992). On the other hand, with faster learning rates the network may not be able to make the fine discriminations possible with a system that learns slower. Adaptive step methods with an algorithm based on a global learning rate is desirable where are all the weights are updated in the network (Rojas, 1996). The idea of the method is to use the negative gradient direction to generate two new points instead of one. The point with the lowest error is used for the next iteration. If it is the farthest away, the algorithm accelerates, by making the learning constant bigger. If it is the nearest one, the learning constant is reduced. The family of second-order algorithms considers more information about the shape of the error function instead of the gradient. A better iteration can be performed if the curvature of the error function is also considered at each step. In second-order methods a quadratic approximation of the error function is found to be of superior performance when compared to standard back propagation techniques (Battiti, 1992). The Taylor Series, which approximates the error function $E(u)$, as given by

$$E(u) = E(u_1, u_2 \ldots \ldots . u_n) \tag{4-43}$$

The Taylor series for this function about the point $"u*"$, in $"u"$ is,

$$\begin{aligned} E(u) &= E(u^*) + \frac{\partial}{\partial u_1} E(u) \Big|_{u = u^*} (u_1 - u_1^*) \\ &\quad + \frac{\partial}{\partial u_2} E(u) \Big|_{u = u^*} (u_2 - u_2^*) + \cdots \\ &\quad \ldots + \frac{\partial}{\partial u_n} E(u) \Big|_{u = u^*} + \frac{1}{2} \frac{\partial^2}{\partial u_1^2} E(u) \Big|_{u = u^*} (u_1 - u_1^*)^2 \\ &\quad \ldots + \frac{1}{2} \frac{\partial^2}{\partial u_1 \ \partial u_2} E(u) \Big|_{u = u^*} (u_1 - u_1^*) \quad (u_2 - u_2^*)^2 \end{aligned} \tag{4-44}$$

This may be written in Matrix form as shown in equation (4-45),

$$\begin{aligned} E(u) &= E(u^*) + \nabla E(u)^T \Big|_{u = u^*} (u - u^*) \\ &\quad + \cdots \frac{1}{2} (u - u^*)^T \nabla^2 E(u) \Big|_{u = u^*} (u - u^*) \end{aligned} \tag{4-45}$$

where $\nabla E(u)$ is defined as the gradient given by equation (4-46),

$$\nabla E(u) = \left[\frac{\partial}{\partial u_1} F(u) \quad \frac{\partial}{\partial u_2} F(u) \quad \ldots \quad \frac{\partial}{\partial u_n} F(u) \right]^T \tag{4-46}$$

and the $\nabla^2 E(u)$ is the Hessian matrix which is given by equation (4-47),

$$\nabla^2 E(u) = \begin{bmatrix} \frac{\partial^2}{\partial u_1^2} "E(u)" & \frac{\partial^2}{\partial u_1 \ \partial u_2} " E(u)" & \ldots & \frac{\partial^2}{\partial u_1 \ \partial u_n} "E(u)" \\ \frac{\partial^2}{\partial u_2 \ \partial u_1} "E(u)" & \frac{\partial^2}{\partial x_2^2} " E(u)" & \ldots & \frac{\partial^2}{\partial u_2 \ \partial u_n} " E(u)" \\ \vdots & \vdots & & \vdots \\ \frac{\partial^2}{\partial u_n \ \partial u_1} " E(u)" & \frac{\partial^2}{\partial u_n \ \partial u_2} " E(u)" & \ldots & \frac{\partial^2}{\partial u_n^2} " E(u)" \end{bmatrix} \tag{4-47}$$

The gradient of the error function can be computed by differentiating equation (4-46) and since a minimum of the error function is required, this is equated to zero. The minimization problem can be solved in a single step if the Hessian matrix and the gradient have been previously computed under the assumption of a quadratic error. However, computing the

Hessian matrix can become quite a difficult task and approximation is carried out using the inverse Hessian shown in (4-47).

4.6.4 The Levenberg-Marquart Algorithm

The Levenberg-Marquart method is one of the standard methods for the minimization of mean square error criterion, due to its rapid convergence properties and robustness. A version of the method was applied with the primary difference being that the size of the elements of the diagonal matrix added to the Gauss-Newton approximation of the Hessian matrix is adjusted according to the size of the ratio between actual decrease and predicted decrease (Norgaard et al., 2002). The Gauss-Newton algorithm was designed for minimizing functions that are sums of squares of other non-linear functions, which is well suited for neural network training where the performance index is the mean squared error (MSE) or the normalised sum of squared error (NSSE).

Network complexity, size, architecture, learning rules employed, and desired accuracy must be given due consideration. These factors play a significant role in determining the training duration. Most learning functions depend on a learning rate, which may be fixed or variable. Most of these laws are some sort of variation of the best-known and oldest learning law, Hebb's Rule (Hebb, 1949). The Levenberg-Marquart method is one of the standard methods for minimization of mean square error criterion, due to its rapid convergence properties and robustness (Levenberg, 1944). Levenberg proposed an algorithm based on this observation, whose update rule is given as

$$x_{i+1} = x_i - (H + \lambda\, diag[H])^{-1} \nabla f(x_i) \qquad (4\text{-}48)$$

where H is the Hessian matrix evaluated at x_i.

The update rule (Ranganathan, 2004) is used in the following way:

- If the error goes down following an update, it implies that the

quadratic assumption on $\mathbf{f}(\mathbf{x_i})$ is working and therefore, it needs to be reduced by $\boldsymbol{\lambda}$ to reduce the influence of gradient descent.

- On the other hand, if the error goes up, the gradient will be followed more and so $\boldsymbol{\lambda}$ is increased by the same factor.

The Levenberg algorithm is as follows:

i. Provide an initial learning rate, $\boldsymbol{\lambda_0}$.
ii. Do an update as directed by the rule above.
iii. Evaluate the error of the new parameter vector.
iv. If the error has increased as a result the update, then reset the weights to the previous values and increase the new $\boldsymbol{\lambda}$ by some significant factor. Go back to step (ii) and try an update again.
v. If the error has decreased due to the update, then keep the weights at the new values and decrease $\boldsymbol{\lambda}$ by a factor.

4.7 Improve & Optimise Performance

The Optimal Brain Surgeon (OBS) is the most important strategy, and it is consequently the only method, which has been implemented for dynamic systems. The method was originally proposed by (Hassibi and Stork, 1993). A modification of the method was derived so that it can handle networks trained according to the regularized criterion, and defined a saliency as the estimated increase of the unregularized criterion when a weight is eliminated (Larsen, Hansen, Svarer, and Ohlsson, 1996).

A new expression for the saliences is obtained where the saliency for weight ζ_j is defined as

$$\begin{aligned}\zeta_j = \frac{\lambda}{N} e_j^T H^{-1}(\theta^*) D\theta^* + \ \ldots\ldots\ldots\ldots \\ \ldots\ldots\ \frac{1}{2}\lambda_j^2\, e_j^T\, H^{-1}(\theta^*)\, R(\theta^*)\, H^{-1}\,(\theta^*)\, e_j\end{aligned} \tag{4-49}$$

where θ^* specifies the minimum and H(θ^*) the Gauss-Newton Hessian of the regularized criterion

$$H(\theta^*) = R(\theta^*) + \frac{1}{N} D \tag{4-50}$$

where e_j is the jth unit vector and λ_j is the Lagrange multiplier, which is determined by.

$$\lambda_j = \frac{e_j^T \theta^*}{e_j^T H^{-1}(\theta^*) e_j} = \frac{\theta_j^*}{H_{j,j}^{-1}(\theta^*)} \tag{4-51}$$

The constrained minimum (the minimum when weight j is 0) is then found from,

$$\delta\theta = \theta^* - \theta = -\lambda_j \, H^{-1}(\theta^*) \, e_j \tag{4-52}$$

Notice that for the unregularized criterion, where $R(\theta^*) = H(\theta^*)$, the above algorithm will degenerate to OBS scheme (Hassibi and Stork, 1993).

A modification to the algorithm to address the situation was made which does not allow a single weight to a unit in the hidden layer to be removed whilst it is still connected to the outer layer (Norgaard et al., 2002).

The variable **J** is defined as the set of indices to the weights leading to and from the unit in the hidden layer. Let E_J be a matrix of unit vectors corresponding to each element of the set **J**. In order to calculate the saliency for the entire unit, the above expressions are then modified to:

$$\zeta_J = \lambda_J^T E_J^T H^{-1}(\theta^*) \, \frac{1}{N} D\theta^* + \frac{1}{2} \lambda_J^T E_J^T H^{-1}(\theta^*) R(\theta^*) H^{-1}(\theta^*) E_J \lambda_J \tag{4-53}$$

$$\lambda_j = \left[E_j^T H^{-1}(\theta^*) E_J \right]^{-1} E_J^T \theta^* \tag{4-54}$$

$$\delta\theta = \theta^* - \theta = -H^{-1}(\theta^*) E_J \lambda_J \tag{4-55}$$

When a weight (or unit) has been removed, it is necessary to obtain the new inverse Hessian before proceeding to eliminate new weights. If the network has been retrained, it is necessary to construct and invert the Hessian once more. However, if the network is not retrained, inversion of

partitioned matrices can be used for approximating the inverse Hessian of the reduced network (Pedersen, Hansen, and Larsen, 1995).

Assuming that the pruned weights are located at the end of the parameter vector, $\boldsymbol{\theta}$, the Hessian is then partitioned as follows in equation (4-56),

$$H = \begin{bmatrix} \widetilde{H} & h_J \\ h_J^T & h_{JJ} \end{bmatrix} \tag{4-56}$$

where $\widetilde{\mathbf{H}}$ is the 'new' Hessian, which is to be inverted and partitioning the inverse Hessian in the same way yields equation (4-57),

$$H^{-1} = \begin{bmatrix} \tilde{P} & p_{JJ} \\ p_J^T & p_{JJ} \end{bmatrix} \tag{4-57}$$

The new inverse Hessian is then determined as the Schur Complement (Burns, Carlson, Haynsworth, and Markham, 1974) of $\tilde{P}$ and is given by equation (4-58),

$$\widetilde{H}^{-1} = \tilde{P} - p_J p_{JJ}^{-1} p_J^T \tag{4-58}$$

4.8 Summary

In this chapter, the proposed algorithm was described, and the description of the various approaches was outlined. Due to the high co-linearity of the input variables, opportunities were identified to reduce the number of input variables to those that significantly contributed to the derivation of the critical flowing bottomhole pressure (CFBHP). PCA is a technique that maps the input vector or predictive variables only, the method is extended to principal component regression (PCR). In most real-life applications, systems are non-linear and can be modelled by a non-linear time series. Causal modelling is introduced and how the principles of systems identification can be used to model complex non-linear systems. The use of artificial neural networks with reference to the multilayer perceptron was discussed. The simplest and most widely used approach for modelling

nonlinear dynamics using neural networks was extending the ARX model with a neural network to form the Neural Network Auto Regressive with Exogenous inputs (NNARX) model. The model structure of the NNARX model and its corresponding regressors was introduced. The Lipschitz function is used to estimate the order to observe a reasonable performance. The underlying details of the neural network in terms of its activation functions, learning algorithm were under-pinned. In order to address the problem of over-fitting and improve the performance of the network, the concepts of pruning were introduced.

CHAPTER 5

RESULTS AND DISCUSSIONS

5.1 Introduction

Having determined the measurements of process parameters that were required to design a representative model of the sand prediction tool, an automated and smart data pre-processing module was designed for rapid prototyping and simulation of the archived data. For a pre-analysis of the input data, a suitable subset was selected such that there was sufficient excitation. With these multiple inputs, the neural networks effectively identified a system without a priori knowledge. In this case, a selected dataset consisting of multiple inputs from the process measurements and the corresponding output of the sand erosion loss measurement has been implemented to model a Multiple Input Single Output (MISO) system. Model training and validation constitutes an important aspect of modelling to minimise the problem of overfitting when presenting new data to the model. Model training was adopted methodically, and with a prior knowledge, parameters of the model was adjusted to obtain the optimum model based on a specific dataset.

5.2 Data Pre-processing

The neural network was trained with the training subset. After training, the weights of the trained network model were rescaled with the scaled mean and standard deviation before it was validated with the validation subset. In the algorithm, the dataset is divided into 3 parts; namely the training subset, validation subset and test dataset. The training subset was allocated a portion and the remaining portion was equally divided between the validation and test subsets. The dataset was comprised of the following

independent input variables, IV in Table 5-1 from the literature. (Gharagheizi).

Table 5-1: Independent Variables

Variable	Description	Units
BHFP	bottom hole flowing pressure	Kg/cm2
BHSP	bottom hole static pressure	Kg/cm3
COH	cohesive strength of the formation	Kg/cm4
CTD	critical total drawdown	Kg/cm5
DD	drawdown pressure	Kg/cm6
EOVS	effective overburden stress	Kg/cm8
Hperf	thickness of perforation interval	metres
LGR	Liquid Gas Ratio	number
ProdLife	Production Life	years
Qg	gas production rate	Ksm33/day
Qw	water production rate	litres//day
Sand	Sand detected	categorial (1,-1)
SPF	shot per foot	number
TT	transmit time	microsec/ft
TVD	total vertical depth	metres

The dependent variable, DV for the output was the presence of sand at these wells.

Normalization allows the removal of systematic bias in the data. Before training, the inputs and targets were scaled so that they fell around zero. Therefore, scaling was applied to obtain a mean of zero and a variance of unity. This effectively standardized all the measurements of the process parameters that were used in the neural network. One reason for the use of the variance in preference to other measures of dispersion was that the variance of the sum (or difference) of independent random variables is the sum of their variances.

A change in the combination of the variables' measurement provides an indication that sand is being produced downhole in the reservoir. The phenomenon cause sand to be produced to the surface and if the velocity

is high enough, this will result in sand erosion. Sand erosion in the flowline caused metal loss in the flowlines and equipment.

5.2.1 PCR Variance

The sum-of-squares is proportional to the covariance matrix and re-writing (4-9) as in (5-1),

$$E_M = \frac{1}{2} \sum_{i=M+1}^{d} u_i^T \Pi u_i \tag{5-1}$$

where $\mathbf{\Pi}$ is the covariance matrix of the set of vectors $\mathbf{u^n}$ and is given in equation (4-10) as shown in (5-2),

$$\Pi = \sum_{n} (u^n - \bar{u})(u^n - \bar{u})^T \tag{5-2}$$

The minimum occurs when the basis vectors selected are the eigenvectors with the largest eigenvalues of the covariance matrix.

In taking the eigenvalues of the covariance matrix, the principal component variances of the eigenvectors are given in Table 5-2 below.

Table 5-2: Eigenvalues or Variances of PCA Eigenvectors

Eigenvector	Eigenvalue	% Variance	Cumulative %
PC1	2.18	54.6%	54.6%
PC2	1.17	29.3%	83.8%
PC3	0.55	13.7%	97.5%
PC4	0.10	2.5%	100.0%

From the table it can be seen that the first principal component, PC1, was only able to explain 54.6% of the total variance. Generally, 80% of the variance were to be explained and it took at least the first two principal components, i.e., PC1 and PC2 in order to explain 83.8% of the total variance.

5.2.2 PLSR Variance

The SIMPLS algorithm computes a partial least squares (PLS) regression of the dependent variable, y on a number of predictor or independent variables, u using the PLS components or latent factors, and returns the predictor and response loadings.

u is a matrix of predictor variables, with rows corresponding to observations and columns to variables while y is a response matrix. In the predictor loadings, $uLoadings$, each row contains coefficients that define a linear combination of PLS components that approximate the original predictor variables. In the matrix of response loadings, $yLoadings$, each row contains coefficients that define a linear combination of PLS components that approximate the original response variables. The predictor scores, $yScores$, is an orthonormal matrix with rows corresponding to observations, columns to components and are the PLS components that are linear combinations of the variables in u. The response scores are the linear combinations of the responses with which the PLS components predictors scores have maximum covariance. The response scores matrix is neither orthogonal nor normalized.

The SIMPLS algorithm centres u and y by subtracting off column means to get centered variables $u0$ and $y0$. The relationships between the scores, loadings, and centered variables $u0$ and $y0$ are,

$$uLoadings = u0^T * uScores \tag{5-3}$$

$$yLoadings = y0^T * yScores \tag{5-4}$$

where $Xloadings$ and $Yloadings$ are the coefficients from regressing $x0$ and $\mathrm{y0}$ on $XScores$.

The partial least squares regression (PLSR) computes a 2-by-4 matrix that contains the percentage of variance explained by the model. The percent of variance explained for X and Y is computed using,

$$Var_u = \frac{\sum uLoadings^2}{\sum u0^2} \tag{5-5}$$

$$Var_y = \frac{\sum yLoadings^2}{\sum y0^2} \tag{5-6}$$

For the PLSR, the percentage variance explained in u by each PLS component or latent factor is given in Table 5-3.

Table 5-3: Variance for each PLSR component or Latent Factor

Latent Factors	Variance	Variance(%)	Cumulative %
PLS1	0.54	54.4%	54.4%
PLS2	0.12	12.4%	66.8%
PLS3	0.07	7.5%	74.3%
PLS4	0.26	25.7%	100.0%

From the table, there are four latent factors corresponding to the four PLS components. In order to explain at least 80% of the total variance, three PLS components were not sufficient as it cumulated to only 74.3% as the fourth PLSR component, PLS4 alone explained 25.7% of the variance. For comparison, the cumulative percentage variances for PCR and PLSR are plotted in Figure 5-1. It took all of the four PLS components because it required more information in the predictor variables that were important in fitting the response variable, y. Partial least squares regression (PLSR) finds components from u that are also relevant for y. PLSR searches for a set of components or latent vectors that performs a simultaneous decomposition of u and y with the constraint that these components explain as much as possible of the covariance between u and y. It is followed by a regression step where the decomposition of u is used to predict y. The goal of partial least squares regression is to predict y from

u and to describe their common structure. The PC curve is uniformly higher and suggests that PCR with two components, relative to PLSR, constructs components to best explain the predictors.

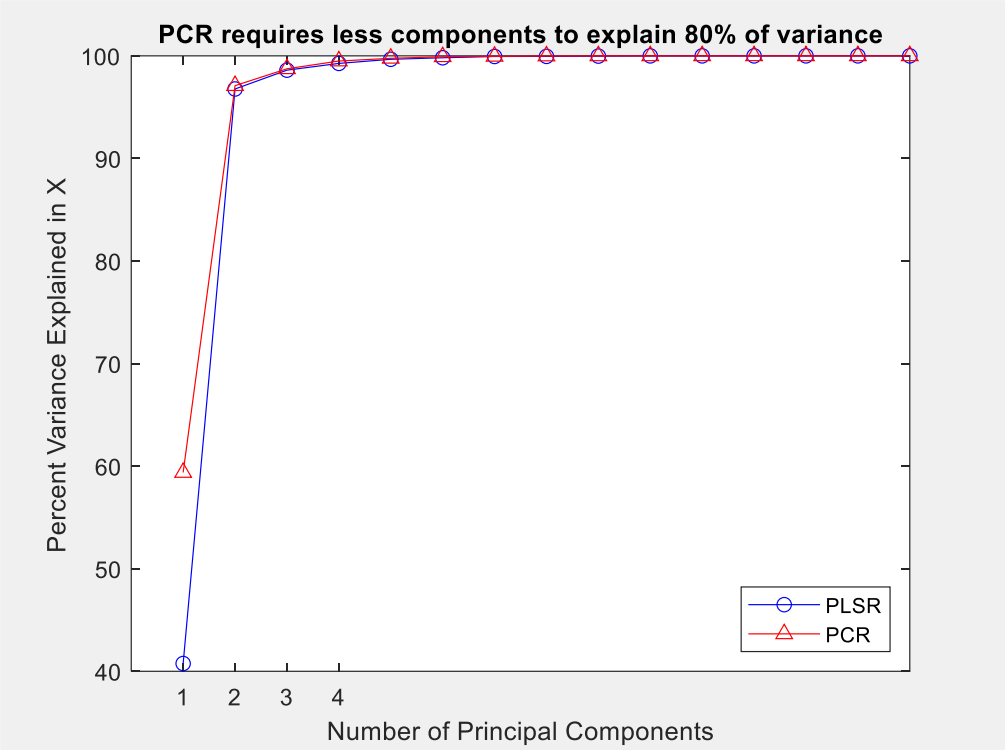

Figure 5-1: Model can be represented by 2 PCR Components

This is because in PCA, only the predictor variables were used to explain the variance without the need for any regression in y. PCR performs a principal component analysis of the u matrix and which then uses the principal components of u as regressors on y.

5.2.3 K-fold Cross-validation

Cross-validation is a more statistically sound method for choosing the number of components in either PLSR or PCR. It avoids overfitting data by not reusing the same data to both fit a model and to estimate prediction error. Thus, the estimate of prediction error is not optimistically biased downwards. The technique of cross-validation was used to determine the optimum number of principal components by calculating the mean squared prediction error (MSPE).

In principal components regression 10-fold cross-validation a vector of sum of squared prediction errors for principal components regression models with 0 to 10 components is produced, (with training data and test data). The 0^{th} model is just the mean of the training response data. It computes the PCA loadings from the training predictor data and regresses the first ten (10) principal components on the centred training response data. It then computes predictions for the first through the 10^{th} model. In partial least squares regression 10-fold cross-validation, a matrix containing the estimated mean squared errors for PLS models with 0 to 10 components is computed. The first row of the matrix contains mean squared errors for the predictor variables in u and the second row contains mean squared errors for the response variable(s) in y. The MSPE is calculated for the principal components (PC) for both PLSR and PCR regression models using the 10-fold cross validation technique and is tabulated in Table 5-4 below. It can be seen that the principal component 2 and 3 in PCR does not decrease the prediction error of the model, suggesting that the combination of predictor variables contained in that component is not strongly correlated with the dependent variable. This stems from the fact that PCR constructs components to explain variation in the predictive variables rather than the dependent variable. On the other hand, with two or three principal components for PLSR, the error approaches continue to steadily decrease and attains a minimum of 0.827.

Table 5-4: 10-Fold Cross validation for PLSR and PCR

	Mean Squared Prediction Error	
PC	**PLSR**	**PCR**
0	1.000	1.000
1	0.858	0.864
2	0.843	0.864
3	0.829	0.854
4	0.828	0.827

5.2.4 Model Parsimony

From the comparison of the MSPE, the different aspects need to be considered as to which model is more parsimonious between that of the PLSR or PCR. The PLS weights are the linear combinations of the original variables that define the PLS components. Similarly, the PCR loadings describe how influential each component in the PCR depends on the original predictor variables. In selecting the PCR components that best represent the predictor variables, the eigenvalues of the eigenvectors for can be plotted for the PCR loadings. Likewise, the PLSR weights of each of the PLSR components or latent vectors can be graphically depicted for comparison as shown in Figure 5-2.

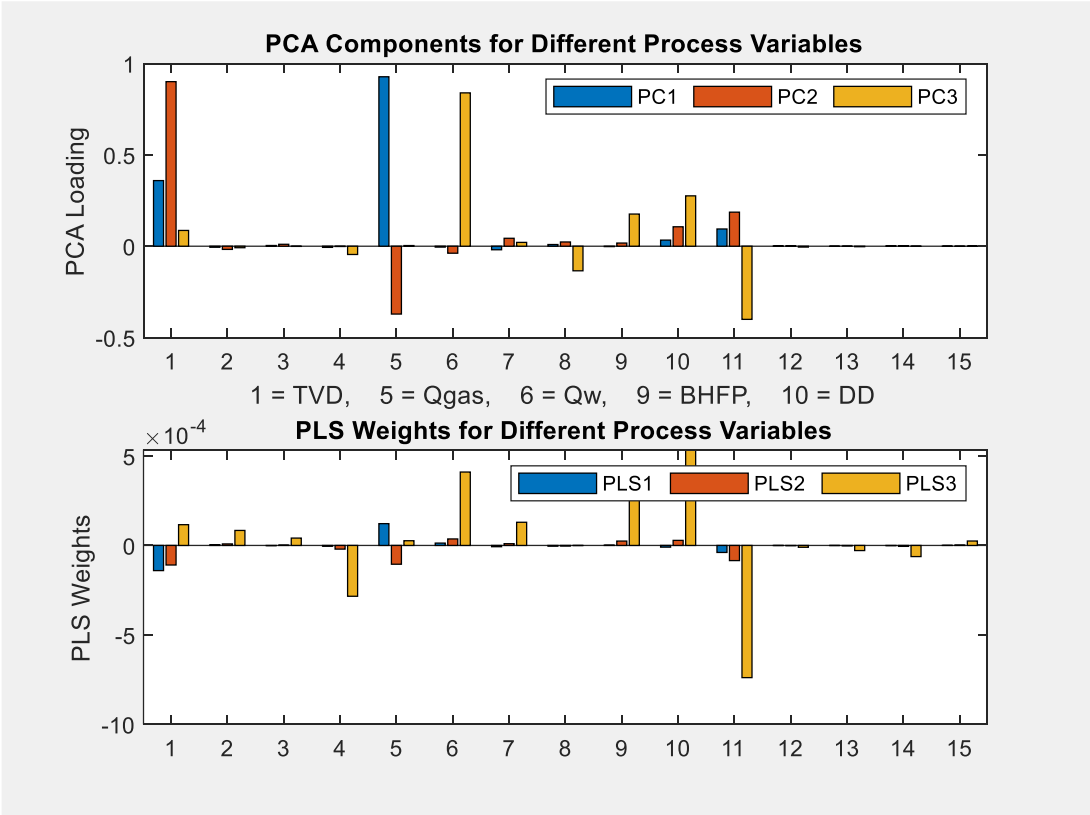

Figure 5-2: Comparison PCR Loadings and PLSR Weights

It can be seen that predictor variables TVD(1), Qgas(5) and Qw(6) have maximum PCALoadings for PCR principal component PC1, PC2 and

PC3. On the other hand, PLSR weights are largest for principal component for Qw(6), BHFP(9) and DD(10).

5.3 Model Structure

5.3.1 Regressors

Due to the complexity, uncertainty and nonlinearity a large class of systems, appropriate models it is difficult to derive accurate and complete equations for input-state-output representations of the systems from first principles. Input-output models based on input-output data are employed to represent the unknown nonlinear systems. The identification from sampled input and output signals involve the identification of model orders and nonlinear function approximation. In order to obtain a valid neural network model based on prediction error principle, the model orders as shown in Figure 5-4 and the number of hidden units must be determined.

Figure 5-3: Order lag space of inputs and outputs

The model order is represented the number of regressors comprising of past outputs and past inputs of a specific input-output pair in a SISO

network. For a MISO network, the model order is effectively the number of regressors associated with each individual input-output pair for each variable. Hence, for a network with 5 input variables and a single output variable, there would be as many regressors as the sum of all the regressors for each input-output variable pair.

The number of regressors were taken into account for the 5 independent variables. For e.g., for the input variable TVD, there are 4 past inputs, and they are fed into the neural network as regressors. There is only one dependent variable, DV, and hence, in the case of TVD, 4 previous outputs are fed back fed into the neural network as regressors. If a SISO model was implemented with TVD as a single input and SAND as the output, then the NNARX network would be the sum of all the regressors of the past inputs and past outputs. In this case, the total no. of regressors would be the sum of the 4 past inputs of TVD and the 4 past outputs of SAND. Hence, the total no. of regressors would be the size of the input layer, and with the example given, the size of the input layer would be 8 neurons, while the size of the size of the output layer would be 1 neuron. In this instance, the total number of regressors for the SISO Model using the NNARX structure would be 8.

Likewise, if two variables were selected instead, a MISO model would be implemented, and the total no. of regressors would be the sum of the 4 past inputs of the first variable, sum of the 4 past inputs of the second variable and the sum of the 4 past outputs. In this case, the 4 past outputs required for the first variable takes precedence to the 2 past outputs of the second variable. In implementing the MISO model using two input variables each with 4 different past inputs but with 4 past outputs and 2 past outputs respectively, the total number of regressors is twelve instead of ten.

Essentially, in the implementation of MISO models, the input variable with the maximum no. of past outputs dictates the no. of past outputs to be used in the summation of the total no. of regressors. On the other hand,

if the input with the minimum no. of past outputs is considered, then the input variable which would have required 4 past outputs would be deprived from information from the two past outputs (regressors) that have been omitted. The drawback would be that the NNARX model would take a longer processing time due to 2 additional past output regressors for the two variables. However, the benefit that is obtained from not omitting the 2 required past outputs each for the first variables outweighs the slightly longer processing time for the next variables.

Consider the case where 5 input variables are used to build a MISO model with NNARX structure, to predict the onset of SAND production. The schematic of the neural network is depicted with 4 past inputs for variables TVD and Qgas, while 3 past inputs for variable Qw, and 2 past inputs for variable BHFP while no past input for variable DD. Hence, 13 past inputs of the input variables. For the dependent variable, SAND which is to be predicted, 4 past outputs were selected to build the model and the NNARX structure is shown in Figure 5-4.

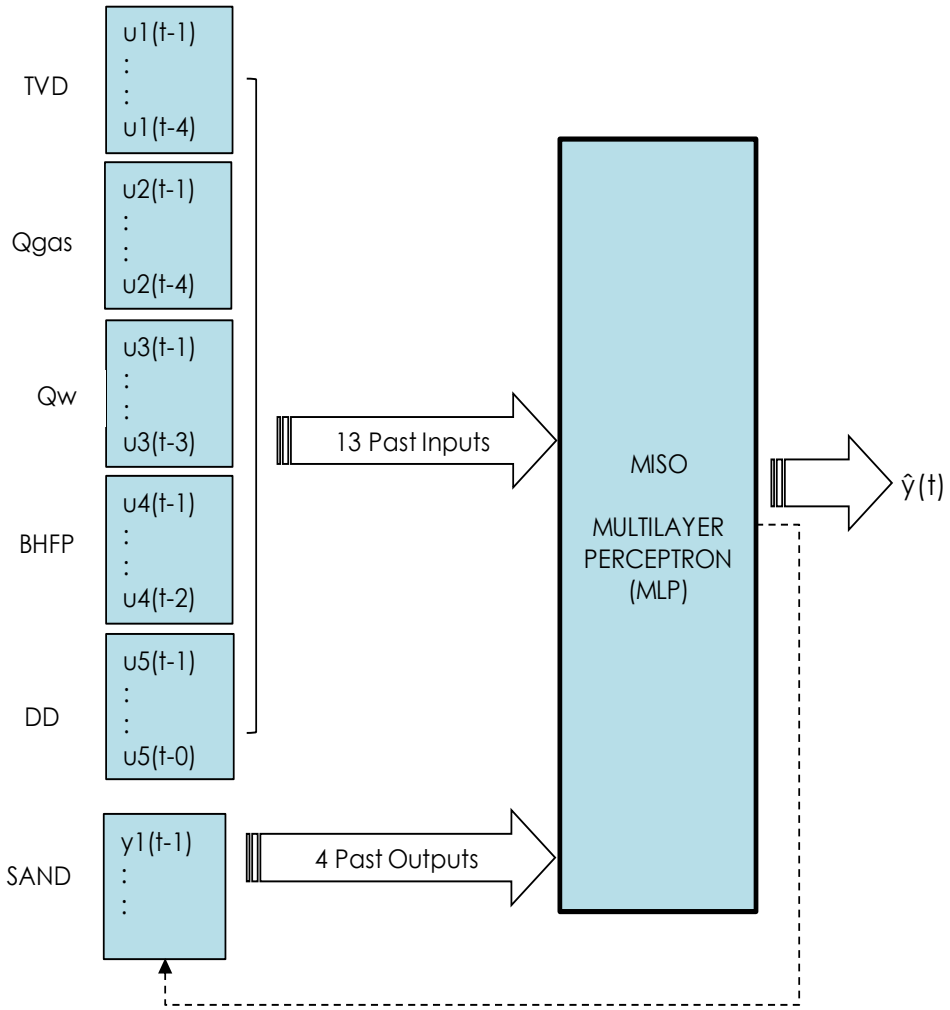

Figure 5-4: Regressors for a 5-Input Single Output (MISO)

5.3.2 Training, Validation and Test Data-subsets

The need to validate the neural network model was required to ascertain the confidence level of any model. Validation was carried out by computing the cross-correlations and autocorrelations to determine the performance index. The dataset is subdivided into the following proportion; Training Subset (40%), Validation Subset (40%) and Independent Test Subset (20%). The dataset sub-division was illustrated as shown in Figure 5-5.

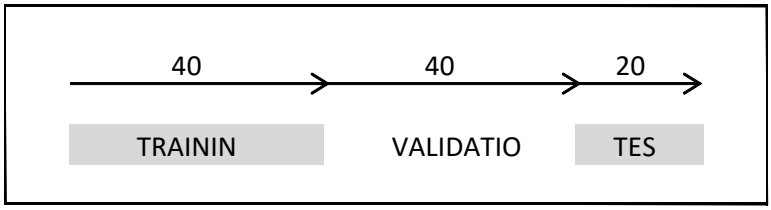

Figure 5-5: Model Validation with 40-40-20 Ratio

The validation set was used together with the training set to prune the neural network. Due to the network ending up in a "bad" local minimum, it should be trained starting from different initial weights. Regularization has a tremendous smoothing effect on the local minimum. Nevertheless, local minima remains one of the major problems for nonlinear regressions and pruning has to do with obtaining the optimal network architecture selection.

5.3.3 Neural Network Parameters

The parameters of the neural network in terms of its structure, regression vectors, no. of hidden layer, no. of input and output neurons, activation function used in the hidden layer and training algorithms are shown in Table 5-5 below. The architecture for the neural network was a multilayer perceptron (MLP) with four inputs, with an arbitrary determined number of hidden neurons in the hidden layer and a single linear neuron in the output layer.

Table 5-5: Network Parameters

Parameter	Description of Parameter
Model Structure	Nonlinear Auto Regressive with Exogenous inputs (NNARX)
Regression Vector	[na nb nk] na = number of past outputs nb = number of past inputs nk = delay (typically =1)
Network Architecture	Number of Input Layer Neurons = 4 (IV)
	Number of Hidden Layers = 1
	Number of Hidden Layer Neurons = 6
	Number of Output Layer Neurons = 1 (DV)

Parameter	Description of Parameter
Activation Functions	Hidden Layer: Fast Hyperbolic Tangent Function (tanh)
	Output Layer: Linear Function
Training Algorithm	Levenberg-Marquart Algorithm

5.3.4 Performance Indices

The number of hidden neurons in the hidden layer was determined during training of the network by measuring the performance indices of the training and validation and test subsets. The performance of the network is measured by determining the normalised sum of squared error (NSSE).

- Performance Index of Training Subset: $NSSE_{Train}$
- Performance Index of Validation Subset: $NSSE_{Valid}$
- Performance Index of Test Subset: $NSSE_{Test}$

Moreover, in order to prevent overfitting, the trained network was further pruned, and the performance indices of the pruned neural network was measured accordingly.

- Pruned Performance Index of Training Subset: $NSSE_{Train_P}$
- Pruned Performance Index of Validation Subset: $NSSE_{Valid_P}$
- Pruned Performance Index of Test Subset: $NSSE_{Test_P}$

A total of six performance indices were computed for the dataset and was recorded in the Performance Database. Residual analysis of the performance indices facilitated and enabled model selection of the neural network in terms of the required number of neurons in the hidden layer of the neural network and its corresponding learning rate, λ.

5.4 Residual Analysis

Residuals are differences between the one-step-predicted output from the model and the measured output from the validation data set. Thus, residuals represent the portion of the validation data not explained by the

model. Residual analysis consists of two tests, namely the whiteness test and independence test (Ljung, 1999). The most common method of validation is to investigate the residuals (prediction errors) by cross-validation on a validation subset. The autocorrelation function of the residuals and cross-correlation function between controls and residuals were used to validate the test set.

5.4.1 Autocorrelation

For sampled signal, the autocorrelation is defined as either biased or unbiased for $m = 1, 2, \ldots\ldots, N+1$ for both the unbiased and the biased cases (Rodgers and Nicewander, 1988).

For the Unbiased Autocorrelation:

$$R_{uu}(m) = \frac{1}{N - |m|} \sum_{n=1}^{N-|m|+1} u(n)u(n+m-1) \tag{5-7}$$

For the Biased Autocorrelation:

$$R_{uu}(m) = \frac{1}{N} \sum_{n=1}^{N-|m|+1} u(n)u(n+m-1) \tag{5-8}$$

According to the whiteness test criteria, a good model has the residual autocorrelation function inside the confidence interval of the corresponding estimates, indicating that the residuals are uncorrelated (Hipel, McLeod, and Lennox, 1977).

5.4.2 Cross-correlations

The cross correlation function measures the dependence of the values of one signal on another signal (Rodgers and Nicewander, 1988). For sampled signals, it is defined as,

$$R_{yu}(m) = \frac{1}{N} \sum_{n=1}^{N-|m|+1} y(n)u(n+m-1) \tag{5-9}$$

for $m = 1,2 \ldots\ldots (N+1)$ and where N is the number of samples.

Cross-correlation is a measure of similarity of two waveforms as a function of a time lag applied to one of them, while the auto-correlation is the cross-correlation of a signal with itself. According to the independence test criteria, a good model has residuals uncorrelated with past inputs. Evidence of correlation indicates that the model does not describe how part of the output relates to the corresponding input (Haugh, 2010). A peak outside the confidence interval for lag k means that the output $y(t)$ that originates from the input $u(t-k)$ is not properly described by the model.

5.5 Model Estimation

5.5.1 Validation Before Model Pruning

The performance index for the training subset before pruning, *NSSE_Train* was recorded for network architecture comprising of an arbitrary value of five (5) neurons in the hidden layer, HL. The measure of the performance index used was the minimum Normalised Sum of Squared Error (NSSE_min). The network was trained and validated using the training and validation data-subsets, respectively. The corresponding performance index was measured for these subsets and the values for $NSSE\_\min\ \_Train$ and $NSSE\_\min\ \_Valid$ were recorded.

The performance of the validation data subset was higher than the training data subset. This was due to overtraining as a result of having too many weights. After the network has been trained and validated, the test data-subset was used to predict SAND and the performance index of the test subset, $NSSE_{Test}$.

The performance index of the test data-subset was much lower than that of the training data-subset. Residual analysis using the whiteness and independence tests were carried out on results of the model estimation. Both tests under the residual analysis failed indicating that there were lag

orders which exceeded the 95% confidence limit. However, although the $NSSE_{Test_P}$ error was a minimum, the result was rejected as it did not pass both the whiteness and independence tests. Hence, there was a requirement for residual analysis to be successful for the result to be accepted. In this instance, the minimum value of the normalised sum of squared error of the test datasubset, $NSSE_{Test_P}$, was not a sufficient condition for acceptance of the result. This is due to the fact that the model had too many redundant weights and it was a case of overfitting, and hence, the result was rejected. In order to remove the redundant weight, the network was pruned using the OBS strategy.

The model was pruned and the corresponding performance indices of the training ($NSSE_{Train_P}$), validation ($NSSE_{Valid_P}$) and test ($NSSE_{Test_P}$) data-subsets.

The pruning strategy adopted worsened the performance index of the training error from a minimum value of $\mathbf{NSSE_{Train}}$ of 1.42E-12 to a value of $NSSE_{Train_P}$ after pruning to 1.32E-00. The reason for this is that training data is trained with a much-reduced number of weights. These weights are the weights that have remained after the network has been pruned and represents the optimum pruned network. However, there is a significant improvement on the validation data-subset as a result of pruning from a value of $NSSE_{Valid}$ of 2.16E-01 to three orders of magnitude better to a value of $NSSE_{Valid_P}$ of 1.1E-01. This improvement in the validation data-subset is attributed to the absence of redundant weights which have a relative lower value. Those weights with lower relative values are removed as they contribute less to the network. When tested with an independent set of test data-subset, the pruned network exhibited a significant improvement $NSSE_{Test}$ of 8.85E-00 to a value of $NSSE_{Test_P}$ of 1.35E-00. The marked improvement underwent a residual analysis. In both the whiteness and independent tests, the auto-correlations cross-correlations respectively were stayed within their standard deviations. Since the predictions were

not as good as the validation data, these tests indicates that the neural network is overfitting the data.

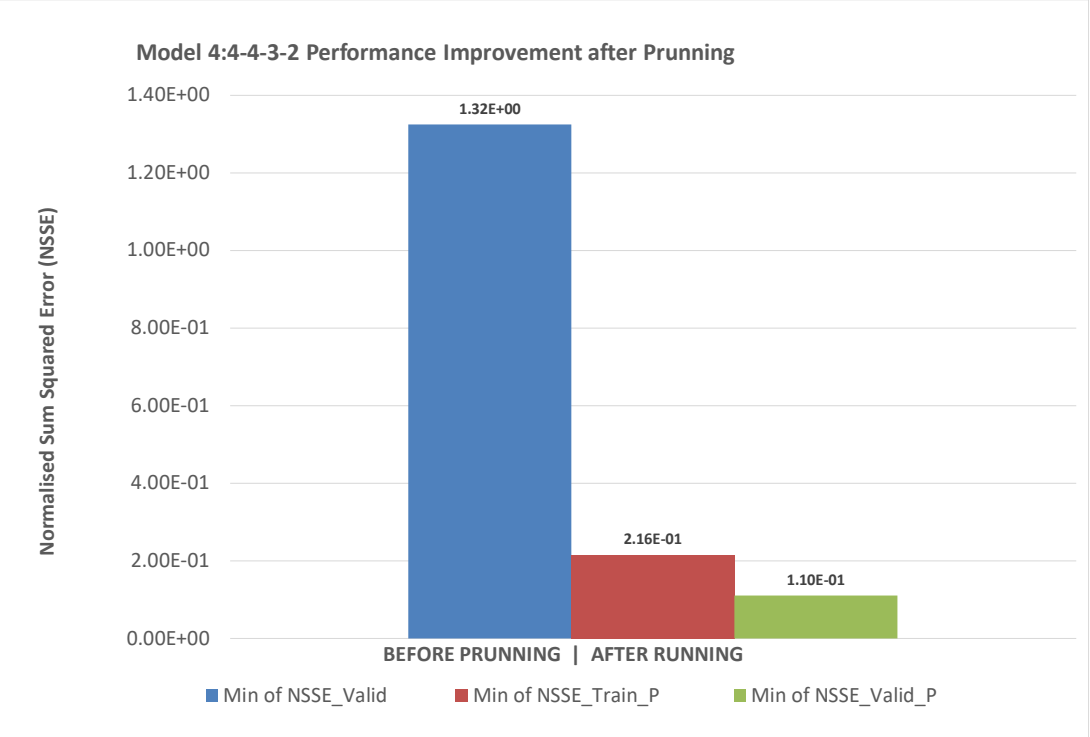

Figure 5-6: Normalised Sum of Squared Error Before/After Prunning with 13 Neurons

The final regressor selected for the Neural Network Auto Regressive with Exogenous inputs (NNARX) model was [4:4-4-3-2] i.e., with a total of 17 exogenous inputs (4 past outputs and 13 past inputs).

5.6 Regression models

Sand production can be measured with a correlation to all the four process variables. In terms of which combinations of process variables or components have a stronger influencing contribution to the sand production, principal component analysis was conducted. A linear regression model using the dataset subsets testing for the fitting of the 5 predictor variables with the response variable to obtain the principal components. The minimization of the expected error in predicting the response from future observations on the predictor variables selected the

number of principal components. A large number of components will fit the current observed data but will cause overfitting. Therefore, the model will give an optimistic estimate of the expected error with a poor generalization for new prediction.

5.6.1 Hidden Layer Neurons

There are many rule-of-thumb methods as shown in Table 5-6 for determining the correct number of neurons to use in the hidden layers.

Table 5-6: Rules of Thumb for No. of Hidden Layers

Claims	Description of Claim	Symbolic
1	The number of hidden neurons, N_{HL} should be between the size of the input layer, S_I and the size of the output layer, S_O.	$S_O < N_{HL} < S_I$
2	The number of hidden neurons, N_{HL} should be 2/3 of the size of the input layer, S_I plus the size of the output layer, S_O.	$N_{HL} = 2/3 * S_I + S_O$
3	The number of hidden neurons, N_{HL} should be less than twice the size of the input layer, S_I.	$N_{HL} < 2 * S_I$

The above rules of thumb were taken into account when designing the neural network based on the generalisation of test error. Based on rules of thumb for choosing the no. of hidden layers, the total number of neurons in the input layer depends on the model order of the corresponding input variables.

5.6.2 Plots of Residual Analysis

Figure 5-7 shows an analysis of the network response was performed by feeding the entire data set through the network (training and test) employing the autocorrelation of the prediction error.

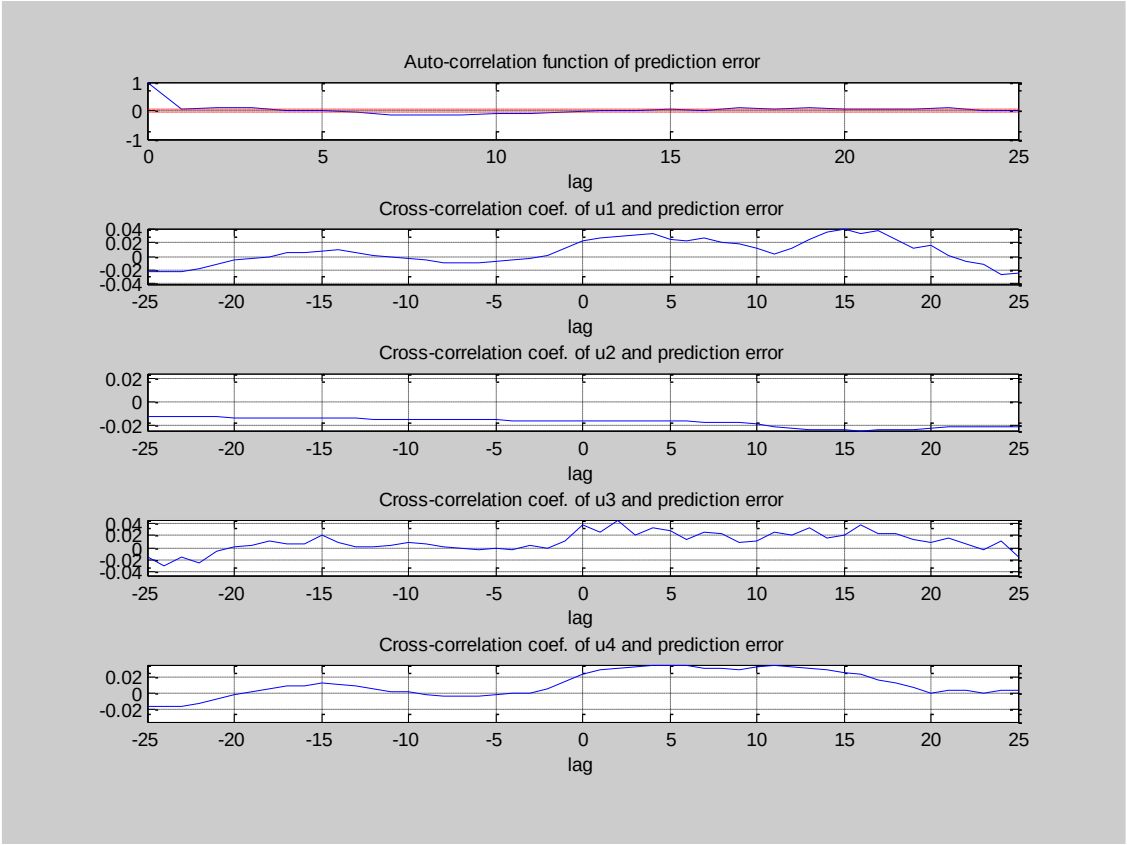

Figure 5-7: Autocorrelations and cross-correlations after pruning based on 4 input variables

5.6.3 Initial Learning Rate, $NSSE_{Test_{ILR}}$

The initial learning rate is varied between 0.1 and 0.9 and the performance index of the Test subset is recorded as $NSSE_{Test_{ILR}}$ and shown in Figure 5-8.

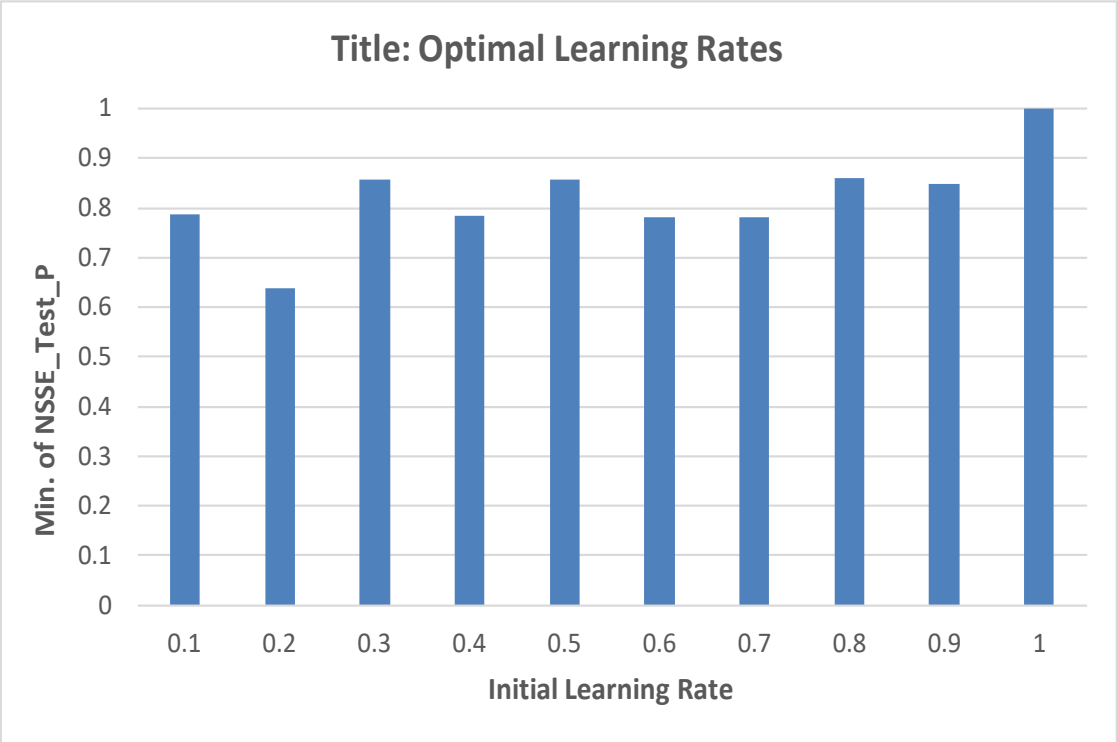

Figure 5-8: Improved performance at low initial learning rate of 0.2

5.7 Summary

Model training and validation constitute an important aspect of modelling to ensure that the problem of overfitting is minimised. Cross-validation is a statistically sound method for choosing the number of components in PLSR or PCR. With PCR, linear regression can be carried out with the output vector or the dependent variable. A comparison is made with partial least squares to choose the optimum number of components using the k-fold cross-validation to compute the mean square prediction error. The model was validated with an independent test set. In order to increase the robustness of the model, round robin tests using random slices of the dataset that were circularly shifted. The model variation amongst the three different subsets was tested to recreate different ratios for model training and validation.

Information on datasets can be made available in order to realise artificial neural network systems as shown in Figure 5-9. In the absence of

reliable equipment to monitor the onset of sand production, data driven models will become the preferred technique in addressing the high degree of uncertainty.

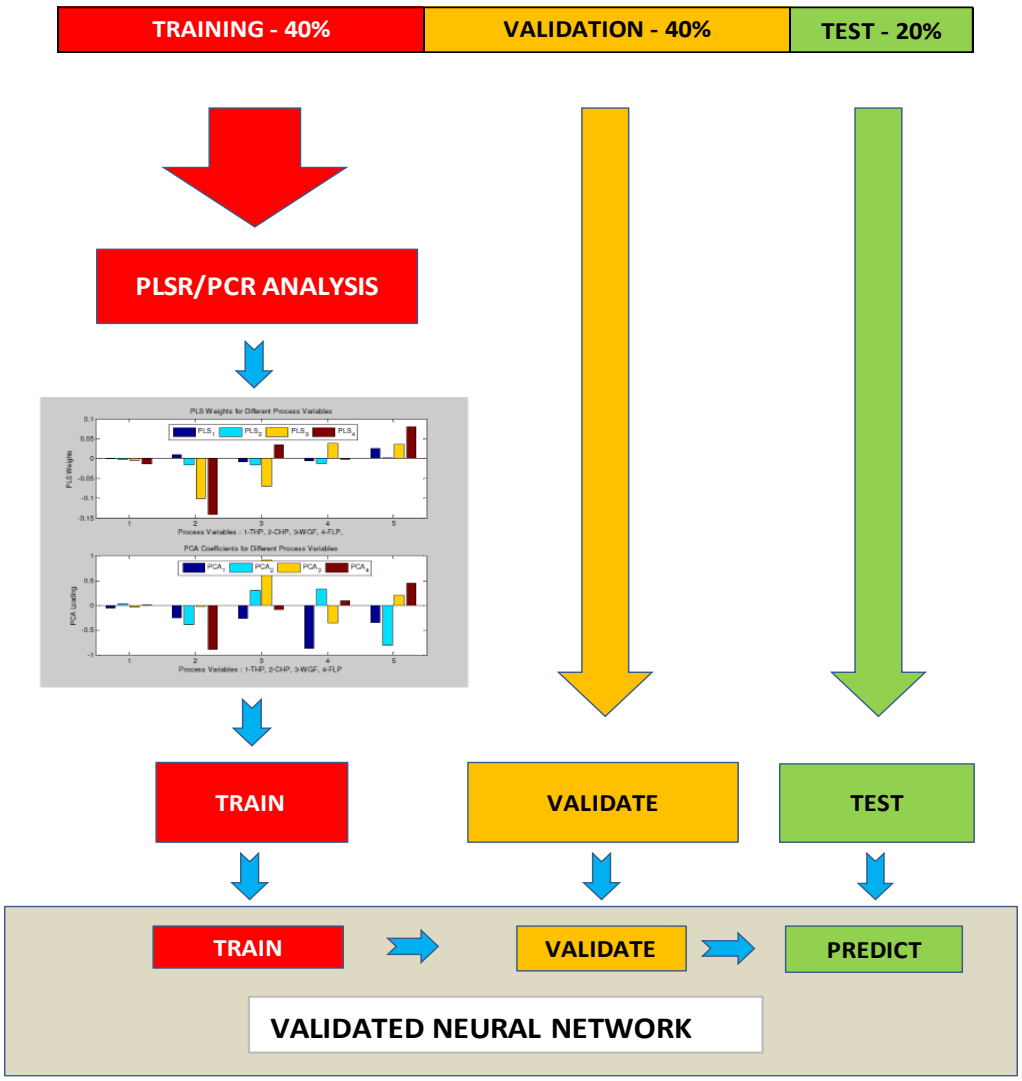

Figure 5-9: ANN-based Sand Prediction System

CHAPTER 6

CONCLUSION AND RECOMMENDATION

6.1 Conclusion

The presence of prolonged sand production has detrimental effects to the continuous and safe production of oil and gas. The prediction of the onset of sand production allows mitigative measures to be taken by production operators in order prevent the erosive and corrosive damage to equipment. Although sand monitoring devices are common in the oil and gas industry to assess the undesirable effects of sand production, the cost associated with the installation, operation, maintenance and replacement of a sand monitoring system is expensive. Besides, there are the indirect cost incurred with the mobilisation of personnel and logistics to carry out these activities. More importantly, the increasing exposure of people to health, safety and environmental hazards when they are involved in activities connected with a sand monitoring system.

6.2 Recommendation

An area that can be explored would be the use of long short-term memory of LSTM's when there is larger datasets available with the application of deep learning networks.

Real time production data and process engineering data from oil and gas wells could be implemented with the present algorithm for the early detection of the onset of sand production, and possibly its commercial viability.

REFERENCES

(n.d.). doi:https://doi.org/10.2118/28066-MS

Abdelgawad, A., Merhi, Z., Elgamel, M., & Bayoumi, M. (2009). Multisensor Data Fusion Methods for Petroleum Engineering Applications., (pp. 17--19).

Ali, J. (1994). Neural Networks: A New Tool for the Petroleum Industry?

Anderson, D., & McNeill, G. (1992). Artificial neural networks technology. *Kaman Sciences Corporation*.

Battiti, R. (1992). First-and second-order methods for learning: between steepest descent and Newtons method. *Neural computation, 4*, 141--166.

Bauer, M., & Craig, I. K. (2008). Economic assessment of advanced process control-A survey and framework. *Journal of Process Control, 18*, 2--18.

Birkeland, R., Lilleland, S. E., Johnsen, R., & Braaten, N. A. (1998). Erosion monitoring manages sand production. *Oil and Gas Journal, 96*, 63--71.

Bishop, C. M. (1995). *Neural networks for pattern recognition.* Oxford university press.

Bratvold, R., Bickel, J. E., & Lohne, H. P. (2009). Value of information in the oil and gas industry: past, present, and future. *SPE Reservoir Evaluation & Engineering, 12*, 630--638.

Brown, G. (1997). External Acoustic Sensors and Instruments for the Detection of Sand in Oil and Gas Wells.

Brown, G. K., & Davies, R. (2000). Solids and Sand Monitoring-An Overview. *CORROSION 2000*.

Burns, F., Carlson, D., Haynsworth, E., & Markham, T. (1974). Generalized inverse formulas using the Schur complement. *SIAM Journal on Applied Mathematics, 26*, 254--259.

Centilmen, A., Ertekin, T., & Grader, A. (1999). Applications of neural networks in multiwell field development.

Chen, S., & Billings, S. (n.d.). Neural networks for non-linear dynamic system modelling and identification. *Advances in Intelligent Control*.

Chitale, A., Stein, M., Arias, B., & Narayanan, R. (2009). A New Methodology To Safely Produce Sand Controlled Wells With Increasing Skin.

Cirrincione, M., Pucci, M., Cirrincione, G., & SimÃµes, M. (2005). A neural non-linear predictive control for PEM-FC. *J. Electrical Systems, 1*, 1--18.

Cybenko, G. (1989). Approximation by superpositions of a sigmoidal function. *Mathematics of Control, Signals, and Systems (MCSS), 2*, 303--314.

Diebold, F. X., Barro, R. J., Marthinsen, J. E., Carbaugh, R., Yarbrough, B. V., Yarbrough, R. M., . . . Hyclak, T. (2005). *Elements of forecasting.* Thomson, 2004.

DNV, R. (1999). O501 Erosive Wear in Piping Systems, 1994, reprint 1999. *DNV, Norway*.

Faga, A., & Oyeneyin, B. (2000). Application of Neural Networks for Improved Gravel-Pack Design.

Falcone, G., Teodoriu, C., Reinicke, K., & Bello, O. (2007). Multiphase Flow Modelling Based on Experimental Testing: A Comprehensive Overview of Research Facilities Worldwide and the Need for Future Developments.

Fortes, J. A. (2003). Future Challenges in VLSI Design.

Fuh, G. F., Ramshaw, I., Freedman, K., Abdelmalek, N., & Morita, N. (2006). Use of Reservoir Formation Failure and Sanding Prediction Analysis for Viable Well-Construction and Completion-Design Options.

Gharagheizi, F. M.-2. (n.d.). Prediction of sand production onset in petroleum reservoirs using a reliable classification approach. Petroleum, 3(2), 280-285.

Gorelick, S. M. (2009). Oil Panic and the Global Crisis: Predictions and Myths. Wiley-Blackwell.

Green, A., Johnson, B., & Choi, N. (1993). Flow-Related Corrosion in Large-Diameter Multiphase Flowlines. *Old Production & Facilities, 8*, 97--100.

Guinot, F., Duncan, J., Douglass, S., Orrell, M., & Stenger, B. (2009). Sand Exclusion and Management in the Okwori Subsea Oil Field, Nigeria. *SPE Drilling & Completion, 24*,

157--168.

Gunningham, M., Addis, M., & Hother, J. (2008). Applying Sand Management Process on the Lunskoye High Gas-Rate Platform using Quantitative Risk Assessment.

Hansen, L. K. (1994). Controlled growth of cascade correlation nets. pp. 797--800.

Hassibi, B., & Stork, D. G. (1993). Second order derivatives for network pruning: Optimal brain surgeon. *Advances in neural information processing systems*, 164--164.

He, X., & Asada, H. (1993). A new method for identifying orders of input-output models for nonlinear dynamic systems., (pp. 2520--2523).

Hebb, D. O. (1949). The organization of behavior: A neuropsychological approach. NewYork: John Wiley & Sons. Hinton, GE (1989). Deterministic Boltzmann learning performs steepest descent in weightspace. Neural Computation, 1, 143--150.

Hernandez, W. (2005). Robust multivariable estimation of the relevant information coming from a wheel speed sensor and an accelerometer embedded in a car under performance tests. *Sensors, 5*, 488--508.

Hornik, K. (1991). Approximation capabilities of multilayer feedforward networks. *Neural Networks, 4*, 251--257.

Huser, A., & Kvernvold, O. (1998). Prediction of sand erosion in process and pipe components., *31*, pp. 217--228.

Islam, M., & Wellington, S. (2001). Past, Present, and Future Trends in Petroleum Research.

Jolliffe, I. T. (1986). *Principal component analysis* (Vol. 487). Springer-Verlag New York.

Kanj, M., & Abousleiman, Y. (1999). Realistic Sanding Predictions: A Neural Approach.

Kim, T., & Adali, T. (2003). Approximation by fully complex multilayer perceptrons. *Neural Computation, 15*, 1641--1666.

Kovalerchuk, B., Todd, C., & Henderson, D. (n.d.). Testing neural networks using the complete round robin method.

Levenberg, K. (1944). A method for the solution of certain nonlinear problems in least squares. *Quart. Appl. Math, 2*, 164--168.

Ljung, L. (1987). *System identification.* Springer.

Ljung, L. (2001). Black-box models from input-output measurements., *1*, pp. 138--146.

Ljung, L. (2013). System Identification Toolbox™ User's Guide 8.2.

Ltd, C. I., No, E., & Instruments, L. (2009). Product Showcase. *Insight-Non-Destructive Testing and Condition Monitoring, 51*, 405--407.

Lunde, G. G., Vannes, K., McClimans, O., Burns, C., & Wittmeyer, K. (2009). Advanced Flow Assurance System For The Ormen Lange Subsea Gas Development.

Marsh, J., Teh, T., Ounnas, S., & Richardson, M. (2009). Corrosion Management for Aging Pipelines--Experience From the Forties Field. *SPE Projects, Facilities & Construction, 4*, 1--7.

Massie, I., Nygaard, O., & Morita, N. (1987). Gullfaks Subsea Wells: An Operators Implementation of a New Sand Production Prediction Model.

Mazumder, Q. H., Shirazi, S. A., & McLaury, B. S. (2008). Prediction of Solid Particle Erosive Wear of Elbows in Multiphase Annular Flow-Model Development and Experimental Validations. *Journal of Energy Resources Technology, 130*, 023001.

McCartney, R., Burgos, A., & Sorhaug, E. (2010). Changing the Injection Water on the Blane Field, North Sea: A Novel Approach to Predicting the Effect on the Produced Water BaSO4 Scaling Risk.

McCulloch, W. S., & Pitts, W. (1943). A logical calculus of the ideas immanent in nervous activity. *Bulletin of Mathematical Biology, 5*, 115--133.

McLaury, B. S., Shirazi, S. A., & Rybicki, E. F. (2010). Sand Erosion in Multiphase Flow For Slug and Annular Flow Regimes. *CORROSION 2010*.

McNichol, J., Getzlaf, D., & Protz, M. (2001). Neural Network Analysis Identifies Production Enhancement Opportunities in the Kaybob Field.

Mevik, B.-H., & Cederkvist, H. R. (2004). Mean squared error of prediction (MSEP) estimates

for principal component regression (PCR) and partial least squares regression (PLSR). *Journal of Chemometrics, 18*, 422--429.

Moricca, G. R. (1994). Basin scale rock mechanics: field observations of sand production. In Rock Mechanics in Petroleum Engineering. OnePetro.

Morita, N., & Boyd, P. (1991). Typical Sand Production Problems Case Studies and Strategies for Sand Control.

Norgaard, M., Ravn, O., & Poulsen, N. K. (2002). NNSYSID-toolbox for system identification with neural networks. *Mathematical and Computer Modelling of Dynamical Systems, 8*, 1--20.

Norgaard, M., Ravn, O., Poulsen, N. K., & Hansen, L. K. (2000). Neural networks for modelling and control of dynamic systems: A practitioners handbook. Springer Verlag.

Nouri, A., Vaziri, H., Belhaj, H., & Islam, M. (2006). Sand-Production Prediction: A New Set of Criteria for Modeling Based on Large-Scale Transient Experiments and Numerical Investigation. *SPE Journal, 11*, 227--237.

Oberwinkler, C., & Stundner, M. (2005). From Real Time Data to Production Optimization. *Old Production & Facilities, 20*, 229--239.

Olufemi, A., & Darlington, E. (2010). Effect of Sand Production on Pressure Drop for Vertical Wells in Gas Storage Reservoir.

Oluyemi, G. F., Oyeneyin, B. M., & Macleod, C. (2010). UCS Neural Network Model for Real Time Sand Prediction. *International Journal of Engineering Research in Africa, 2*, 1--13.

OSU, A. H. (2004). HSE Offshore: Research reports.

Oyeneyin, M., Macleod, C., Oluyemi, G., & Onukwu, A. (2005). Intelligent Sand Management.

Pearl, J. (1987). Evidential reasoning using stochastic simulation of causal models. *Artificial Intelligence, 32*, 245--257.

Pederson, M., Hansen, L., & Larsen, J. (1995). Pruning with generalization based weight saliences., (p. 8).

Pots, B. F., Hendriksen, E. L., & Hollenberg, J. (2006). What are the real influences of flow on corrosion? *CORROSION 2006*.

Priestley, M. (1988). Non-linear and non-stationary time series analysis.

Ranganathan, A. (2008). The levenberg-marquardt algorithm. Georgia Tech College of Computing, http://www. cc. gatech. edu/\~ ananth/docs/lmtut. pdf, last accessed Oct.

Rojas, R. (1996). Neutral Networks: A Systematic Introduction. Springer.

Rosenblatt, F. (1958). The perceptron: A probabilistic model for information storage and organization in the brain. *Psychological review, 65*, 386--408.

Rosenblatt, F. (1962). Principles of neurodynamics: Perceptrons and the theory of brain mechanisms. Spartan Books, Washington, DC.

Salama, M. M. (2000). Performance of Sand Monitors. *CORROSION 2000*.

Sengul, M., & Bekkousha, M. (2002). Applied Production Optimization: i-Field.

Shirazi, S. A., Ali, M., & McLaury, B. S. (2000). Sand Monitor Evaluation in Multiphase Flow. *CORROSION 2000*.

Singh, B., Jukes, P., Wittkower, R., & Poblete, B. (2009). Offshore Integrity Management 20 years On-An Overview of Lessons Learnt Post Piper Alpha.

Singh, B., Krishnathasan, K., & Consulting--JPKenny, I. (2009). Pragmatic Effects of Flow on Corrosion Prediction.

Svedeman, S. (1994). Criteria for sizing multiphase flowlines for erosive/corrosive service. *Old Production & Facilities, 9*, 74--80.

Tan, Y., & Van Cauwenberghe, A. (1996). Nonlinear one-step-ahead control using neural networks: Control strategy and stability design* 1. *Automatica, 32*, 1701--1706.

The MathWorks, I. (2013). *Statistics Toolbox™ User's Guide 8.2.* Natick, Massachusetts, United States: The MathWorks, Inc.

Venkatesh, E. (1986). Erosion damage in oil and gas wells.

Veritas, D. E. (2009). Risk based inspection of offshore topsides static mechanical equipment.

Wallace, M., Dempster, W., Scanlon, T., Peters, J., & McCulloch, S. (2004). Prediction of impact erosion in valve geometries. *Wear, 256*, 927--936.

White, R. H. (1992). Competitive hebbian learning: Algorithm and demonstrations. *Neural Networks, 5*, 261--275.

Yi, X., Valko, P., & Russell, J. (2004). Predicting critical drawdown for the onset of sand production.

Yinghong, Z., Mingming, Q., Min, Z., Benjing, D., Cunzhi, C., & Zuokun, Z. (2008). Questions and comprehensive economic evaluation model for sand management.

Zhang, Y., McLaury, B. S., & Shirazi, S. A. (2009). Improvements of Particle Near-Wall Velocity and Erosion Predictions Using a Commercial CFD Code. *Journal of Fluids Engineering, 131*, 031303.

Publications derived from the Research:

Jayasuriya T D, Chekima A. 2010. Optimizing Learning Rates in Neural Network Applications. 1st Graduate Science Student Research Conference, Bandar Seri Begawan, Brunei Darussalam

Jayasuriya T D, Chekima A. 2010. Green Computing: Neural Network-based Virtual Instrumentation. In Proceedings of the 2nd IET Brunei International Conference, Bandar Seri Begawan, Brunei Darussalam.

Jayasuriya T D, Hamid M Y, Sainarayanan G, 2006. Sigma-based Data Pre-processing for Rapid Neural-Network Training, 3rd International Conference on Artificial Intelligence and Engineering Technology (ICAIET 2006), Universiti Malaysia Sabah, Kota Kinabalu, Malaysia

Jayasuriya T D, 2004. Prediction of Quiting of Oil Wells, Shell Research Grant, GameChanger, Holland

Jayasuriya T D, 2005. Neural Network-based Tools for Continuous and Optimised Production, Conference on Intelligent Wells: Implementation and Optimizations, Miri, Malaysia

Jayasuriya T D,, Pandian P M, 2005. Neural Network-Based Sand Prediction Tool With Enhanced Data Pre-Processing, 2nd Brunei International Conference on Engineering and Technology, Bandar Seri Begawan, Brunei Darussalam

Jayasuriya T D, Yaacob S, Nagarajan R. 2004. Neural Network-Based Virtual Sand Rate Production Prediction Tool. In Proceedings of the 2nd International Conference on Artificial Intelligence in Engineering and Technology, Kota Kinabalu, Malaysia.

Jayasuriya T D. 2004. Implementing Data Analysis Techniques To Optimize Neural Network-Based Sand Prediction Tool. Sand Control and Management in the African Oil and Gas Industry, Capetown, South Africa (accepted)

Jayasuriya T D. 2004. Sand Production Prediction – A Novel Approach in Implementing Artificial Neural Networks. Sand Control and Management –A Holistic Approach Conference. Kuala Lumpur, Malaysia

Jayasuriya T D, Yaacob S, Nagarajan R. 2003. Sand Prediction Model Implementing

Neural Network Based System Identification. In Proceedings of the 1st International Conference on Chemical and Bio Process Engineering, Kota Kinabalu, Malaysia

Jayasuriya T D, Yaacob S, Nagarajan R. 2001. Process Plant Information : Realizing Real-time Neural Network Controllers. In Proceedings of the 20th Conference of ASEAN Federation of Engineering Organizations (CAFEO), Phnom Pehn, Cambodia.

Jayasuriya T D, Yaacob S, Nagarajan R. 2002. An Intelligent Control system Employing Neural Adaptive Feedback Linearization. In Proceedings of the 1st International Conference on Artificial Intelligence in Engineering and Technology, Kota Kinabalu, Malaysia.

Jayasuriya T D, Yaacob S, Nagarajan R. 2001. Using Application & Analytical Software to Validate an Intelligent Model of a Variable-Frequency Induction Motor Drive. In Proceedings of the 19th Conference of ASEAN Federation of Engineering Organizations (CAFEO), Gadong, Brunei Darussalam.

Jayasuriya T D, 2001. Computer-based Tools: An Imperative Energizer for Augmenting the Teaching-Learning Process. In Proceedings of 6th International Conference on Science, Mathematics & Technical Education, Brunei Darussalam.